Escola de Camins
Escola Tècnica Superior d'Enginyeria de Camins, Canals i Ports
UPC BARCELONATECH

TREBALL FINAL DE MÀSTER

Theoretical Research on the Behaviour of Floating Offshore Wind Turbine Concrete Structures under Fatigue

Treball realitzat per:
Pablo Ángel Plou Nogueira

Dirigit per:
Climent Molins i Borrell
Alexis Campos Hortigüela

Màster en:
Enginyeria de Camins, Canals i Ports

Barcelona, 23 de juny de 2016

Departament d'Enginyeria Civil i Ambiental

Abstract

TITLE Theoretical Research on the Behaviour of Floating Offshore Wind Turbine Concrete Structures under Fatigue

Author Pablo Ángel Plou Nogueira

Supervisors Climent Molins i Borrell
Alexis Campos Hortigüela

KEY WORDS Fatigue, Offshore, Floating, Concrete, Wind Turbine

Floating offshore wind turbines technology is being developed worldwide as a solution to society's upcoming requirements on energy production. Current research tries to assure its viability by working on many different aspects, among which the development of economical floating substructures stands out.

The structural technology research group in the *Departament d'Enginyeria Civil i Ambiental* of the *Universitat Politècnica de Catalunya* is developing its own design, named WindCrete, which consists of a monolithic concrete spar buoy. Such a proposal is framed on an incipient technology context, in which previous similar experiences are limited and cost reduction becomes crucial in order to achieve success.

Therefore, it is necessary to characterize as better as possible the structure behaviour on the current previous design phase, considering all possible factors that may influence its operation conditions and the structural response. Given the WindCrete's offshore environment, highly determined by the constant application of high magnitude cyclical loads such as wind and waves, the verification of fatigue strength turns to be critical to assure the structure's resistance and viability.

A theoretical research on the fatigue behaviour of floating offshore wind turbine concrete structures has been taken to term, by approaching the problem of WindCrete's fatigue design. A model for the characterization of fatigue resistance of the conceptual structure has been developed and implemented as a complex numerical computation tool. Aspects as a dynamic simulation and load time history determination according to environmental conditions have been duly accounted, for which its own models have been created. Ultimately, the developed code has been employed to characterize the fatigue strength of the WindCrete, as well as for evaluating its fatigue resistance response on variations of design parameters.

Resum

TÍTOL Estudi Teòric del Comportament a Fatiga d'Estructures Flotants de Formigó per a Aerogeneradors

Autor Pablo Ángel Plou Nogueira

Tutors Climent Molins i Borrell
Alexis Campos Hortigüela

PARAULES CLAU Fatiga, Alta Mar, Flotant, Formigó, Aerogenerador

La tecnologia d'aerogeneradors flotants està sent desenvolupada arreu del món com una solució a les demandes socials emergents en relació a la producció energètica. La recerca actual procura assegurar-ne la viabilitat treballant en diversos aspectes, entre els quals destaca el desenvolupament de subestructures flotants assequibles.

El grup de recerca en tecnologia estructural del Departament d'Enginyeria Civil i Ambiental de la Universitat Politècnica de Catalunya està desenvolupant el seu propi disseny, anomenat WindCrete, consistent en una estructura monolítica de formigó tipus spar. Tal proposta s'emmarca en un context de tecnologia incipient, en la qual el nombre d'experiències similars anteriors és limitat, i la reducció de costos esdevé crucial per tal d'assolir l'èxit.

Per tant, és necessari caracteritzar tan bé com es pugui el comportament de l'estructura a la fase de disseny previ, tenint en compte tots els factors que puguin incidir en les seves condicions operatives i la seva resposta estructural. Donat l'entorn d'alta mar del WindCrete, altament determinat per l'aplicació constant de càrregues cícliques d'alta magnitud com el vent o les ones, la verificació de la resistència a fatiga esdevé crucial per a assegurar-ne la fermesa i viabilitat.

S'ha dut a terme una recerca teòrica sobre el comportament a fatiga d'estructures flotants de formigó per a aerogeneradors, tot abordant el problema de disseny a fatiga del WindCrete. S'ha desenvolupat un model per a la caracterització de la resistència de l'estructura conceptual en aquests termes, i s'ha implementat com a eina de càlcul numèric complexa. S'ha tingut en compte aspectes com la simulació dinàmica i la determinació de la sèrie històrica de càrregues segons condicions ambientals, creant-hi models propis. En darrer terme, el codi desenvolupat s'ha emprat per a caracteritza la resistència a fatiga del WindCrete, així com per a avaluar-ne les seves variacions en front a variacions sobre els paràmetres de disseny.

Resumen

TÍTULO Estudio Teórico del Comportamiento a Fatiga de Estructuras Flotantes de Hormigón para Aerogeneradores

Autor Pablo Ángel Plou Nogueira

Tutores Climent Molins i Borrell
Alexis Campos Hortigüela

PALABRAS CLAVE Fatiga, Alta Mar, Flotante, Hormigón, Aerogenerador

La tecnología de aerogeneradores flotantes está siendo desarrollada en todo el mundo como una solución a las demandas sociales emergentes entorno a la producción energética. La investigación actual intenta asegurar su viabilidad trabajando en varios aspectos, entre los cuales destaca el desarrollo de subestructuras flotantes rentables.

El grupo de investigación en tecnología estructural del *Departament d'Enginyeria Civil i Ambiental* de la *Universitat Politècnica de Catalunya* está desarrollando su propio diseño, llamado WindCrete, consistente en una boya monolítica de hormigón tipo spar. Esta propuesta se enmarca en un contexto de tecnología incipiente, en el cual el número de experiencias similares anteriores es limitado y la reducción de costes adquiere un carácter crucial para alcanzar el éxito.

Por consiguiente, es necesario caracterizar tan bien como sea posible el comportamiento estructural de la fase de diseño previa, tomando en consideración todos los factores posibles que puedan incidir en sus condiciones operativas y su respuesta estructural. Dado el entorno de alta mar del WindCrete, fuertemente determinado por la aplicación constante de cargas cíclicas de alta multitud como el viento y las olas, la verificación de la fatiga resulta crítica para asegurar la resistencia y viabilidad de la estructura.

Se ha llevado a cabo una investigación teórica acerca del comportamiento de la fatiga en estructuras flotantes de hormigón para aerogeneradores, en una aproximación al problema de diseño a fatiga del WindCrete. Se ha desarrollado un modelo para la caracterización de la resistencia a fatiga de la estructura conceptual, y se ha implementado como herramienta de cálculo numérico compleja. Se han tomado en cuenta aspectos como la simulación dinámica y la determinación de la serie histórica de cargas acorde a las condiciones ambientales, incluyendo la creación de modelos propios. Finalmente, el código desarrollado se ha utilizado para caracterizar la resistencia a fatiga del WindCrate, así como para evaluar su respuesta frente a variaciones de parámetros de diseño.

I. Table of Contents

II. Units, Symbols and Acronyms

Acronyms

ABS	American Bureau of Shipping
CAPEX	Capital Expenditures
CM	Centre of Mass
COB	Centre of Buoyancy
Cur	Current
Dir	Wind/Wave Directionality
DLC	Design Load Case
DNV	Det Norske Veritas
EC2	Eurocode 2
EWC	Extreme Wind Conditions
FLS	Fatigue Limit State
FOWT	Floating Offshore Wind Turbine
HCL	Hollow Core Link
IEC	International Electrotechnical Commission
LCOE	Levelised Cost of Energy
LRFD	Load and Resistance Factor Design
LS	Least Squares Method
LSD	Limit States Design
MC10	Model Code 2010
MH	Metacentric Height
MLE	Maximum Likelihood Estimation
MoM	Method of Moments
MSL	Mean Stillwater Level
NSS	Normal Sea State
NTM	Normal Turbulence Model
NWC	Normal Wind Conditions
NWH	Normal Wave Height
NWP	Normal Wind Profile
RAO	Response Amplitude Operator

TLP	Tension Leg Platform
WavC	Wave Condition
WinC	Wind Condition
WL	Water Level

Units

Force	kN, N
Stress	MPa
Strength	MPa
Length	m, cm, mm
Distance	km
Depth	m
Displacement	m
Permeability	m/s
Design Life	Years
Area	m^2
Deformation	-
Density	kg/m^3
Moment	kNm
Velocity	m/s
Acceleration	m/s^2
Rotation	DEG
Time	sec, min, h

Symbols

Latin Characters

A	Area
C_1	SN Curve Structural Component Placement Parameter (DNV)

C_A	Added Mass Coefficient
C_D	Frictional Drag Coefficient
C_L	Lift Coefficient
C_M	Inertia Coefficient
c	Wave Celerity
D	Diameter
D	Fatigue Damage
D_{lim}	Limit Fatigue Damage
$E_{cd,max}$	Maximum Compressive Stress Level
$E_{cd,min}$	Minimum Compressive Stress Level
F_b	Buoyancy Force
f_{ck}	Characteristic Resistance of Concrete
$f_{cd,fat}$	Design Fatigue Strength of Concrete
f_S	Vortex Alternation Frequency
H	Wave Height
H_{m0}	Spectral Significant Wave Height
H_{RMS}	Root Mean Square Wave Height
H_S	Significant Wave Height
I	Intertia Moment
K_C	Keulegan-Carpenter Number
k	Wave Steepness
k_{xx}	Hydrostatic Stiffness, in *xx* Degree of Freedom
m	Structural Mass
m_{added}	Added Mass
m_v	Dynamic Mass
N	Number of Fatigue Resisting Cycles
n	Number of Fatigue Acting Cycles
p	Dynamic Pressure
$\bar{q}$	Morison's Equation Force per Unit Length
$\overline{q_1}$	Inertia Force per Unit Length
$\overline{q_D}$	Drag Force per Unit Length
R_d	Design Resistance
S	Strouhal Number
S_{max}	Maximum Stress Level

S_{min}	Minimum Stress Level
S_d	Design Load Effect
T	Wave Time Period
T_m	Mean Wave Period
T_{m02}	Spectral Mean Wave Period
T_P	Peak Wave Period
T_R	Return Period
t_0	First Load Application Day on Concrete
U_{10}	10-Minute Mean Wind Speed
$U_{10,hub}$	10-Minute Mean Wind Speed at Hub Height
u	Flow Velocity
$\dot{u}$	Flow Acceleration
$u_{current}$	Current Velocity
u_{waves}	Wave Velocity
V	Volume
V_{ref}	Wind Turbine Reference Wind Speed
v_{in}	Wind Turbine Cut-In Speed
v_{out}	Wind Turbine Cut-Out Speed
V_{hub}	Wind Velocity at Hub level
w	Angular Velocity
$\ddot{x}$	Acceleration Vector

Greek Characters

α	Stress Gradient Redistribution Factor (DNV)
α	Weibull Distribution Scale Parameter
β	Weibull Distribution Shape Parameter
β_{cc}	Factor for Concrete's Strength at First Load Application Day
γ	Weibull Distribution Location Parameter
$\gamma_{c,fat}$	Fatigue Partial Safety Coefficient for Material Concrete
γ_{E_d}	Partial Safety Coefficient for Load
γ_f	Partial Safety Coefficient for Load
γ_m	Material Factor
η	Limit Fatigue Damage

η_c	Stress Gradient Redistribution Factor (MC10)
λ	Wave Length
ρ	Density
$\sigma_{cd,max}$	Maximum Fatigue Cycles Stress
$\sigma_{cd,min}$	Minimum Fatigue Cycles Stress
σ_U	Standard Deviation of the Wind Speed
$\sigma_{U,c}$	Characteristic Wind Speed Deviation

1. Introduction

1.1 Motivation

Offshore wind power is the energy generation method which consists on the transformation of the kinetic energy of wind into electricity, by means of wind turbines placed in shallow or deep waters. Although offshore wind turbines appeared not so long ago, have been proved to be a secure and reliable source of energy.

Nowadays offshore wind power is positioned at the same level of profitability as other renewable energy sources. Despite presenting higher costs (mainly related to installation, operation and maintenance) in comparison with, for example, onshore production facilities; the stronger wind velocities available out at sea, in addition to the higher design life and the reduction of location related problems, have turned offshore wind power into a successful energy supply [1].

Although its young age, offshore wind power is today a well-established energy source, which has undergone an intense growth. The inauguration of the first offshore wind farm installation dates back to 1991 in the southern part of Denmark (Vindeby). Located 2.5 km from the coast, the farm was projected with 11 wind turbines 450 kW each, featuring a total capacity of 4.95 MW [2]. Since this first incipient development of the offshore wind industry, the sector has increased its global capacity exponentially. At the end of 2014, the total figure has raised up to 8759 MW, with 1713 MW installed during 2014 and twelve projects under construction that will add 2900 MW [3]. A potential of 150 GW wind capacity, meeting 14% of the EU's total electricity consumption by 2030, is predicted. This tendency can be clearly seen on Figure 1.

Offshore wind energy industry has positioned itself as well as a solid economy agent, becoming a strong asset for many countries. Employment figures are substantially prominent, having reached around 75000 full time equivalent jobs in 2014, a value the triple than five years ago [4].

The reduction of the cost of offshore wind energy has played and plays a very important role on its development. Lately, industry has focused its innovation and expenditure decrease efforts on foundations and moorings, which have resulted into a driven factor of this economic sector. The improvements developed thanks to the gained experience in the last years have helped to reach large growth rates. Nevertheless, the employed technology is still considered to be young. Costs can and need to be more competitive, especially for floating wind turbines,

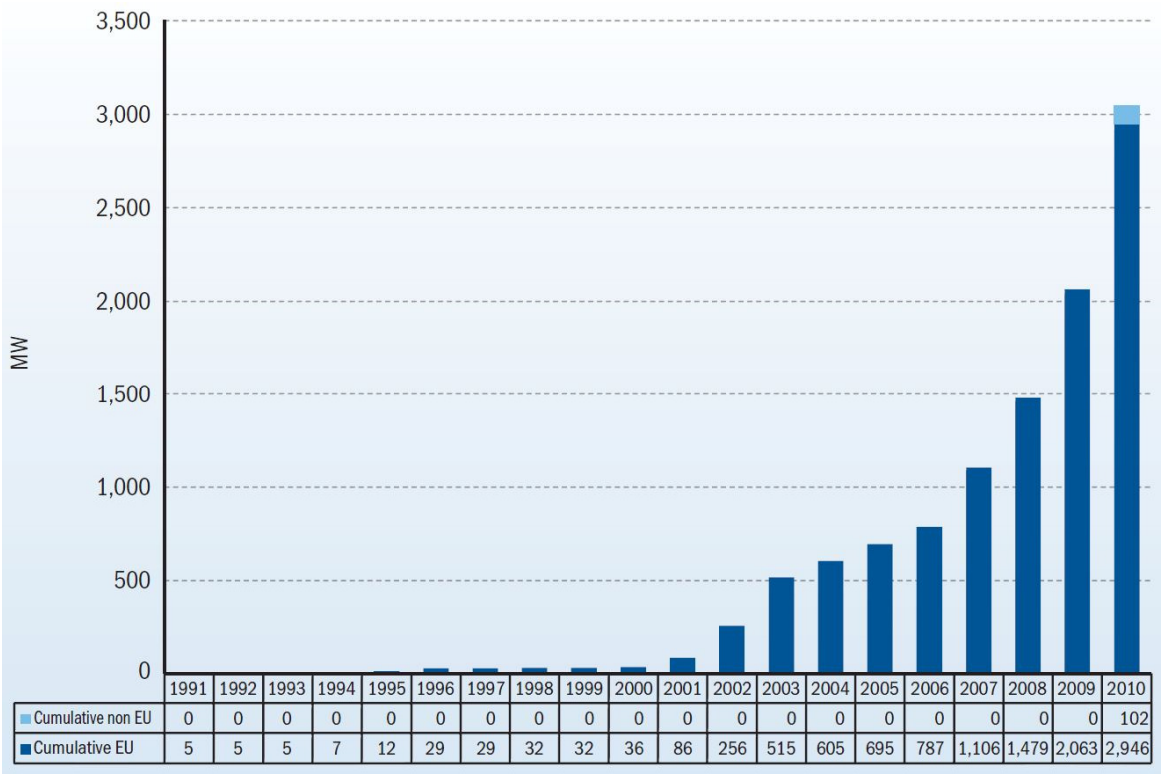

	1991	1992	1993	1994	1995	1996	1997	1998	1999	2000	2001	2002	2003	2004	2005	2006	2007	2008	2009	2010
Cumulative non EU	0	0	0	0	0	0	0	0	0	0	0	0	0	0	0	0	0	0	0	102
Cumulative EU	5	5	5	7	12	29	29	32	32	36	86	256	515	605	695	787	1,106	1,479	2,063	2,946

Figure 1 Evolution of the worlwide cumulative installed offshore wind capacity *[2]*.

for what a considerable investment in research and development related to turbines, supply chain optimization, transmission, operations and maintenance is necessary [5].

The benefits obtained from an impulse of offshore wind energy are unquestionable. As a large productive, profitable and completely renewable source of energy, it can be a fundamental player on the transformation of the electricity generation system. Its highly positive repercussions over the economy of productive related maritime areas, and globally over the energy consumer society, are certain [6].

Current future trends show the sector intention to keep growing. In this regard, cost reduction appears again as the agent that will condition the development of the sector. It is not only needed to take the maximum profit of the production, but also to ensure and make effective the enormous expansion potential benefits of offshore wind power. It will condition industry profitability, and the interest of the stakeholders into investments on enlargement and development projects. Taking the maximum profit of such an enormous and beneficious expansion potential involves efforts and work on many different topics; from the legislative frameworks to the development of a price competitive technology [7].

Among the many cost reduction objectives which are needed to facilitate this expansion, there is one which stands out due to its magnitude and its enormous influence over the potential of the sector: floating offshore wind turbine technology development.

Actual fixed-bottom technology does not offer competitive solutions on deep waters. Floating wind turbines appear as the natural solution to save up costs, by basically reducing high priced budget items such as material, installation and foundations. A vertical extent of 50 m is determined as the minimum depth for which floating offshore wind cost would be below fixed-bottom installations expenditures. On preliminary studies, it has been qualitatively determined that the maximum depth that would ensure the profitability is 200 m [6].

Floating offshore wind can be considered to be a long term and global solution to the actual development problems of the offshore wind industry. It would allow to economically make the most of all the available localizations with wind resources, introducing all those zones between 50 m and 200 m depth [8]. In addition, the exploitation of the wind resources over maritime areas far from shore would allow to avoid problems related to spatial planning and take profit of the stronger wind velocities present, for which larger turbines, which would not be supported by fixed bottom solutions, will optimize the production [6].

If the current growth rates are not wanted to sink, the necessity of technological solutions

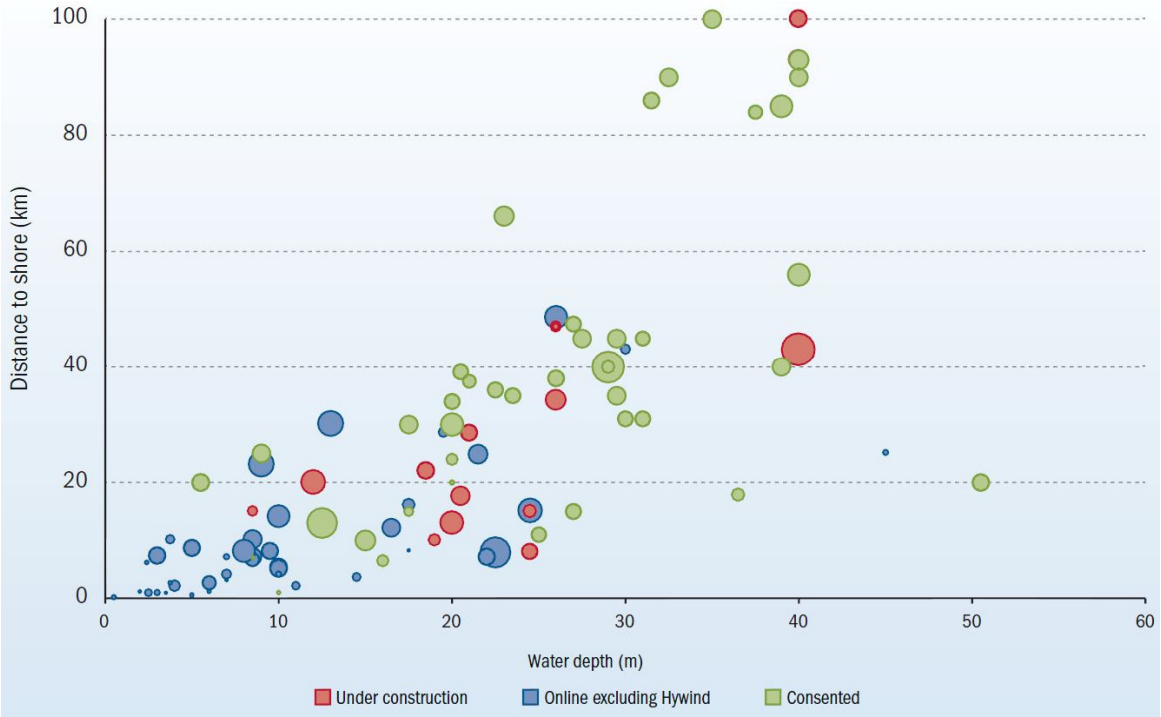

Figure 2 Distance and water depth of constructed, under construction and consented offshore wind farms *[2]*.

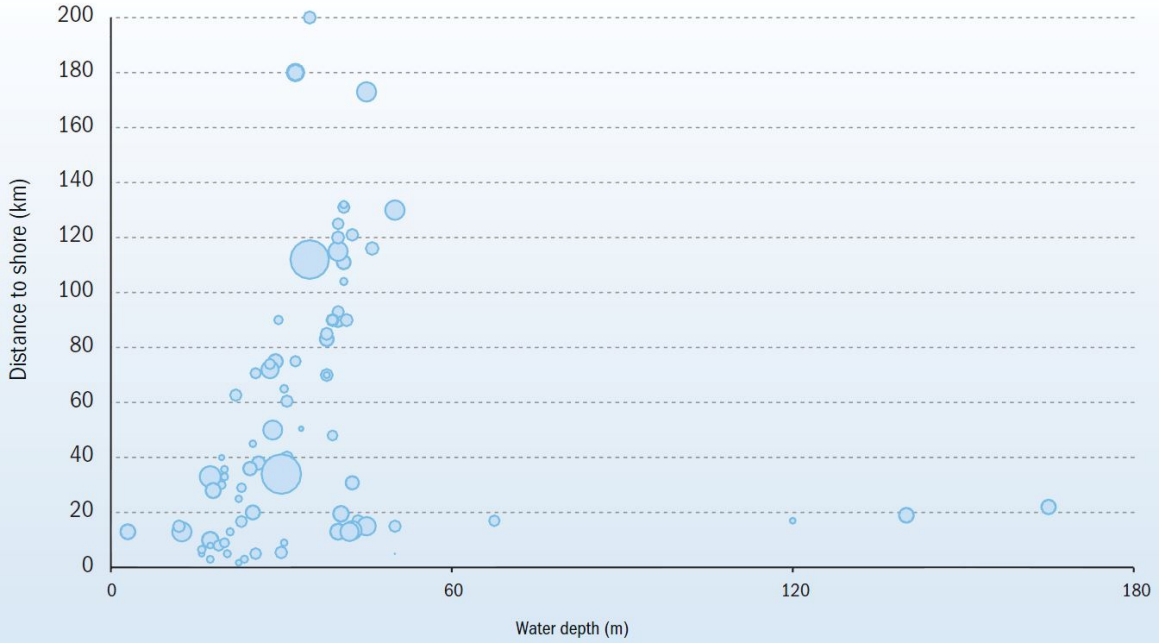

Figure 3 Distance and water depth of planned offshore wind farms *[2]*.

that can guarantee the expansion is clear. Existing expansion trends of the offshore wind deployments show that a translation from the actual locations into further from coast and inherently deeper positions is required, for which offshore wind turbines appear as the best solution. The data shows that in 2012 operative wind farms presented an average value of 29 km distance from shore and 22 m of depth, with interest on planning wind farms which go up to 200 km from shore and depth of 215 m. It is easy to see this trend in Figure 2 and Figure 3, where the distance to shore and the water depth of the placements for respectively constructed and planned wind turbines is plotted.

In similar terms, future wind production installations are demanding larger turbines (76 % of the ones planned in 2012 larger than 5 MW) to take profit of the economies of scale that are unrestricted in the sea [6]. New offshore designs will need to adapt to the presented trends, for what floating offshore appears to be a cost effective good solution.

This need for floating solutions for the global sector development can be justified as well on other reasons. The development of offshore wind production in many of the world key markets would exclusively accept floating wind solutions to adequately take profit of their wind resources. Data contrast on some of this countries reaffirms it: 61% of the USA offshore wind resources are located in water depths of more than 100 meters, nearly all of Japan’s are in deep water, 66% of the North Sea presents depths comprised between 50 and 220 m, and the

Mediterranean bathymetry does not allow to exploit its wind resources on fixed bottom solutions.

Moreover, on a long term scenario, the development of cost effective floating solutions would provide sufficient solutions for energy scarcity. Taking into account the suitable water areas for the installation of floating turbines in the North Sea, and assuming 10 MW generators, an energy production that could meet the European Union consumption 4 times over is estimated [6].

Despite these advantages that the floating solutions present, the unwanted cost increment is inherent. Operation, maintenance and grid connection infrastructure would be affected, on a framework where the construction of the wind turbine will cost as much as 5 times the price of a fixed bottom solutions [9]. Expenditure cut is therefore needed, for what the research for floating solutions that meet the expansion problems of the sector in a cost effective way appear as a challenge for the industry [10].

In this regard, a large number of floating offshore wind substructure projects are being developed worldwide. Different concepts, based on various flotation principles, are being proposed, trying to answer the industry requirements by taking chances on different strengths [11].

In this context, researchers of the Structural Technology Group (STRUCTECH) of the Department of Civil and Environmental Engineering (DECA) of the *Universitat Politècnica de Catalunya* (UPC) have committed itself to the expansion of the floating offshore wind power by devising an ambitious, thorough and extensive project on the development of a substructure for floating offshore wind turbines. Analysing the industry problem, and taking profit on the broad and deep civil engineering expertise of the research team, a concept focused on minimizing the cost of the energy has been proposed [12].

Starting on 2012, the former AFOSP (Alternative floating offshore substructures for offshore wind farms) project, now turned into WindCrete, is still being developed, entering at this time (2016) the scaling tests phase. The design involves a large sized spar-buoy (approximately 230 m length) constructed as a monolithic continuous pre-stressed concrete cylinder, as rendered on Figure 4. The concept tries to respond to the enlargement trend of the industry, answering with a design capable of supporting large wind turbines (up to 10 MW on this first design) and taking advantage of the high wind resources on deep waters. At the same time, the concrete structure reduces enormously the material and fabrication and cost, ensuring as well a cost-effective installation and low maintenance need.

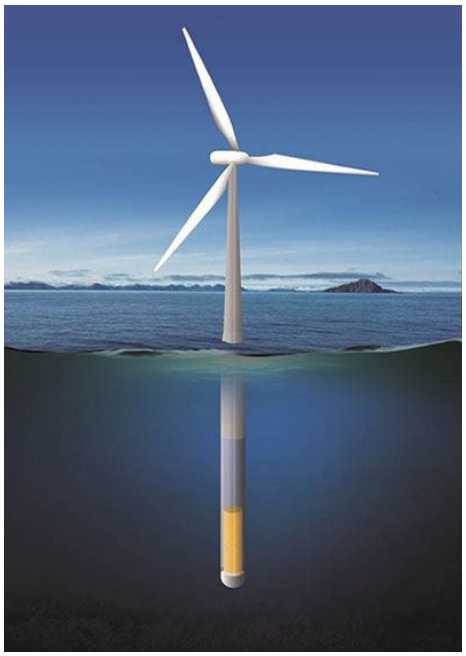

Figure 4 3D render of the WindCrete conceptual concrete structure for floating wind turbines.

The process of studying and developing such a special, unique and innovative concept requires of many efforts that involve technical, economical, financial and commercial studies [6]. Among them, the technical efforts stand out as the ones that would condition the others the most, and globally, have influence over the viability of the project [13].

In this regard, every single developable aspect of the technical project must be carefully considered. The development of such an enormous structure, taking into account the lack of references on similar designs and the need for cost optimization requires of a series of well planned, extensive and meticulous studies on the subject. The maximum advantage of the design phase must be taken to reduce as much as possible the uncertainty, guaranteeing the return of such a huge investment and reducing the possible losses, contingencies and risks to its minimum [14].

1.2 Problem Definition

The required technical and scientific research work differs considerably from those of any other innovation project civil engineering related. Not only by its highly innovative nature, the characteristic large size, or the high cost optimization necessity; but because of its location on a very special environment with harsh service conditions [15].

Two main factors with direct influence on the engineering design can be outlined among the different operating circumstances of the wind turbine. First, the loads present on a maritime deep sea differ significantly from any other system of loads. Many combined actions will affect the structure. Among those wind and wave stand out due to its high magnitude and cyclic properties [16].

Second, farms located at large distances from shore entail a high cost related to maintenance (on a fixed-bottom wind farm, up to 22-40% of the total cost [17]). This cost is also linked to the technical difficulties of repairing such a special structure on deep sea. In addition, the sea environment (humidity, chemical agents, etc.) entails a rapid aggravation of the structural properties when a minor harm is produced, mostly fostered by such repetitive and intrusive load as wave. In this scenario, the only possible solution to ensure the reduction of those costs and the maximization production's profitability is guaranteeing a large design life, during which maintenance will not be needed and the operation requirements will not be affected. The monolithic design of the spar structure has been designed to avoid complications concerning this problem [12].

In this context, a design condition must be highlighted among the others: fatigue resistance. Fatigue can be defined as the process causing a degradation of the material due to cyclic loading. Its effects influence the structural behaviour in different detrimental ways, including the increase durability problems and the possibility of material sudden collapse [18].

The most important loads affecting the structure, which are the wave and wind load, are cyclic. Consequently, the presence of fatigue effects is evident. Taking into consideration the necessity of avoiding any structural maintenance, it must be ensured that fatigue effects will not compromise the design life of the wind turbine nor its structural response.

Due to the singular nature of fatigue, most codes only impose its verification on extraordinary cases. Basically, it is reserved for those special structures subjected to cyclic loading (crane-rails, high traffic bridges, etc.) [19]. As a consequence, fatigue design is reduced to a small group of structures, among which offshore constructions only comprise a short sum. Additionally, when compared to other structures that must verify fatigue conditions, offshore structures are subjected to larger numbers of stress cycles and higher loads which tend to respond to stochastic processes. The exceptionality of fatigue design referred to floating wind turbines is indisputable.

In addition to this problematic, it must be outlined that the research on fatigue is very young and superficial. Only a few simple theories and established application methodologies have

been obtained, and a high uncertainty over the phenomena is still present, being a current investigation topic nowadays [20].

The doubts on fatigue design that the described scenario implies are increased by the use of concrete as the material of the designed floating wind turbine concept. The development of the offshore industry related to the naval and to the oil and gas sector in the last century has involved the production of some research related to deep sea structures, including fatigue related topics. Despite the vast differences between wind power and those industries, mainly related to cost optimization necessity due to the velocity of investment amortization, its available knowhow has been used by offshore wind turbines producers on the developing of technical solutions and processes [14] [21] [22]. As a consequence, the initial development of the industry has been based on the steel construction, which is the main material used by the naval and the oil and gas industries. This, has influenced considerably its expansion and the following research. In this regard, the reduced experience on offshore fatigue design is based on steel structures, leaving a high uncertainty level over concrete behaviour on those cases.

In conclusion, the design conditions of the floating wind turbine concept make necessary the assurance of fatigue effects not affecting the serviceability of the structure. The background on offshore wind turbines design must be taken into account and adequately exploited, despite presenting limited conclusions

The fatigue design processes of concrete structure for floating offshore wind turbine have to be studied in order to ensure the desired service life.

1.3 Aim Definition

It is the pretension of this master thesis to approach the fatigue resistant behaviour of the floating offshore wind turbine structures made of concrete, in order to help the development and establishment of the in the previous section introduced WindCrete conceptual structure.

A work process has been established through the definition of accordingly selected tasks, which shall contribute to establish a well-documented, rigorous and reliable procedure for the fatigue processes characterization of the WindCrete.

The fulfilment of the next developed objectives has been considered necessary to accomplish successfully this endeavour.

On a first step, it is considered to be indispensable to understand the mechanical and resistant behaviour of the WindCrete. Its floating character and the offshore environment in which it is placed present an inherent added complexity which shall be duly apprehended.

On a second phase, a deep insight in the fatigue phenomena shall be taken to term. The gathering of the basics and the state of the art related research will be necessary to approach the ultimate WindCrete fatigue behaviour description in the better possible way. When possible, this information shall be related to concrete structures and/or offshore environments.

On a further third phase, an original approach on the numerical simulation of the fatigue phenomena on concrete floating offshore wind turbine structures shall be set. Necessary considerations will have to be taken to term in order to define a characterization process which must account for its applicability on a structure such as WindCrete, providing reliable results while maintaining assumable levels of realization. Existing design codes specifications shall be considered in this regard. In case of conflict between the requirements of those, comparisons must be taken to term, trying to evaluate its functioning.

A fourth step shall account for the transformation of the defined approach into an analysis model. It must serve as a comprehensive and practical tool to undergo researches on the fatigue response of the floating concrete structure. Its numerical implementation on the Matlab programming language will be necessary, providing a resourceful and competitive coding environment that must set for a flexible and optimized usage.

Finally, a fifth last phase shall document the employment of the designed and implemented model on the fatigue behaviour analysis of the WindCrete conceptual structure. Its resisting properties and the main parameters influencing them shall be accounted.

1.4 Procedure

Given the stated project's ambition, which is boosted by a context of difficulties such as the ones described in the motivation section (Section 1.1), the taken to term work has been categorized and presented in an extensive set of chapters and sections. An overview of the content of each of them is given next.

On Chapter 2, a global state of the art research is documented. The relevant aspects of the established knowledge on the related research areas have been gathered, organized and studied.

First, the state of the art regarding floating offshore wind turbine technology (Section 2.2) and its mechanical simulation methods (Section 2.3) have been taken into account. It has provided a deeper understanding on the characteristics of its structural behaviour governing principles, both general and for the particular ones of WindCrete. Moreover, the research on its simulation methods has as well provided interesting information over the simplifications and hypothesis which these approaches presented, which are necessary to be known for the assuring of the fatigue behaviour results reliability.

Second, the state of the art regarding fatigue phenomena on floating offshore wind turbines has been studied and documented. The generality of such a phenomena has needed of an extensive and detailed literature research process, which has started on the basic knowledge existing on the description of the fatigue phenomena, both in general materials and in concrete (Section 2.4), and has ended on its practical evaluation techniques on concrete structures (Section 2.5).

Third, a description of the state of the art on fatigue design is presented. The resolution of real engineering problem needs of some approaches for which theoretical descriptions of a phenomena may not be adequate. In this sense, the analysis of existing fatigue design methods allows the obtaining of a practical view of the problem approach. The existing design codes which include fatigue verification have been detailed and compared (Section 2.6). Finally, procedures on fatigue design for offshore and floating offshore wind turbines are introduced as presented by different guidelines and codes (Section 2.7).

On Chapter 3 the produced method for fatigue resistant behaviour analysis on the WindCrete conceptual structure is presented. A global approach has been given to the presentation of the chapter's contents, for which problem statement, resolution approach proposal, numerical code implementation, and results obtaining, are described all together; following the linearity of the different steps in which the model has been divided. Hypothesis, further considerations and conceptual details are included along the chapter.

In the frame of Chapter 3, and on first place, a complete description on the geometrical and resisting properties of the WindCrete structure has been performed (Section 3.2).

Second (Section 3.3), the hypothesis in relation to location which have been assumed in order to give a real application character to the fatigue design problem of the conceptual structure have been introduced. Spatial location will condition the loads on the structure, given its dependence of environmental conditions magnitude. An original approach for the loads determination on the analysed structure has been presented. The load time histories that fatigue

analyses requires and the high stochastic character of the sea environment loads, have led to the production of this comprehensive method for its determination. Finally, the results obtained in this terms for the proposed WindCrete problem are presented.

Third, the obtained loads have been introduced into a model for the mechanical simulation of the WindCrete (Section 3.4). The characteristics of the model and its functioning are described. Output values in terms of displacements and forces are obtained.

Fourth, the output simulation values allow for a characterization of the fatigue damage that those will be causing on the structures. A complete analysis in this terms has needed of the stress and damage computation proceeds, along with the careful definition of many other necessary parameters (Section 3.5).

Fifth, and as a last section of Chapter 3, the produced and implemented model has been used to analyse the fatigue resistant behaviour of the WindCrete, in the context of the problem defined along the chapter. Results on fatigue life and parameter influence have been accounted (Section 3.6).

Finally, Chapter 4 presents the conclusions which have been derived from all the work taken to term and results obtained on the different sections, along with some interesting suggestions for future research on the matter.

2. State of the Art

2.1 Introduction

Specific studies on the fatigue behaviour of offshore concrete floating structures cannot be found on the actual literature. Given the novelty of such an area of research, no specialized or deep publications can be found on that precise subject.

Therefore, a primary research stage for the elaboration of this master thesis has required the gathering of the available specific information on each of the topics that relate to it. The obtaining of a first knowledge base has been pretended, attempting to get to know the associated knowledge areas, extract conclusions and settle the further research steps.

As mentioned on Chapter 1, newness is present on all the matters that relate to the fatigue on concrete floating offshore wind turbines (FOWT), for which some of the topics are not as rooted as desired. In this regard, the establishment of clear, rigorous and wide theoretical fundaments becomes crucial in the developing of further knowledge.

With these objectives in mind, a documentation and literature research has been performed on the different topics which compose fatigue design on concrete FOWT. This process has included a first overview on the state of the art of the FOWT technologies, followed by a dissertation about its mechanical simulation and modelling possibilities. Next, the contemporary knowledge on fatigue is presented, accompanied of a brief historical review of the phenomena investigation. Finally, the actual practical engineering theories and methods used for fatigue design are introduced.

On each of the worked topics, the pursuit of collecting information that best could approach the final topic of this master thesis has been seek, instead of reducing it to the specific subject itself. In this regard, for example, the research on FOWT simulation has focused on the modelling of fatigue loads; or the fatigue reviews are presented along its behaviour for concrete structures.

In these chapter, a global overview on the results of the conducted primary research for each of the subjects is presented; attempting to lead the reader into the fundaments that have been employed for the proposals, methods and conclusions which will be introduced in the next sections of this thesis.

2.2 FOWT Technology

Floating offshore wind technology is being developed as a solution to many of the problems that the growing offshore wind energy sector faces.

Although fixed-bottom offshore technology advances have reached a high maturity level, and this kind of technology is expected to dominate the offshore wind energy production in a short term horizon, an approach to the characteristics of a long term scenario suggests the appearance of many expansion requirements that will be difficult to answer to. The increasing power and size of wind turbines require more exigent site conditions, where a higher level of wind resources can be found. It makes it necessary for wind farms to search adequate locations further from shore, involving higher water depths. This poses challenges associated to installation, operation and maintenance; involving huge costs related to the structure, foundations and construction logistics [2].

Floating offshore wind appears as an answer to these difficulties, allowing to ignore the high depth limitations and take profit of the advantages of very deep water areas where it was impossible for fixed-bottom solutions to act. These benefits include proximity to the coast, along with its inherent cost reduction; and high and constant wind velocities zones.

Nowadays floating offshore wind energy production is still incipient and needs a set of complete development processes where commercial models can be created and optimized in order to enhance the energy production and take the cost reduction potential up to its maximum. As a consequence of the actual developing stage, feasibility of floating wind has to be proven by means of prototype and pre-commercial projects. The natural path of development of such a new technology is being followed, guaranteeing all along its way, the overcoming and discard of all possible problems and difficulties of the market-oriented evolution process.

In this context of nascent developments and lack of consistent previous experience, many floating concepts have been developed focused on the promotion of different strengths that answer to a wide range of aspects of the original problem approach and cost drivers, such as water depth, seabed conditions, local infrastructure or local supply chain capabilities [22].

2.2.1 FOWT Typology

Among the current on-development concepts, a basic classification based on the stability response of the floating substructure is made.

There are three types of flotation principles which are combined in order to achieve structure static stability [8]. Namely:

- Ballast
- Mooring
- Water plane stabilisation

Ballast stabilisation manages to ensure the heavier components of the structure are located on the lowest levels, in confrontation with the lighter materials in the upper part. This way, the centre of gravity is much lower than the centre of buoyancy. The flotation and stability of the structure are ensured.

Mooring stabilisation provides balance through tensioned slack lines connected to the sea bed. The cables are accordingly disposed and stressed to provide enough restore moment. Water plane stabilisation refers to a large weighted area in contact with water, resulting on an automatic restore moment when the destabilizing loads act.

In respect of real concepts, designers will seek to combine adequately the three available stability systems to achieve the design objectives; specifically, best functionality or lowest cost. In consequence all the designs use a combination of the three principles. Nevertheless, and as a result of a focused design, one of the stabilization mechanisms will always be predominant [8].

In this regard, a global view over the up-to-date proposed floating concepts results into three main typologies of floating structures, regarding the stability responses that they combine [6]:

- Tension Leg Platform (TLP)
- Spar Buoy
- Barge
- Semisubmersible

TLPs are high buoyancy structures which mainly obtain stability from a tension mooring system. Spar buoys consist of a very large cylindrical buoy that stabilises the wind turbine using ballast. Barge obtain flotations and stability from its large water plane area, given the extensive horizontal cross section area.

Semisubmersible floating structures differ from the other types on the fact they do not focus on a single stabilization principle. A combination of ballast and water plane effect help

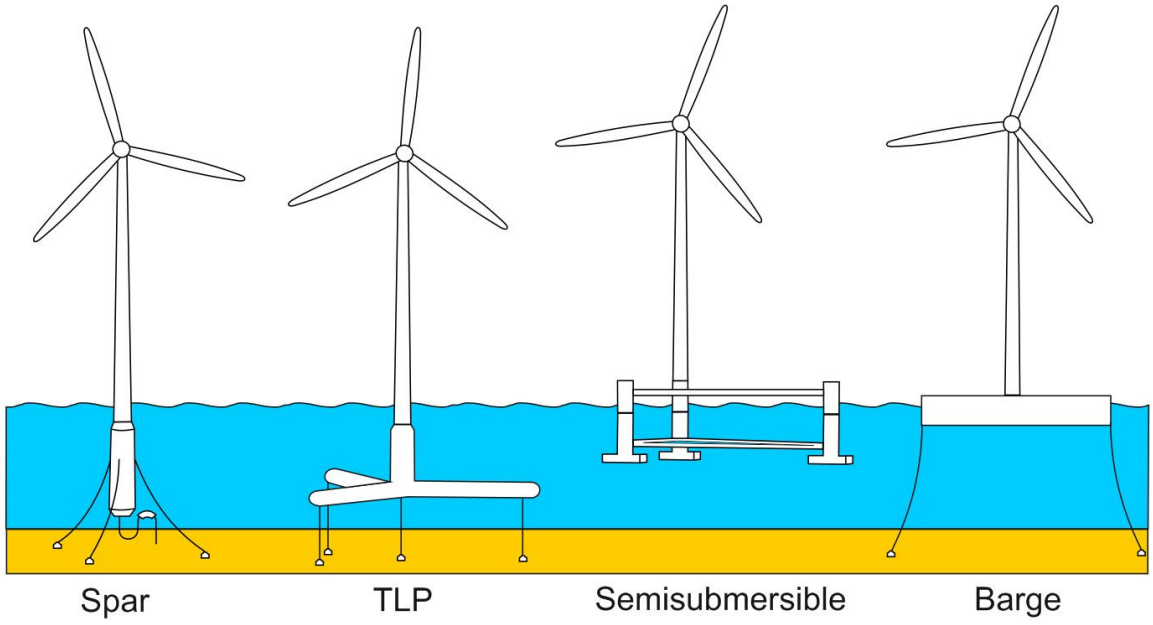

Figure 5 Main typologies of floating offshore wind turbines.

balance these high buoyancy structures which are geometrically designed in this regard. No taut mooring lines are needed [14] [23]. More combinations of stability systems are found on other singular designs.

In Figure 5 the graphical representation of the four presented types of FOWT can be observed; while in Figure 6 each of them is plotted on a three dimensional space representing the combination of floating principles, which each typology takes advantage of.

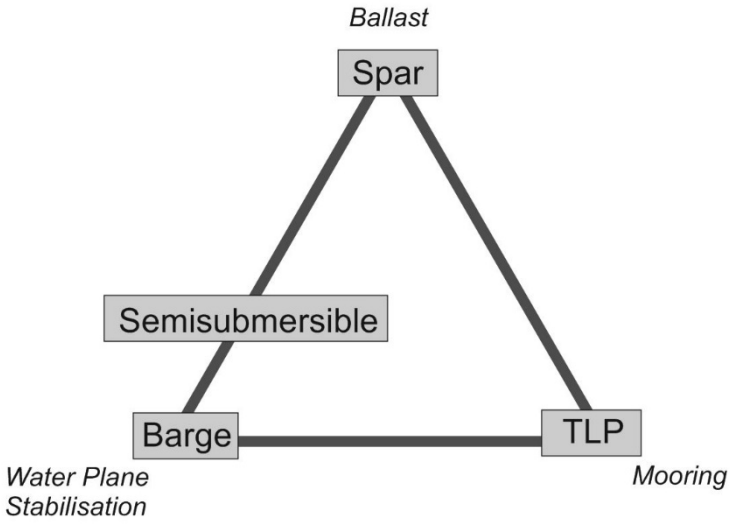

Figure 6 Flotation principles in which each FOWT typology design is based.

As an indicator of the design tendencies which will be later exposed in this text, it is interesting to know that the oil and gas floating platforms also take profit of these three main typologies. Regarding the production system, apart from the typologies mentioned above which usually work as a support structure for one turbine, other minor special designs such as multi-turbine platforms and hybrid wind-wave devices happen to be as well [23].

Available estimated data on the different concepts has make it possible to carry out a preliminary qualitative comparison on the advantages of these typologies. Capital expenditures (CAPEX), which is the cost concept including investment and deployment; and the levelized cost of energy (LCOE), defined as the total cost of deploying and operating a power-generating asset, divided by the total electricity production of that asset, have been analysed and compared on the literature. On average, the results show similar values between the three main typologies. Some semisubmersible platforms show a lower LCOE value related to smaller installation costs. Some other spar and TLP concepts present a flatter CAPEX value. It is worth mentioning, all of

	Floating Substructure Types		
Substructure Design Challenge	**Barge**	**LTP**	**Ballast**
Design Tools and Methods	-	+	-
Buoyancy Tank Cost	-	+	-
Mooring Line System Cost	-	+	-
Anchors	+	-	+
Load out	+	-	/
Onsite	+	-	+
Decommissioning	+	-	+
Corrosion	-	+	+
Depth	+	-	-
Sensitivity	+	-	+
Minimum	-	+	-
Wave	-	+	+
Impact of Stability Class on Turbine Design			
Turbine weight	+	-	-
Tower Top Motion	-	+	-
Controls Complexity	-	+	-
Maximum Healing Angle	-	+	-

+: relative advantage
-: relative disadvantage
/: neutral effect

Table 1 Pros and cons trade-off of the three main floating platform types *[8]*.

them present a lower CAPEX on the concrete structures over the steel alternatives [22].

As for a more specific and technical view, [8] categorized the pros and cons trade-off in terms of a series of predicted design challenges [24]. Table 1 determines the proposed criteria for the three main types of stability principles. Relative advantage, disadvantage or neutral affection of a balance class, in relation to a design topic, is indicated through a symbol system. It is very important to outline the context of concept-development context in which this classification takes place. It must be understood as an indicative preliminary categorization without major experience on optimization potential, and therefore heavily dependent on factors such as specific design or location site.

Different proposed alternatives can be found on [22]. A wide variety of typologies, origin countries and design stages can be found among the gathered concepts.

2.2.2 Materials

A remark is made regarding the floating offshore structure construction materials. Special interest has been placed on the benefits and disadvantages of each of them. Resistance, durability, cost or scalability are taken into account as important factors.

As a better way to organize information related to material usage, it is convenient to divide the floating support structure into different parts, according to its basic properties. Namely:

- Floating Substructure
- Tower
- Mooring
- Anchors

The floating substructure and the tower are the two main components that form the floating wind turbine structure. The tower extends from a defined elevation above the water level to just below the generator. The substructure comprises the rest of the structure. In some designs, a differentiation between the two parts might not be possible [25].

In Figure 7 the main material components of a floating offshore wind turbine are plotted over the scheme of a spar buoy type substructure.

Steel and concrete are the main materials that can be found on these wind turbine parts. A quick view among existing offshore structures concepts and designs states the predominance

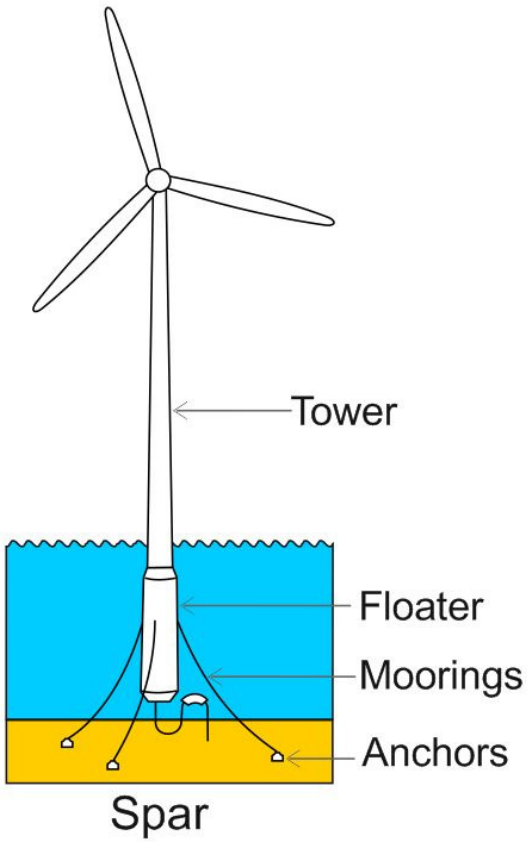

Figure 7 Material components of a floating offshore wind turbine.

of steel usage. Other materials as stainless steel are also employed on singular parts where its corrosion resistance properties are needed, such as difficult maintainable members.

2.2.2.1 FOWT Steel Structures

The use of steel is extensive to all kinds of structures. Offshore industry has specially taken profit from its benefits. High strength and easy complex geometries shaping can be outlined. Distinctively, a high resistance to weight ratio eases offshore logistics operations, where the complications of using cranes and transport vessels increase.

Nevertheless, steel presents a big disadvantage that influences the design life and the cost of the structure: low corrosion resistance. This steel property becomes substantially harmful on offshore environments, where the presence of attacking agents is much higher. Although it can be battled and prevented, the cost increase is inevitable. Regular maintenance, cathodic protection or coatings are some of the possible expensive methods that can be used.

Additionally, steel manufacture needs of an intense quality control and highly specialised work force during manufacture. The addition of fatigue processes consequences, very significant on offshore steel structures, in combination with the corrosion sensitivity mentioned above, is also a remarkable disadvantage.

2.2.2.2 FOWT Concrete Structures

The benefits of concrete as structural material stand out on marine and offshore environments. It presents a high resistance to corrosion and erosion, providing high durability results. WindCrete concepts takes advantage of these properties on its proposal [12].

Historically, concrete has been widely used on marine environments, especially on harbours. The first experiences of its usage on offshore structures dates back to the 70s, when the oil & gas industry, which traditionally used steel, saw a profitability source on the minimum maintenance cost of concrete.

At present, it has proven to be a reliable and fully functional material. Its durability expectations have been extensively proven to be true. In this regard, a study conducted on the 80s, confirmed its full operational safety and the protraction potential of its design life [26]. That study was based on data gathered from the first maintenance and repair reports of concrete offshore structures, which were constructed using a very limited concrete knowledge and technology. Even so, a lifetime greater than 60 years was expected for most of them [26] [27] [28].

In spite of having a much better durability behaviour than steel, concrete presents some concerns in this sense that can affect its design life. These problems are mainly originated by reinforcement corrosion, mainly related to chlorides; and by the reactions between aggregates and hydrate cement, which are produced inside the concrete internal structure [29]. Erosion problems may also be present, for which sharp edges will be preferably avoided on the design.

The solutions to concrete durability problems are assorted. A strict quality control during the concrete production [26], protecting the reinforcement bars using cathodic systems or epoxy coatings [30] [31], or even using stainless steel reinforcement bars are some of the possible solutions. In any case, durability increase through one of these methods or any other additional ones will suppose a rise on the total structure cost.

Nowadays, concrete technology has suffered a very intense development. A compressive

strength higher than 100 MPa and a permeability below 13 m/s can be easily reached [27]. In the same way, concrete mixtures have also advanced significantly, being able to respond to the durability related cost optimization desire of the offshore designs. Most of them take profit of low water – concrete ratios (below 0.4), a high reinforcement cover (over 100 mm), or the use of additions (silica fume, slag, etc.) [32]. Despite these advances, extraordinary measures to ensure durability as the ones described before will have to be adopted as well.

Other concrete typologies such as fiber reinforced concrete and light weight concrete, whose development is very young, present interesting properties which can be beneficial on a marine environment. Design processes should take into account the possibility of its use.

2.2.3 Mooring Systems

Mooring systems are an essential component of floating offshore structures. Stability, movement control and, of course, structure anchorage, are some of its purposes. Moorings will need to be adequately designed, taken into account that its behaviour will depend on the floating structure characteristics. Functional criteria, that ensure a good behaviour of the total structural ensemble; and strength criteria, that guarantee an enough resistance to resist the present loads applied both over the floating part of the structure and over the mooring system itself, need to be taken into account when designing.

Traditional offshore mooring systems, such as chains or wire ropes, have been progressively substituted by more advanced systems which try to be cost effective, due to the expansion of the industry to deeper waters. The need for cost optimization on floating offshore wind turbines appears here as an extra factor to this evolution.

Nowadays, the existing types of mooring systems can be distributed in two groups:

- Steel catenary mooring
- Synthetic taut mooring

Steel catenary moorings base the reduction of motions on the counteraction of the mooring lines' self-weight. This behaviour determines its characteristic shape once deformed, called catenary, which change its position with respect to the seabed when the structure drags the lines. Steel is the main material used due to its contribution to self-weight.

Three parts can be distinguished on a mooring line, namely:

- Fairlead (upper zone, connection to the structure)
- Intermediate zone
- Bottom zone (connection to the anchor)

Each zone has some service demands which determine the type of steel mooring used on them. In this regard, chains are used on the bottom and upper zone, where erosion and corrosion respectively make it necessary for the mooring to present a higher resistance in those terms. Steel wires are commonly used on the intermediate zone, where erosive and corrosive actions are not a problem but displacements and deformations that can lead to fatigue complications are important [15]. Stud-link and stud-less chains are used all along with different kinds of steel wires, depending on its final structural requirements.

Synthetic taut mooring are often used on deep water applications. They present advantages in regard to its low weight, flexibility and resilience; which make them convenient to absorb large imposed dynamic motions. Reduced seabed footprint and easier transportation due to smaller weight can be found among its extra advantages. Nylon, kevlar, dacron or ploypropylene are some of the materials used on this kind of moorings. They offer high corrosion resistance, great strength to immersed weight ratios and a large service life [15].

Nevertheless, its complexity and an early stage material technology lead to conservative design which prevent from taking their maximum profit in order to guarantee safety [15]. Degradation due to fish bites and plastic flow of the fibres are some of the other problem that this type of mooring face.

Besides these two mooring system technologies, there exist some other developments which are worth to mention, resulting from the high depth requirements of some of the floating concepts of the oil and gas industry. Hollow cylindrical links (HCL) were created in this regard. They increase the strength to immersed weight ratio by adding buoyancy, which counteracts the internal high tensions created by the self-weight. Usually, they are made of pinned links which dispose of an internal buoyancy chamber [33]. Application on floating offshore deployments might not be necessary on a mid-term, taking into account previsions on this regard. In any case, it might be interesting to be conscious about its existence and behaviour in order to conceive further optimization developments and to confront future designs on larger water depths.

Finally, a remark on anchors is made. Anchors must ensure the correct behaviour of the

mooring system by resisting forces applied on them without varying its position. Three types of anchoring system are commonly used on offshore installations:

- Embedded anchors
- Suction piles
- Self-weight anchors

Embedded anchors and suction piles are usually made of steel. They are directly connected to the seabed and ensure attachment by transmitting its forces to the seabed using different connection systems. In the case of self-weight anchors, they oppose acting forces only taking profit of gravity force. A good balance between material volume cost and density must be found, which usually results into the use of concrete, much more competitive in this sense than steel.

The choice of anchors must be done taken into account the characteristics of the floating structure which they support, and the properties of the mooring system itself. Normally, it is preferred to use high specific weight moorings to obtain smaller anchor systems, which tends to result in a more economical solution. On those other cases where a self-weight anchoring is cheap due to the low cost of concrete, or due to the high availability of dredge material that works as ballast, designs tend to use these kind of fixation systems [33].

2.2.4 FOWT Technology Development Tendencies

Floating offshore wind turbines technology is expected to evolve until it becomes an established cost-competitive technology, being able to serve as an alternative for fixed solutions on almost every possible location.

As a new technology still being developed, there are many challenges that the different floating concepts will have to face [34]. Some of them stand out among the others. On one hand, modelling systems and computational tools will have to be developed in order to adequately validate floating concepts, for what interaction between the aerodynamic and structural behaviour will be very important. On the other hand, the concepts will have to respond to the competitiveness of the market.

In this direction, the maximum exploitation of the installations based on larger turbines will be basic, which will help to optimize the system. Because of that, efforts on bettering and optimising the interaction between turbine and substructure are needed, all along with the

developing of new materials. In this sense, motions due to environmental loads have to be controlled along with the rotor functioning and energy production enhancement. Finally a last factor that will condition floating offshore deployment is the connection to the grid. To the difficulties related to distance from shore and network connection availability, the technical problems caused by cables in movement due to the non-perfect stability of the structures must be added [6].

The design of FOWT must be framed in the context of a new technology incipient developing. At the moment, there is no standard design process established.

There are some FOWT design specifications, which are usually adapted from the oil and gas codes. Those specifications offer disperse and general instructions, mostly relating to other codes and recommendations, and maintaining a high level of uncertainty for the wind turbines design singularities [15].

According to this technology development situation, some authors have proposed a milestone list to be fulfilled on the proposal of a conceptual design. Henderson [14] makes the following proposal:

- Comprehensive modelling capability; design and optimization of the complete systems including loads, motions, controllers and performance.
- Development and demonstration of reliable installation and repair procedures.
- Demonstration of a successful grid-connected prototype.

In the same context of previous studies, publications have been made exposing the expected main factors that will condition the design of a floating offshore solution. On a general field, Chakrabarti [15] refers to:

- Weight control and stability as key drivers
- Dynamic response governing loads on mooring and equipment
- Fatigue
- Environmental conditions on special areas
- Installation
- New materials

In regard to more specific FOWT conditioning factors, Henderson [14] states:

- Wind turbine thrust and wave loads, as dynamic loads governing among the actions.
- Deviations of the turbine position with respect to the wind directions, due to longitudinal spin (yaw) of the support structure.
- Cost, as a great importance driven factor.

On a similar way, the authors make predictions for the design of a spar-buoy floating concept solution, which results in high interest due to the typology coincidence with WindCrete.

Referring generally to spar floating solutions, Chakrabarti [15] considers important aspects to take into consideration:

- Maximum weight
- Deck eccentricities
- Small pitch motions, even for extreme events
- Simplifications on installation process
- Vibration mode period of vertical movement (heave) much greater than the peak storm period.

The same author defines the following parameters as key for the hull sizing:

- Diameter
- Fixed Ballast
- Draft
- Fairlead Elevation

In regard to the actual challenges that a spar-buoy design faces, Henderson anticipates:

- Control of the spar-buoy structure size
- Tower (upper part of the structure) strengthened enough to contend bending moment and motion of the heel
- Assembly of the wind turbine on to the spar.

2.3 FOWT Simulation

2.3.1 Introduction

FOWT simulations pretend to model the behavior of the wind turbines in order to obtain its response in different real conditions. A numerical code solving a series of adequately selected equations that answer to the physics of the turbine are applied over input data defining the structure geometry, properties and loads.

A representative simulation allows to design cost effective floating wind turbines while assuring its performance and structural integrity [24].

The simplified scheme on the most important parts of a FOWT simulation would consist of an ensemble of physical processes which mostly represent environmental phenomena. The modeling of the structure consists on the representation of each of these through its own scheme, which are later combined on the global scale. Therefore, a normal FOWT simulation is usually divided in the modeling of its different physical subsystems all along with its interaction.

Different modeling equations, concepts and theories; with a wide range of possibilities related to reliability, input data considerations and computational cost; can be found on each of those parts.

In general terms, a complete simulation would involve a numerical tool that is labeled as aero-hydro-servo-elastic. Aero and hydro refer to the incorporation of aerodynamic and hydrodynamic models, servo to the inclusion of the wind turbine control system effects, and elastic to the assumption of a dynamic structural response on small deformations. The term *fully coupled* may appear as well, determining the consideration of the complete interdependence among the outputs and inputs of each of the mentioned subsystems [24].

An overview of the state of the art on the technical simulation of floating offshore wind turbines is presented in this section.

2.3.1.1 Degrees of Freedom, Global Coordinates.

A remark is made here regarding the categorization and nomenclature of the degrees of freedom which are used in the simulation and design of a floating wind turbine.

Given its simplicity and effectiveness when working on them, the in Figure 8 presented

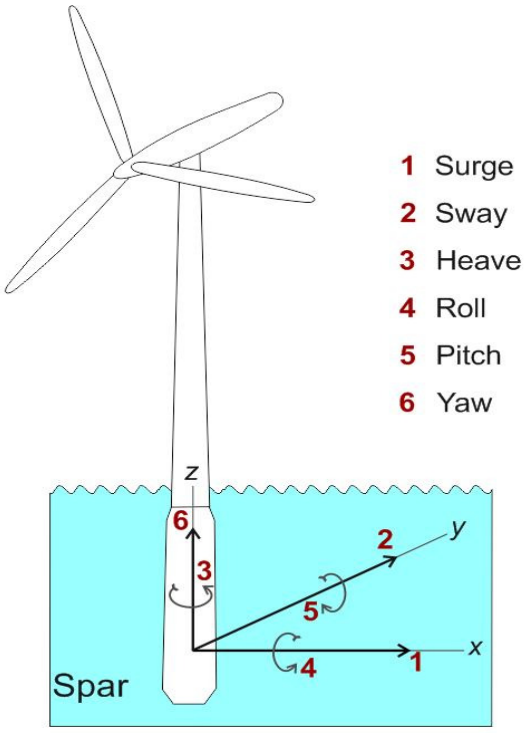

Figure 8 Nomenclature of the degrees of freedom of a floating structure.

degrees of freedom system, is the most employed. A name is given to each movement, namely displacement and rotation, over each global coordinate reference system axis. It will be used along the developments of this thesis, for what is interesting to have it present.

2.3.2 FOWT Subsystems, Loads Simulation

A complete list of the physical subsystems which participate on the global wind turbine model are listed next, including a special mention on those which contain processes that will be modelled as loads.

- Hydrodynamics (incl. wave loads and currents)
- Aerodynamics (incl. wind loads)
- Structural Dynamics
- Control System (incl. rotor loads)

A schematic representation of them has been included in Figure 9.

The main loads acting on a floating offshore wind turbine, as can be found in the literature,

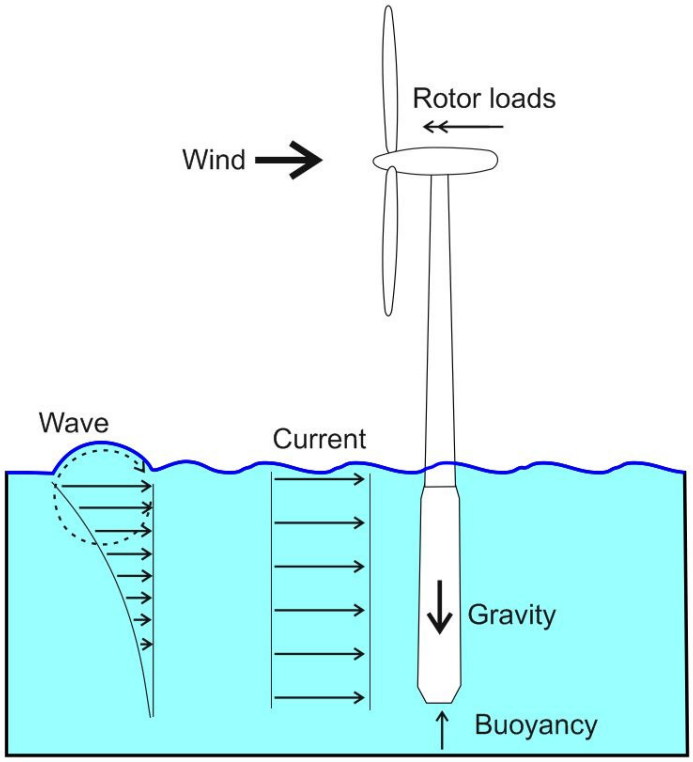

Figure 9 Basic loads which describe the mechanical behaviour of a floating wind turbine.

are included in the over detailed list [24] [13] [15] [35]. Extraordinary loads, which would only be necessary for a verification phase on a detailed design level such as earthquake or ice have not been included, leaving the list for the most important actions that help explain the behavior of the FOWT system.

In order to obtain a better insight on the interacting loads of the floating typologies, a comparison with onshore placed turbines can be made. Those include gravity, wind inflow and inertial loading due to the turbine movement would refer to identical physical processes. Plenty of references and experience exist on the modeling of these loads [25]. The inclusion of the wind turbine on an offshore environment involves the consideration of additional actions, mainly related to hydrodynamic loading, but also incurred by possible floating debris or sea ice. Finally, it must be outlined that the consequence of a floating offshore design results in the necessity of simulating the dynamic coupling between motions of the structure and the variation of the present loads, conditioned by the interaction with the mooring system.

Different considerations can be done when simulating the applied loads. The complexity of some of the actions make it necessary to model them using simplified theories, which differ on complexity and reliability, and which may be more or less adequate depending on the type of analysis.

In the case of floating offshore wind turbines, it is especially necessary to characterize adequately wave loading and the hydrodynamic structural response. In this regard, it is important to remark the selection of an adequate wave theory to simulate the water kinematics, and the possible inclusion of hydrodynamic effects such as diffraction and radiation.

In the next sections the state of the art possibilities regarding the modelling of each of these physical subsystems and its related loads are detailed.

2.3.3 Hydrodynamics

The modelling of the interaction between the structure's movement and the water body requires the definition and implementation of its own model. The hydrodynamic subsystem will contemplate all the loads, forces and kinematics on the structural system caused by its interaction with the water body, the ocean in this case.

It is necessary to understand and have in mind the most important properties of such a model and the parameters that represent it

2.3.3.1 Hydrodynamic Modelling Approach

The hydrodynamic simulation has to be able to represent the mechanical behaviour of the particles of the water body and, which is even more important, its interaction with the structure. Therefore, it will be crucial to take adequately into account the structural dynamic behaviour as well, given that forces and displacements of water particles and the structural body will depend on each other.

Such a complex problem can be simulated in many different ways, all of them based on approaches which try to simplify the resolution process through different engineering procedures.

A very common approach in this regard, is based on the employment of two different approximations to the hydrodynamic processes simulation, which affect different subsystems.

First, the determinants on the structural dynamics subsystem generated by the body of water in which it is contained are modelled. The hydrodynamic properties of the system in which the structure tries to displace itself will condition the mechanics of the structure. Second, the

modelling and description of the kinematics inherent to the sea water particles, produced by natural phenomena such as wind and waves, and its interaction with the structure in form of loads.

Further details on the conceptualization on this modelling approach are next presented, through the characterization of each of the two separated simulation parts.

2.3.3.1.1 Structural Dynamics Characterization

The dynamics of the structure will be simulated taking into account all the response forces which the structure suffers given its movement inside water. Different processes and phenomena are considered and modelled. Some insight on the theoretical tools used are given next.

The main phenomenon controlling the hydrostatics of a body inside a body of water it is the Archimedes' Principle, which helps understanding the forces interacting on the structure stability. A hydrostatical approach considers the forces and moments acting on the structure to be in a stable system. If those forces and moments do no present equilibrium, the system will try to conduce the structure into an equilibrium state.

On the instants where no equilibrium is reached, the structure will suffer displacements. These will be conditioned by the kinematic and dynamic interaction of the structure and the water body. The dynamics of the water displaced by the structure movements will be conditioned on the structure kinematic properties at each time instant, which at the same time will depend on the forces produced by the water body as a reaction to the structure which tries to displace them.

Modelling this phenomena is usually tackled from the structure dynamics point of view, taking into account the determinants inherent to its displacement on a water body. The simulation of this interaction is usually made through added mass coefficients, determining the contribution to the inertial movement produced by water; and damping coefficients, referring to the forces which will react to its displacement. Reference to the modelling and quantification of these phenomena can be found along this section.

2.3.3.1.2 Ocean Hydrodynamics Modelling

Ultimately, the mechanical ocean behaviour modelling translates into the simulation of the two main phenomena which determine the natural movement of water particles, namely waves and currents. It is necessary to model its kinematics in order to characterize the forces that will be applied onto the structure.

Models presenting different considerations and levels of reliability are employed for this endeavour. Given the studied structure, the hydrodynamics needs to be simulated on an oceanic fluid model with free surface boundary. In this regard, most of the current analysis are based on potential flow theory.

Potential flow theory assumes incompressible, inviscid and irrotational flow. An algebraic equation, based on free-surface and seafloor boundary conditions, models the dynamic pressure field over depth, which results of the spatial integration of the velocity potential. It provides acceptable results at a much more reduced computational cost than computed fluid dynamics based models, like the Reynolds averaged procedures.

The possibility of using similar but more advanced models exist as well. Those can include the consideration of non-linear waves through higher order fluid mechanics model, which are usually employed to describe the interaction on severe sea states or breaking-wave conditions.

Once all the actions over the structure are modelled and quantified, the resultant fluid structure interaction forces are computed. This process is generally taken to term via an integration of the static and the dynamic pressures over the submerged surface, for which several procedures are available. Those are classified according to the considered fluid structure coupling when computing the flow field around the floating body.

Commonly, industry related computations, tend to compute the flow field generated by the model independently from the floating body. This implies the necessity for a correlation of the fluid particle kinematics to forces, for which empirical parameters are used.

The most known and used approach in the regard of computing forces from wave fluid flow kinematics are the Morison's equation, which takes into account viscous damping and the contribution of an acceleration dependent added mass [36]. The Morison's equation, despite being configured for its application on slender, cylindrical, fixed-bottom structures, can be applied as well to floating slender cylinders, as the one object of our study, with a relative formulation [37]. Many computation tools for the calculation of FOWT, such as the HAWC2, take profit of this procedure

A further approach in this regard, used by many codes, is based in the separation of the analysis in two types of problems. On one side, a diffraction problem, based on the hydrodynamics of a standstill structure with exciting incident waves; and on the other, a radiation problem, fundament on an oscillating structure at still sea. Therefore, the influence of the moving body over the flow is taken into account when modelling this way. Wamit, Ansys Aqwa or Sesam take profit of this approach to compute the hydrodynamics load, which can be used later on an aero-hydro-elastic FOWT simulation code like fast.

2.3.3.2 Hydrostatics

The very first approach that needs to be considered on the simulation of a floating system is the one regarding its hydrostatic properties. Hydrostatics study the static equilibrium of a partially or totally submerged body.

They form a very important base on the floating structures design as long as the forces that participate on the rest state of the structure will be as well the main actions governing the structure mechanics before reaching the equilibrium state, and therefore, will be essential for its appropriate conceptual design.

The main phenomena regarding hydrostatics, and consequently the general hydrodynamic interaction of a floating system, is the Archimedes' principle of buoyancy, for which there exists an upwards force called buoyancy acting on the centre of gravity of the portion of a body's submerged in water, with a value equal to the weight of the volume of water displaced.

The inclusion of the Archimedes' principle on a dynamic problem is modelled through the computation of the so called restoring forces, which are the forces and moments which act on the structure trying to bring it to a static flotation state.

These forces and moments must be defined according to a position for the combination of interacting hydrodynamic forces at each time instant. Usually a still-water level point inside the structural body is used, which will provide intuitive information about the structure's dynamic behaviour.

It is interesting to get a deeper insight on the interacting hydrodynamic actions that will form this matrix to understand the physical background of this system. A calculation on the previously mentioned still-water level point would provide a series of translational and rotational

restoring actions.

Translational restoring is normally only existent on the vertical direction, as long as horizontal movements are usually zero. It is the result of the integration of hydrostatic pressure under the submerged volume. Rotation restoring is the results of the action of three different causes. First, the so called water plane area effect, for which the additionally elevated or additionally submerged volumes of the structure tend to reach its equilibrium static position. The cross sectional shape perpendicular to the axis of rotation is the main parameter conditioning this phenomena, and therefore an important design factor for the structure. As a second contributor to the restoring forces, the moment generated by the buoyancy force on the submerged body can be found. This force will be acting on the geometrical centre of the submerged volume. Finally, the last contribution action is provided by the moment correspondent to the weight of structured, computed on its centre of gravity.

A good hydrodynamic design of the structure tries to maximize the stability of the structure, which will be determined by the projected geometry. A determinant parameter for the stability in this sense is the distance between centre of gravity and centre of buoyancy, also called metacentric height.

The equations governing these restoring forces are presented next.

2.3.3.2.1 Hydrostatics Equations

The main concept regarding hydrostatics is the Archimedes' principle. As a basic previous procedure it ensures the correct flotation given its properties and the desired draft [38], being it the vertical distance between the waterline and the bottom of the hull. On TLPs applications, it also provides the resultant force to be supported by the moorings. The Archimedes' principle equations is given next.

$$F_b = V \cdot \rho$$

Where F_b is the buoyancy force, ρ is the fluid density (around 1025 kg/m^3 for sea water) and V is the structure's submerged volume.

Structural stability on the design of a floating structure is ensured when the distance between the centre of buoyancy (geometrical centre of the submerged part of the body) and the structure bottom is bigger than the distance between this last point and the centre of mass of the structure. This position relation, which also must take into account the effect of the restoring

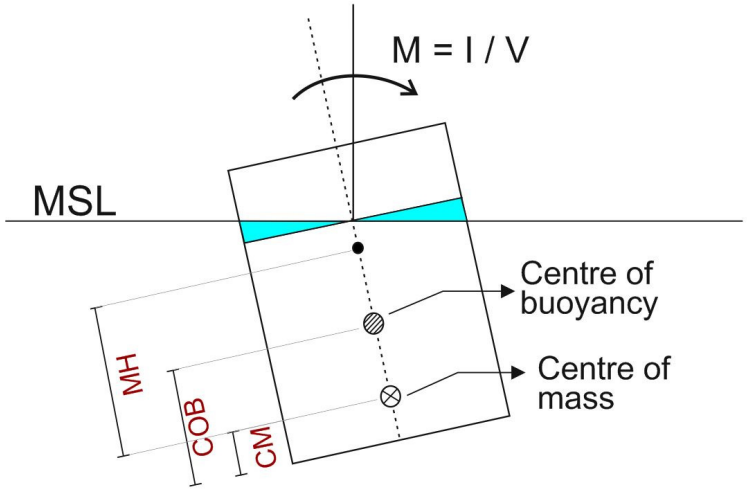

Figure 10 Graphical representation of the main geometrical parameters defining hydrostatical stability.

moment due to water plane area, is called the metacentric height.

The next equation and Figure 10 exemplify this behaviour.

$$MH = COB - CM + \frac{I}{V}$$

Where MH is the metacentric height, COB is the centre of buoyancy and CM is the centre of mass. The term I/V makes reference to the water plane area restoring moment contribution, being I the second moment of area of the structure cross section and V is the displaced volume.

In Figure 10 a floating structure in form of parallelepiped can be seen. The main stillwater level correspond to the MSL acronym. Its centre of buoyancy and centre of mass are indicated. According to the over stated equation, the base distance of the centre of buoyancy (COB) minus the base distance of the centre of mass (COM) plus the water plane area restoring moment, will define the metacentric height (MH), which is graphically represented through the distance between an untagged point and the centre of mass.

The relation between the parameters that contribute to the metacentric height determine the floating structure type. Spar structures present a negligible water plane restoring moment, and ensure a large metacentric height through a low centre of mass thanks to ballast fill. On the other hand, semisubmersible and barge structures may have a centre of mass above the centre of buoyancy, but its large restoring water plane moment ensures stability.

The relation between relative displacements of the structure and the correspondent hydrostatic force response is commonly given through the hydrostatic stiffness matrix. It is a 6x6

matrix regarding the forces and moments in each degree of freedom with the rest of degrees. When only hydrostatics is considered, and no external restraints such as mooring lines are modelled, coefficients related to horizontal displacements (surge and sway) and vertical axis rotation (yaw) are zero, reason why this matrix can also be presented on a 3x3 form.

Further detailed equations describing the previously described interactions along with a more detailed explanation can be found on the literature [39].

2.3.3.3 Added Mass Coefficients

Fluid mechanics states that an accelerating or decelerating body inside a fluid causes the movement of the surrounding fluid, given the body and the fluid cannot occupy the same space at the same time instant. In this situation, the fluid suffers acceleration in all the degrees of freedom, behaving on a very complex way.

In a simplified way, this phenomenon can be modelled as a certain mass of fluid moving with the body, which takes the name of added mass, and are represented through added mass coefficients on the second Newton's law. This equation is presented next. Mass term results into dynamic mass term, which is the sum of standard mass and added mass. It is represented through a matrix which relates acceleration and force, with size 6x6 given that it represents all degrees of freedom.

$$\boldsymbol{F} = \boldsymbol{m_v} \cdot \ddot{\boldsymbol{x}} = (\boldsymbol{m} + \boldsymbol{m_{added}}) \cdot \ddot{\boldsymbol{x}}$$

Where $\boldsymbol{F}$ is the forces vector, $\boldsymbol{m_v}$ the dynamic mass matrix, $\ddot{\boldsymbol{x}}$ the accelerations vector (second derivate of position with respect to time), $\boldsymbol{m}$ is the structural mass and $\boldsymbol{m_{added}}$ is the added mass matrix.

The added mass coefficients are dependent on the movement's frequency of the structure and the structure geometry among others.

2.3.3.4 Structural Damping

A mechanic system formed by a body inside a fluid subjected to dynamic excitation presents many different types of damping, generated by different sources. These damping sources can be categorized in three different types: viscous damping, radiation damping and

mooring damping.

Viscous damping is generated by the friction between the water particles and the structure's surface in contact with water. Its quantification is not trivial, implying the combined use of computational fluid dynamics numerical tools to obtain a first approach and scale model testing for a final calibration, which will need to be carefully extrapolated. Its calculation for slender bodies tends to be easier, as long as a great portion of it results from flow separation, which can be well modelled by the Morison's equations.

Radiation damping is produced by the radiated waves which are generated by the relative motions between fluid and structural body on structures with large dimensions compared to the wave length. Nevertheless, for floating structures it tends to zero.

Mooring damping, which is generated by the interaction with the mooring lines, becomes a great importance. Mooring, despite being designed on a limited sway and surge motions basis, has a large influence on roll, pitch and heave motions.

2.3.3.5 Wave Forces

The modelling of the system's interaction between fluid and structure includes different aspects which must be taken into account.

A complete model considering all the important factors and interactions, could be reached through sophisticated computational fluid dynamics systems. Nevertheless, simplifications of those are often used given its good results and the in comparison low computational cost. In this sense, linear potential flow theory, which has proved to give good results is usually applied.

Linear potential flow theory assumes no contribution of friction. Using it, a two parts problem approach appear. On one side, the radiation problem, which considers the waves radiated by the floating oscillating body; and on the other, the diffraction problem, which by assuming a fixed body, models the incident waves encountering it.

A different and classical approach to the modelling of the fluid structure interaction is the use of the Morison's equations, a semi-empirical method with a now large number of applications and tests. These equations associate the fluid structure relative velocities and accelerations on every depth with a correspondent force. Morison's equations account for the hydrodynamics using an added mass coefficient as explained on previous sections.

This approach faces the problem by modelling a radiation problem, as the ones explained in the previous paragraph, with some particularities. Radiation damping and radiated waves re-coupling are neglected. However, viscous damping is empirically accounted.

Each of the presented ways to face the problem have their own application regimes. Morison's equations are valid for problems where flow separation is of importance, losing its validity when diffraction becomes important. The capability of each of the methods to model properly a global system is also referenced through dimensionless parameters, such as the diffraction limit, which relates the diameter of the structure and the wave steepness; or the viscous limit, relating water depth and structural diameter.

For the structure studied in this thesis Morison's equations appear as the best possible tool.

Next the Morison's equation is explained and detailed. On a first section, its theoretical background is presented, which is based on the study of the interaction forces between fluid flow and cylinder. On the then upcoming section, the parameters and components of the Morison's equations are definitely explained.

2.3.3.5.1 Fluid Flow – Cylinder Interaction Forces Modelling

The modelling of the hydrodynamic loads on the tower can be simplified to the force that a cylinder receives due to fluid flow, which is a common problem which has been widely studied. The main characteristics and relevant aspects of the proposed solutions are presented next.

A fundamental parameter used by these solutions is the so called inertia coefficient C_M, a non-dimensional parameter which finds its origins on the first hydrodynamic approaches during the end of the 19th century consisting of theories contemplating ideal inviscid flow. The inertia coefficient relates the force per length unit that is required to keep stationary a rigid cylinder in a fluid with uniform and constant free stream acceleration. These relation is stated on the next equation.

$$\overline{q_1} = C_M \cdot \rho \cdot \pi \cdot \frac{D^2}{4} \cdot \dot{u}$$

Where $\overline{q_1}$ is the force per unit length, C_M is the inertia coefficient, ρ is the fluid density, D is the cylinder diameter, and $\dot{u}$ is the constant free stream acceleration.

The inertia coefficient is related to another non dimensional parameter which results of great interest for the hydrodynamic modelling, the added mass coefficient C_A, through the next expression.

$$C_A = C_M - 1$$

Theoretically observed from the above given expressions, the inertia coefficient C_M is directly dependant from the relation between the cylinder's length and diameter, reaching a value of 2 for cylinder lengths much larger than the diameter. In this sense, for a spar geometry like the one of WindCrete, the difference between length and diameter can be considered to be large enough to approximate the inertia coefficient to 2, and therefore the added mass coefficient to 1 [38].

A further related interesting parameter is the frictional drag coefficient C_D on viscous modelling. It related the force per length unit necessary to hold a fully immersed cylinder subjected to a constant free stream fluid velocity, as given by the next expression.

$$\overline{q_D} = C_D \cdot \rho \cdot \frac{D}{2} \cdot |u| \cdot u$$

Where $\overline{q_D}$ is the force per length unit, C_D is the frictional drag coefficient, ρ is the fluid density, D is the cylinder diameter, and u is the constant stream fluid velocity. Absolute value use on one of the right side velocity u terms ensures a force $\overline{q_D}$ that will be always opposing the stream direction.

The frictional drag coefficient has proven experimentally to be related to cylinder roughness and the Reynolds number. It presents values around the unity when the Reynold's number is in the range between 1 000 and 200 000.

Another parameter worth mentioning is the lift coefficient C_L, which would add the effects of a non-circular cylinder, or a rotating one about its axis, to the relation given on the previous stated equation. The lift coefficient, which can be neglected on a problem based on the spar geometry, would be dependent on cylinder roughness, Reynolds number and objects nearby proximity.

Finally, the Keulegan-Carpenter number K_C is presented. Given the case of neither u or $\dot{u}$ constants, but characterized as the result of a single simple plane wave of time period T, a relation between this wave and the forces applied on the cylinder can be established by means of the Keulegan-Carpenter number. The equation defining this correlation is next presented.

$$K_C = \frac{u_0 \cdot T}{D}$$

Where K_C is the Keulegan-Carpenter number, u_0 the amplitude of the wave velocity, T the period of the wave, and D the structure diameter.

2.3.3.5.2 The Morison's Equation

A simple method for the computation of the forces on a cylinder under uniform flow has been presented. Nevertheless, a real hydrodynamic system presents further important phenomena which are not modelled through the previous equations. A commentary in this sense is made next, relating to the periodic wakes or vortices that may form the stationary cylinder.

These vortices behind the cylinder detach alternately on both sides, following a characteristic frequency, which also determines and accompanying top to bottom pressure fluctuation.

A non-dimensional parameter correlating vortex frequency, structure diameter and flow velocity is defined. It takes the name of Strouhal number. Its equations are presented next.

$$S = \frac{f_S \cdot D}{u}$$

Where S is the Strouhal number, f_S is the vortex alternation frequency, D is the structural diameter, and u is the flow velocity.

These kind of vortices occur for values of Reynolds numbers in the range of 60 to 100 000. Inside this range, the Strouhal number is well correlated as well with it [40].

It is important to assure that the periodicity of these vortex cannot generate any damage due to resonance on the structure. Past experiences have shown the destructive power of these vortices. Estimations on the design phase can be done, as well as geometrical surface modifications on the structure to avoid its creation [15].

The Morison's equation [41] provides the total time varying load per length unit on a stationary cylinder subjected to plane flow field with free stream velocity, by combining the equations described in the previous paragraphs which relate to frictional drag coefficient and inertia coefficient. The resulting formulation is presented next:

$$\bar{q} = C_D \cdot \rho \cdot \frac{D}{2} \cdot |u| \cdot u + C_M \cdot \rho \cdot \pi \cdot \frac{D^2}{4} \dot{u}$$

Where the parameters involved follow the same references as in the previous equations.

The equations was first proposed by Morison as the conclusion of a series of empirical studies, and is therefore named after him. Nevertheless, a theoretical base has been given to it, stating that it can be deduced from the principle of conservation of linear fluid momentum conservation.

The determination of the values of the drag coefficient C_D and inertia coefficients C_M presents different approaches. Many databases exist where they are valued as a constant depending on a series of factors [15]. Nevertheless, further research has attributed a new dimension to these parameters by proving its constant behaviour false. Studies over periodic plane flow, which introduces a similar effect as the one of waves, have shown a dependence of both parameters on the Reynolds number, the Keulegan-Carpenter number and the cylinder roughness.

The theories and formulations presented up to here have been introduced in the context of a fixed cylinder. For floating structures, such as the one object of this thesis, some adaptation on the formulas are needed.

The cylinder movement has to be taken into account, both translation and rotation, providing a good characterization of the absolute displacements all along the structural longitudinal axis. In order to ensure the effectiveness of the Morison's equation, relative velocities between structure and water particles must be as well taken into account. The resulting equations is presented next:

$$\bar{q}(z,t) = C_D \cdot \rho \cdot \frac{D}{2} \cdot |u(z,t) - \dot{v}(z,t)| \cdot (u(z,t) - \dot{v}(z,t)) + C_M \cdot \rho \cdot \pi \cdot \frac{D^2}{4} \cdot \dot{u}(z,t)$$

Where the main parameters take the same nomenclature as the ones on the previous equations, $\dot{v}$ is related to the velocity of each point on the cylinder, and z is the longitudinal axis coordinate.

As a final remark, it is worth mentioning that the good employ of these equations will need of a correct input of the water particles velocities, which has its own modelling requirements. As a previous step to it, it is important to know which phenomena will determine this velocity. As for the application of the works performed in this thesis, waves and currents will be the two important sources, resulting the necessary input velocity on the water velocity due to wave and

the one originated by currents. The next equation states this concept mathematically.

$$u(z,t) = u_{waves}(z,t) + u_{current}(z,t)$$

2.3.3.6 Waves Kinematics

As mentioned before, the calculation of the incident wave and current loading over the structures surface needs of the water velocity input, for which a model of the wave's kinematics is needed.

There many wave kinematic models established, answering to different hypothesis and presenting different levels of reliability.

The Airy wave theory, which is the most basic of the theories, is based on the linear description of the waves. Its main equation is a Laplace equation that takes the form presented next.

$$\frac{\partial \varphi^2}{\partial x^2} + \frac{\partial \varphi^2}{\partial z^2} = 0$$

$$\varphi = \frac{g \cdot H \cdot T}{4 \cdot \pi} \cdot \frac{\cosh\left(\frac{2 \cdot \pi}{L}(z+d)\right)}{\cosh\left(\frac{2 \cdot \pi \cdot d}{L}\right)} \sin\left(2 \cdot \pi \cdot \left(\frac{x}{L} - \frac{t}{T}\right)\right)$$

It describes a closed elliptical motion of the water particles, including a total net transport of mass equal to zero. This neglecting of the net transport mass is a simplification which is not always precise. It can be corrected by the introduction of a current velocity equal to 0.2 knots. It is important mentioning as well that this theory provides only information about water velocities under the mean still level water surface.

The developing of this previous presented equation results into a series of expressions defining the velocities and accelerations, in both vertical and horizontal directions, among other parameters.

These expressions differ slightly depending on its application on deep or shallow waters, given the influence of distance to seabed, which is taken as a boundary condition. A differentiation criterion is set in order to select which set of equations must be used. It is based on the division of water depth over wave length, given that for large enough depths in comparison with wave length, the influence of seabed can be neglected.

The before mentioned expression are included next, being presented on its configuration for deep waters, given that the analysis object of this thesis is only usable on those kind of ocean zones. The water depth – wave length relation for deep waters, and therefore for the next equations, must be greater than one half in order to enable its applicability.

$$\eta = \frac{H}{2} \cdot \cos\left(k \cdot \left(x - \frac{w}{k} \cdot t\right)\right)$$

$$u = \frac{g \cdot k \cdot H}{2 \cdot \omega} \cdot e^{k \cdot z} \cdot \sin\big(k \cdot (x - c \cdot t)\big)$$

$$v = \frac{g \cdot k \cdot H}{2 \cdot \omega} \cdot e^{k \cdot z} \cdot \cos\big(k \cdot (x - c \cdot t)\big)$$

$$\dot{u} = \frac{g \cdot k \cdot H}{2} \cdot e^{k \cdot z} \cdot \cos\big(k \cdot (x - c \cdot t)\big)$$

$$\dot{v} = \frac{g \cdot k \cdot H}{2} \cdot e^{k \cdot z} \cdot \sin\big(k \cdot (x - c \cdot t)\big)$$

$$p = \rho \cdot g \cdot \frac{H}{2} \cdot e^{k \cdot z} \cdot \sin\left(k \cdot \left(x - \frac{w}{k} \cdot t\right)\right)$$

Where η is the wave profile height, u and v make reference to the horizontal and vertical velocities respectively, $\dot{u}$ and $\dot{v}$ to the accelerations in the same directions, and p to the related dynamic pressure.

Further parameters included in those equations and its definition are included next.

$$c = \frac{w}{k}$$

$$\lambda = \frac{g \cdot T^2}{2 \cdot \pi}$$

$$k = \frac{2 \cdot \pi}{\lambda}$$

$$w = \frac{2 \cdot \pi}{T}$$

Where c is the wave celerity, λ is the wave length, k is the wave steepness and w is the angular velocity.

It is important to see, that after all the proper substitutions, the final parameters that define the wave kinematics are H, defined as the wave height; and T, defined as the wave period.

2.3.3.7 Eigenfrequencies

Another parameter on the floating structure design and analysis is the structural own frequency, in other terms, the frequency at which the structural global system tends to oscillate in the absence of any driving or damping force. Eigenfrequencies assessment is crucial on design in order to avoid resonance problems when similar own frequency and load frequency exist.

Own frequencies can be obtained from the second Newton's law based equation for each degree of freedom independently. The mentioned equation is presented next:

$$F = m_v \cdot \ddot{x} + c \cdot \dot{x} + k \cdot x$$

Where F is the resulting force, m_v the dynamic mass, c is the damping coefficient, k is the hydrostatic stiffness, x is the structure's displacement, and $\dot{x}$ and $\ddot{x}$ the correspondent derivate with respect to time.

The neglecting of damping effects and a new arrange of the previous equation provide directly an expression for eigenperiods evaluation, which is presented next for a single degree of freedom, indicated with the sub index xx.

$$T_{p,xx} = \frac{2 \cdot \pi}{\sqrt{\frac{k_{xx}}{m_{v,xx}}}}$$

It is interesting to notice that the eigenfrequencies here defined differ slightly from those of the classical structural engineering, given that the added mass coefficient will depend on the frequency of the structure's movement, which at the same time is determined by the loads frequency as explained in the previous sections. Therefore, natural periods will depend on the load frequency, for what it will be necessary to understand them as periods with highly amplified loads.

The critical degrees of freedom in the floating structure design are pitch, roll and heave; for which they will have to be considered in the predesign phase.

2.3.3.8 Response Amplitude Operators (RAOs)

Response amplitude operators are a very powerful tool to describe the behaviour of

floating structures embedded on a system. They are a set of engineering statistics that are used to indicate the mechanical behaviour of the floating body in operation. RAOs are presented as transfer functions which as an input become a free-surface elevation, and provide the amplitude variation of different mechanical parameters of the structures as an output.

Its obtaining can be performed through model computations or experimental studies. The structure is excited with plane harmonic waves on progressive frequency sets, for which the resulting amplitudes on the different degrees of freedom of interest are measured.

Ultimately, response amplitude operators are resonance functions, providing clear information about the resonance behaviour of the structure in each excitation mode. In this sense, RAOs provide direct and clear information which is very useful to select the correct geometry of the structure which avoids resonance problems.

In this sense, a previous study can provide interesting data about the resonance behaviour of the structure through the estimation of the RAOs. Response amplitude operators are strongly connected to the eigenfrequencies of the structure. A qualitative estimation of them is therefore possible by regarding the system as a single mass oscillator, with and embedded hydrostatic stiffness, moving on a fluid which is modelled through an approximated added mass.

The conceptual design process of the structure has needed of this estimation in various moments, for which good results can be obtained by conservatively assuming previously defined constant added mass coefficients, making it almost automatic to obtain the structural eigenperiods.

The response of the structure must then be optimized for each of the degrees of freedom of interest. Some guidelines exist in this regard, which focus on the heave behaviour, on one side; and on the pitch and roll optimization on the other. Some remarks about them are made next.

Heave response is mainly dependant on the cross-section of the body at the water level, also called the water plane area of the structure. A bigger surface increases the hydrostatic stiffness of the vertical movement. If the necessity of lowering the resonance frequency exist, so called heave or damping plates can be added to the system, which increase the added fluid mass of the system and avoid the addition of extra area.

The pitch and roll movements are the most harmful ones for the correct service conditions of the wind turbine. As a first principle to avoid it, oscillation frequencies must be compulsory kept away of the resonance zone. In this regard, a big water plane area will increase wave

sensitivity to rotation around horizontal axis. Mass or inertia can be added to dismiss its negative effects, which is usually applied away from the body centre.

2.3.4 Mooring System

An additional subsystem with important implications on the dynamics and the design parameters of the floating offshore wind turbine is the mooring system.

Its precise modelling is not an easy task, and therefore, solutions involving simplifications have been developed. These simplifications can neglect the dynamic effects of the mooring lines, what is not always considered to be a safe approach.

Two main types of approaches on the mooring system simulation are found on the state of the art studies: A quasi-static method neglecting any dynamics effects, and a dynamics finite element or multi body model using Morison's equation. Some of them are in the following lines.

The quasi-static method might be applied in different ways. One of them is the employment of an analytical method. It solves the mechanical mooring system as a static system for each time instant, providing the forces that will be transmitted to the main structure and which will be used in its dynamic computation. This method can take into account the apparent weight of the mooring line in fluid, the elastic stretching of the mooring line and the friction on the seabed anchorage points.

Further approaches compute the mooring line as dynamics system, obtaining a force-displacement relationship which is applied on the main structure by means of a nonlinear spring with the same properties. This method provides similar results to the quasi-static implementation.

The ultimate approach would consist on the coupling of mooring line and wind turbine dynamic analysis codes. Nevertheless, modelling difficulties make it difficult for it to be a consistent and useful solution, leading in most cases to a numerical instabilities.

Another approach worth mentioning, presented by Matha [42], considers a dynamic analysis by dividing the lines into multibody elements, each of them modelled as a rigid or flexible, which are connected by spring-dampers. Hydrodynamic interaction is performed through the application of the forces obtained with the Morison's equation.

2.3.5 Computational Methods

Codes used for the computation of the structure dynamic system are often combined solutions of finite element methods (modal or linear) and multibody system dynamics representation.

It is possible to adapt the different components of the model to the best corresponding analysis method. In this sense, the wind turbine blades are typically modelled on finite beam elements assuming small deflections, while the drivetrain is approached to a linear spring with damping properties.

For the floating structure, a rigid body simulation with six degrees of freedom has proved to be an efficient practice.

2.3.5.1 Structural Simulation Tools

Many commercial programs can be used for the structural simulation of the floating structure. Most of them are based on the finite element method. An example list could include ANSYS, ABAQUS; MSC NASTRAN or PERMAS among other. This codes present a high level of maturity and can be effective used for precise optimization development.

This type of software requires of a high levels of computational demand, reason why often they are not applied as fully coupled simulation tools, being mostly employed for detailed component design after the mechanical behaviour of the structure has been studied and valuated, introducing the existing modelled loads as an input and developing an optimization based on the computed stresses.

2.4 Fatigue Phenomena

Fatigue is defined as the degradation of a material caused by cyclic loading that can lead to material failure, being the maximum value of the load cycle lower than the ultimate resisted load [25]. Collapse of materials due to fatigue is typified by its sudden occurrence.

A deeper insight on this phenomenon leads to fracture mechanics [43]. Fatigue is a consequence of the growth of subcritical cracks. Load repetition contributes to the development and propagation of the possible micro cracks on the element. When the velocity of fissure growth overpasses a certain threshold, precipitated material failure is imminent.

The origin of research on the fatigue phenomenon dates back to the 19th century, being substantially significant the contributions of Wöhler on the 1850 decade. Great developments were performed on the 20th century, being nowadays a current engineering research topic that offers very little and superfluous knowledge.

Since the response of materials subjected to fatigue is complex, and is known to present a diverse behaviour on different materials, it is difficult to give a rigorous qualitative explanation on it. Nevertheless, there is consensus about the main factors that induce a fatigue failure. Fatigue will have special relevance on those elements subjected to large number of load cycles, high stress ranges, and stress concentrations on singular geometric details [44].

Structural design is often not influenced by fatigue resistance, given that a vast majority of the existing structures suffer small load variations on a low number of repetitions basis. The constructions that shall be verified against fatigue resistance is reduced. It includes, among others, slabs subjected to traffic, footings attached to vibrating machinery, support of overhead travelling cranes, offshore structures subjected to wave action and some constructions under special wind loading [44].

Concrete codes only indicate the verification of the so called fatigue limit state on a reduced amount of structural types. In this sense, as an example, the Spanish concrete code EHE-08 suggests which structure may not need fatigue verification [45], and Eurocode 2 provides a list of structural elements that tend to present no need for fatigue considerations [19].

Offshore structures appear on the literature [44] as a weak construction against fatigue. A high number of large magnitude loads (waves, wind, etc.) is present on an environment in which material degradation due to fatigue can become heavily accelerated by a very aggressive environment.

Research on fatigue, from the viewpoint of engineering applications, is set out on a three topic scheme: predicting fatigue life, increasing fatigue life, and simplifying conclusive fatigue tests [20].

Fatigue life of a structural element is limited by that of its weakest member against fatigue, and, in some instances, by its weakest section [20].

2.4.1 Historical Fatigue Review

In this section a brief review about the historical development of fatigue research is presented. Different conceptualizations, theories, points of view all along with its evolution; which may be interesting to be completely aware of the current stage of fatigue research and fully understand available and forthcoming knowledge, are included.

2.4.1.1 19th Century, First Knowledge

The first experiences on the research of the fatigue phenomena date back to 1837, when the first fatigue test results were published. Its author, Albert, a mine civil servant, designed and employed a test machine for the mine conveyor chains which used to break [46]. Its research stood out by the testing of actual components rather than just the material [47].

Further publications on the next years by other authors such as Rankine, York or Morin refer to the study of fatigue processes on railway and mail coach axles. Conclusions and proposals to increase service life and reduce maintenance cost are drawn [48] [49] [50].

The concept of fatigue was first mentioned by Braithwaite in 1854. Its paper described different kinds of fatigue failures such as brewery equipment, water pumps, propeller shafts or crankshafts [51].

The grave consequences of the numerous railway accidents due to axle fatigue collapse on the 1850 decade meant a great impulse on the research, and led to the results and theories of Wöhler, which are the base of today's fatigue knowledge [52]. Having the results of his, research in the 1860s, Wöhler [53] took to term railway axles tests, by means of displacement and forces measurements, while the trains were on service.

The conclusions of Wöhler's research regarded stress amplitudes as the most important

parameter on the fatigue process. He also highlighted the influence of mean stress and crack propagations, and defined the concept of fatigue limit, known as the minimum stress range for which fatigue failure is possible. As final statement, his research concluded that a finite service life must be taken into account while designing. All of these factor and concepts, are recognized nowadays as main factors on the determination of fatigue life.

On the 1870 decade, Ludwig Spangenburg worked on Wöhler's research by plotting the fatigue test results, which were given in tables [54], using a linear coordinate system. These graphics were later transformed into a double logarithmic coordinate system by Basquin [52], leading to the first version of the nowadays widely established Wöhler's curves.

By the end of the 19th century, Gerber and Goodman introduced the influence of the stress level on the fatigue behavior [55] [56]. Both of them presented similar representations of Wöhler's fatige test results taking into account the relation between each, the maximum and the minimum stress, and the ultimate tensile strength.

The 19th century appeared concepts are still used nowadays. The results of the on this section presented authors investigation constitutes the basis of the actual employed methods for fatigue calculation and design. The knowledge basis has remained intact, suffering a very slow development through the years, consisting of particular empirical theories [57] [58].

The complexity of the phenomena, has lead the research to the study of the material microstructure behavior, obtaining the during 20th century developed fracture mechanics fatigue related theories. Those have helped to understand the phenomena, but nowadays still remain on a theoretical stage, being employed simplified theories based on the early fatigue research concepts.

2.4.1.2 20th Century, Fracture Mechanics Development

The research during the 20th century was characterized by the development of fatigue theories and models related to crack behavior on the material, known as fracture mechanics.

Fracture mechanics is the study of the stress and displacement behavior in the immediate region to a material defect (fracture) which propagates along time. The origins of its research date back to Griffith, who in 1921 started investigating the effect of surface straight scratches on the stress response of solids [59]. He introduced a failure criterion based in the material's strain and potential energy.

Griffith's theory stablished the first theory on fracture mechanics, although its investigation results where only valid for brittle behavior on pieces that could be studied on a bidimensional plane, making it unsuitable for most of the materials.

Gough, Orowan, Sack, and Head developed during the 1930s the initial Griffith's theories, making it applicable for ductile materials and tridimensional behaviors. The series of fatigue related studies performed by these authors, reached its highest point with the publication of Head's model for description and calculation of the fatigue crack growth [60] [61].

A big leap forward was performed by the research by studying the cracking processes at an atomic level. Stroh postulated in 1955 that the local stresses on crack could become sufficient high to cause division of particles, after taking to term studies on dislocation's stress fields [62].

The final step on the research for the description of the fatigue behavior through fracture mechanics was performed at the end of the 1950s, leading to the acceptance of the ductility exhaustion theory as a consistent approach to model crack behavior. The studies of Forsyth and Ryder concluded that the crack development was generated by load cycle sequences, instead of discrete size increases caused by a strain hardening mechanism [63] [64]. This results lead to the differentiation of two phases on the fatigue phenomena development: crack initiation and crack development.

The study on this two-phase fatigue crack development was widely studied on the 1960s, putting great efforts on the description of the two stages and the transition between them. Among others, Paris published the first remarkable paper on the topic, introducing a relation between the crack growth rate (infinitesimal increase of the crack width over stress cycle) and the stress intensity factor range (factor which indicates the magnification of the piece's stress on the crack), which would be later developed up to the well-known Paris' Equation [65] [66].

The development of the fracture mechanics related fatigue continued through the development of models based on Paris' postulates. Walker, Forman, Collipriest, McEvily, Miller, Gallagher, Pugno, Zheng and Wang are considered to be the authors whose research stood out.

Despite the rich variety of advances on the description of fatigue behavior through fracture mechanics, wide research was also performed on fatigue without relating it to crack behavior. Many authors developed the existing fatigue knowledge based on the concepts proposed on the 19th century. The results of these investigations produced different adjustments of the Wöhlers's curve obtained from tests on different specimen configurations, including notched pieces. It allowed to obtain a deeper understanding of the factors that influence fatigue life and

fatigue limit.

Due to the prevailing bigger problems on industry related application, most of the research up to the date was performed on metal members. Nevertheless, during the late 20th century the first Wöhler's curves for concrete appeared [67].

2.4.1.3 Cumulative Fatigue Damage Theories

The Wöhler's curves, first appeared on the 19th century and developed during the 20th, have a limited applicability, only to constant stress range cycles. Real engineering problems consist of complex loads applied on diverse types of structure with a wide variety of properties and applications, which results into ignorance on the precise stress time history, always characterized by different stress ranges and uncertainty about load values.

Cumulative fatigue damage theories find its origin on the challenge to solve real fatigue problems with satisfactory solution [68]. The use of fracture mechanics theories remained disregarded as long as modelling the internal structure behaviour is too complex to obtain useful results and the resources that must be put on are excessive. In this sense, cumulative fatigue damage theories are based on the extension and combination of the results by the Wöhler's curves, which up to time were enough studied and spread to be sure about its reliability levels.

The first idea regarding fatigue damage accumulation computation was proposed by Palmgren in 1924 [69]. He introduced a method to compute fatigue life for stress cycles with different amplitudes, by defining the relation between applied and resisted cycles (obtained from the corresponding Wöhler's curve) for a given stress amplitude. The consumed percentage cycles by each stress amplitude could then be added to compute the total percentage of the piece's consumed lineal, what results to be a linear addition of the effects caused by each of the cycles. The material would fail once the total added value reach the hundred percent value, implying that, for a given problem, the total factorized average of applied cycles equalises the factorised average of resisted cycles.

Without naming it as so, Palmgren introduced the concept of fatigue cumulative damage, being it the described relation between applied and resisted cycles. Its proposal would be developed and extended during the years, reaching our days as the Palmgren-Miner Rule, also known as the linear cumulative damage hypothesis.

The hypothesis and models that, at the same years, fracture mechanics research was

developing on the research on the fatigue behaviour of the microstructure were used by many authors as a basis to understand the physics behind the Palmgren hypothesis and improve its reliability on real application problems.

In this sense, Langer introduced in 1937 a refinement on Palmgren's hypothesis. Considering the fatigue life division into the two phases proposed by fracture mechanics, i.e. crack initiation and crack growth until failure, he proposed a separate fatigue life calculation for each of them [70].

In 1945, Miner [71] published the conclusions of his research on fatigue. He followed the lead of Palmgren's research by parting on Langer's paper. On a first stage, Miner proposed a physical explanation for Palmgren's method. He named the relation between applied and resisted cycles as damage and stated that it was a direct consequence of the work absorbed by the material, proportional to the number of cycles. On a second aspect, Miner improved the application of the Palmgren's conclusion by reducing the effective fatigue life to the one belonging to the crack initiation life, as described by Langer, and therefore neglecting the resisted cycles while the crack is being developed.

Miner's results implied a linear relation between damage and applied cycles, valid therefore to compute any stress level, and named thereafter as linear damage rule, being it a cumulative damage rule.

Miner's work meant the culmination of Palmgren's proposal, managing to give it physical consistency, which has resulted into the theory in which today's engineering fatigue analysis and design methods are based.

Nevertheless, the first linear damage rule proposal by Miner was proved to have many deficiencies; including load level independence, load sequence independence and lack of consideration of the load interaction. Many authors followed Palmgren and Miner's lead and tried to improve its theories. New theories regarding behaviour of specific materials or new approaches to the physical phenomenon appeared.

Among them stand out Machlin's [72] metallurgical based cumulative theory published in 1949, the development of a plastic strain range linear cumulative damage theory by Coffin [73] in 1950 and its calibration on experimental results by Topper, Biggs or Miller.

Other new cumulative damage theories are to be mentioned as well. Based on Grover's [74] proposal of two separates stages, similar to the previous crack initiation and crack propagation differentiations, the double linear damage rule proposed by Manson in 1966 defined

two different damage increase rates dependent on the crack growth stage [75]. A series of callibrations performed over tests done by Billir [76] in the 1990s lead to the redefinition of the theory by Manson [77] , adapting the name of double curve approach. The equation describing this relation between damage and cycles was later modified by the same Manson [78] , adding to it a term which smoothed the stage transition, resulting into the double damage curve approach.

2.4.1.4 Contemporary Research

Materials like concrete, which present a high non-linear behaviour, did not present good analysis results when considering the previous existing models and theories, given that the description of material damage evolution that those used is too simple for materials with such a complex microstructure. As a solution to this problem, efforts were putted on the description of the fatigue damage continuous evolution process during all the material's life, trying to gain a better understanding on its presence and development, which has resulted into the main objective of research on fatigue during the last 20th century decades and the 21th first ones.

In 1986 Kachanov [79] published for the first time the results of a research based on the continuous description of fatigue damage. Kachanov's work was performed on metals, and would be expanded to concrete later by Mazars. Further investigation was performed, among which the work of authors like Fatemi [80], Schijve [81], Schütz [52] , Sendeckyj [82], Jones [83], Agerskov [84] , Zheng [85] and Huang [86] stand out.

2.4.2 Fatigue in Concrete

As explained before, fatigue is a very complex phenomenon whose research is very young and superficial in general terms. These short experience and lack of deep knowledge are even more patent on the actual state of the art knowledge on fatigue processes on concrete. The complexity of the material or the lower number of fatigue resisting applications, have made its research be a few steps beyond the ones of steel or other metals.

Nevertheless, there is an extended knowledge basis which has growth the most in the recent years and is still a very active field on mechanics and materials research. The concepts and relations which it works with are accepted to explain fatigue processes on concrete and are necessary to explain and understand the procedures and conclusions of this thesis.

The basic concepts of the actual state of the art knowledge about fatigue behaviour, modelling and calculation on concrete are presented in this section. Given the different behaviour of concrete depending on compression and tension, research has focused on the explanation of each of them against fatigue separately, for which the following points will be similarly organized, adding to them the result of combination of both, which would be bending.

2.4.2.1 Fatigue of Plain Concrete under Compression

The first research on fatigue on concrete material dates back to the first years of the 20th Century. Van Ornum took to term different tests on concrete specimens, which resulted to be rudimentary and generally inconclusive. Nevertheless, his results meant the first approach to the nowadays accepted concrete Wöhler's curves [87].

Nordby [88] continued Van Ornum's research on plain concrete under compression during the 1930s. Although his conclusions were very innovative, it was not adequate to use them for design purposes.

Graf and Brener's [89] research contributed to the fatigue by proposing a diagram for compressive repeated loading. For a given fatigue life, expressed in number of resisted cycles, the diagram showed the resisted stress ranges, giving information of the values for the maximal and minimal stress of the range. It resulted to be a very good description of the concrete's fatigue properties and a very useful design tool.

It is important to point out that Graf and Brener's diagram introduced the mean stress of the stress range (by giving its maximal and minimal value) as a concrete fatigue variable, which has resulted to be fundamental on fatigue design. Moreover, and although without further emphasis, its research showed too for the first time the influence of cracking processes on fatigue development.

Many authors continued the research on fatigue concrete during the 1960s and 70s, although no solid or applicable conclusions were obtained. Antrim [90] , Gray [91], Murdock [89] or Lloyd [92] stand out for its research efforts.

Significant advances were made on the 1970s, when the first Wöhler's curves for plan concrete in compression appeared. Different formulations were proposed by authors like Aas-Jakobsen [93], Tepfers [94], Hsu or Holmen [67]; whose publications date from 1970 to 1982.

It is interesting to recall Aas-Jakobsen's formulation, which is the base of the Wöhler's curves which are accepted nowadays, for example the ones defined in the current construction codes.

Aas-Jakobsen's formulation stated a curve corresponding to the next equation.

$$\log N = \frac{1 - S_{max}}{\beta \cdot \left(1 - \frac{S_{min}}{S_{max}}\right)}$$

Where S_{max} and S_{min} are the relation between the maximum or minimum stress of the range and the concrete's compressive strength, and β is a calibrated parameter, which Aas-Jakobsen proposed to be 0.064.

The evolution of this formulation has been extensive and diverse. It includes many different variations on form and on coefficient that respond to different studies based on various approaches. Some of the more significant are mentioned in the next paragraphs.

The Eurocode 2 and the Swiss Guide refer to it with some variations, adding some new relation between parameters and a different calibration of the coefficients.

Other authors have modified them to include other variables such as frequency of loading, like Zhang's proposal in 1996 [95]. Interest was put on Zhang's results as long as it was a complete model with higher safety levels.

Hsu's research, published in 1981, added some interesting concepts which would make its model one of the most extended. He calibrated a model based on Wöhler's curves which differenced effectively between low and high cycle loading, and which took into account the frequency of the cyclic load. Despite being widely accepted and used, Hsu's curves present some limitations, including a concrete strength limit (55 MPa) and a maximum number of load cycles (10^7 cycles).

Another interesting contribution of Hsu's studies is an approach to the mechanism of fatigue failure in concrete. He described three different stages: A first stage called flaw initiation, in which the weak regions of concrete are affected; a second one named micro cracking in which the previous created flaws develop until reaching a critical size; and a final stage where crack are characterized by its instability, growing until failure.

Holmen's studies, published at the beginning of the 80s, are to be pointed out as well. In his endeavor to obtain more precise Wöhler's curves, Holmen concluded that the maximum stress level, defined as the relation between maximum stress and concrete capacity, is the more

important factor controlling fatigue. Additionally, he proposed a formulation which included probability of fatigue failure, which despite being a very innovative and interesting concept, was limited by the model with a lower boundary of the maximum stress level and two prescribed values of the minimum stress levels.

Holmen research contains as well a large number of tests and studies on the physical background of the fatigue behavior of concrete under compression, including damage evolution. He took to term observations on the deformability process of concrete under fatigue and proposed analytical expressions that described the maximal strain capability of the concrete, which took into account the short or long term character of the tests.

The plots of his results show the three stage of deformation introduced by Hsu, to which he added the strain behavior on each them. The first stage (flaw initiation) presents a high strain velocity which decreases when reaching the phase end, due to the difficulties of the micro crack to extend in the bond between cement and aggregates. The second stage (micro cracking) shows a constant strain velocity, given the micro crack stable growth. At the las stage (crack development) the strain velocity increases exponentially as the resistance decreases due to the conversion of micro cracks into macro cracks.

Finally, it is necessary to mention Petkovic's work [96]. Petkovic proposed his own Wöhler's curves formulation, which are characterized by different slopes depending on the number of cycles. His formulation is valid for normal and high strength concrete. It is now widely accepted, given the levels of reliability and safety it presents, reason why it has been included in the Model Code prescriptions.

2.4.2.2 Fatigue of Plain Concrete under Tension

Given its material low tensile resistance, the available research on the behavior of concrete under tension is reduced.

Tensile stress on concrete are inherently related with cracking. The existing Wöhler's curves on concrete under tension describe the fatigue phenomena taking into account cracking, which is modelled in a simplified way.

It is the case of the formulation of the formulation included in the Model Code, which simply adds calibrated parameters to the general Wöhler's curves; or the equations proposed by Cornelissen and Reinhard [97], which in this case add the minimum stress as a variable.

2.4.2.3 Fatigue of Plain Concrete under Bending

Given the interest on obtaining fatigue knowledge that can be used on real concrete structures many authors have based its research on the fatigue behaviour of concrete under flexural forces.

The first investigations date back to 1922, when Clemmer [98] studied the corner failures of pavement slabs. He concluded the presence of fatigue in such structures, obtaining numerical values on the strength reduction and proposing a design curve for plain concrete subjected to flexure.

Contemporary to Clemmer, Hatt [99] took to term their own research. It stands out for the use of complete reversed fatigue loading over the pieces they tested. Comparisons with Clemmer's lead to the conclusion that concrete fatigue strength was clearly limited by its tensile resistance.

Williams [100] continued the research in 1943, taking to term tests with complete stress reversals, similarly to the ones by Hatt. His conclusions stated a total difference between concrete's fatigue strength when subjected to compression and subjected to flexion, being the last one much lower.

Williams work reflects too the first observations on the material evolution during the fatigue loading process. He states that a certain relation between crack propagation and fatigue resistance exists, attributing it to stress raisers on the material imperfections. Nevertheless, he also observes that many fatigue failures are produced on late appearing cracks, motivating the interest of the researchers on the physical explanation of the fatigue behaviour of concrete under flexion.

In 1958 McCall [101] published his work regarding fatigue strength of concrete under bending, in which he introduced the probability of failure as a design variable.

Further studies conducted by different authors presented the results of tests conducted on specimens subjected to bending and axial compression at the same time. Authors like Opie [102] and Dillmann [103] can be mentioned. The conclusions of these studies presented an increase on the fatigue life due to the added compressive stresses. A stress redistribution was proposed to be the cause of the phenomena, for which the internal stresses would be transferred in such a way that the materials parts with less damage would receive more stress than the damaged ones, causing a reduction of general stress levels and an increase of the total number of cycles of load resisted.

2.4.2.4 Fatigue in Reinforced Concrete

The actual fatigue calculation procedures treat reinforced concrete considering three different components: concrete, reinforcement, and its bond; proceeding to check and design independently each of them. These procedure has been used since the beginnings of fatigue design and are still considered to be the optimal method, being prescribed independently for each of the three parts by normatives like the Eurocode or the Model Code.

Experimental research on reinforced concrete started in 1973, being conducted by Aas-Jakobsen [104]. In his tests a constant axial force was applied to the specimens, defining the bending moment as the action causing the fatigue stress variation.

The results of his tests showed a significant difference on behaviour, depending on the load level applied on the specimen. For cases of axial force predominance, concrete controls the redistribution of stresses and, ultimately, is the responsible for the piece's failure. For those systems with a high bending moment contribution, steel reinforcement is the fatigue resistance determinant factor. Such conclusion is a good indicative of the different behaviour and design requirements of reinforced concrete pillars and beams.

This behaviour tendency was corroborated by furthers studies performed by authors like Chang [105] or Eskola [106].

As a complimentary aspect, the bond between concrete and steel bars has proven to be very important on the determination of fatigue life. A reduction of the surface connection properties of steel and concrete caused by repeated cycles leads to rigidity problems, which increase the crack size and generate durability problems, causing as well uneven stress distribution, critical given the low tensile strength of concrete.

Bond properties study, classification and valuation has been performed by various authors parting from the calibration of a stress-stiffening law. Among them stand out Ciampi [107], Eligehausen [108] or Kreller [109].

2.4.3 Fatigue Models for Offshore Structures

There is a complete lack of deep knowledge on the specifics of the fatigue processes on concrete offshore structures. While only a few research exists on reinforced concrete working on maritime areas, wide series of research and studies have been done on steel offshore structures, led by the interest of the maritime navigation industry, as well as the oil and gas,

which historically has worked almost only on this material. It has derived in a superficial knowledge about the properties of the fatigue behaviour on this kind of environment.

Nevertheless, some of the conclusions obtained from the offshore fatigue processes on steel can be interesting to understand the behaviour of concrete in similar environments.

The existing calculation method for steel are based on fatigue crack growth models analysis. Those consist of procedures intended to estimate the fatigue life of ships. Authors like Terai [110], Peeker [111] or Robles [112] stand out.

Most of these methods include two differentiated procedures: the ones referred to the steel fatigue processes which will be taken into account to compute damage, and the ones regarding the load and stress determination on service conditions of the structure. In this sense, many authors proposal differ from each other on the fatigue computation method and propose similar stress time history method with slightly variations, which are interesting to understand as long as they will be the same acting on concrete.

For example, Terai's model for fatigue calculations on ships stated the determination of a structural mean stress, based on the ballast and loading condition of the boat, the calculation of a dynamic loading related stress time history, and the consideration of a relative angle between ship and wave.

Another interesting approach that is extracted from steel offshore fatigue calculations is the spectral based ones, included nowadays as a calculation option in all the offshore structures design codes. It relates linearly the fatigue damage with the different frequencies included on the spectral representation of the waves' long term description. A load spectrum, and the subsequent response spectra of the structure in forms of stress ranges are computed, from which linearly adding the caused damage according to the decided model results to be immediate.

Most of the concrete offshore fatigue calculations procedures use similar methods to define loading and structural load effects, although the existing computation for fatigue damage methods do not reach the levels of development of the steel ones. There is an important lack of research in what concerns concrete offshore fatigue. A cumulative damage evolution based model for offshore concrete does not exist, being the use of S-N curves and the Palmgren-Miner's hypothesis the defined analysis method by all the existing offshore construction codes.

Nevertheless, the few existing research has provided some conclusions which have been

numerically adapted through the calibration of existing S-N curves for offshore environments. In this sense, the only known studies, which were carried by Waagard [113] and Gerwick [114] on submerged reinforced and prestressed concrete specimens, allowed Holmen to adapt his S-N curves to maritime areas, on a compression-tension basis. The research which was reflected on those curves observed a pumping of water through the concrete existing cracks which resulted into an acceleration of the material's degradation process. It remarked as well the beneficial impact of rest periods to resistance on the submerged concrete, enabling an increase of the endurance limit, although this effect was not included on Holmen's modified curves.

In the recent times, other authors have proposed model to compute the effects of maritime degradation on concrete offshore fatigue processes. In 2010, Stemberk [115] proposed a fuzzy logic model that took into account the effect of chloride penetration, making it possible to take into account the damage increase process of the concrete due to the loss of material properties because of degradation.

2.5 Fatigue Evaluation of Concrete Structures

The currently used procedures for fatigue design and verification are formed by simplified methods based on the concepts previously explained. The complexity of the fatigue phenomena and the uncertainty which characterizes the fatigue problems, taken into account together with the non-critical condition of fatigue resistance in most concrete applications, have made it sufficient to establish the use of simple methods, which are included in the normative construction codes, given that the existing more complex procedures will only suppose a resources waste increase without better real results due to the existing uncertainty, on problems in which fatigue will not usually be the failure cause. There is no sense in considering the detailed fatigue process, or all the detailed properties and the complete material behavior.

In this section the range of methods for fatigue design and verifications which are used nowadays are presented, framed in the context of its origin, properties, advantages and usefulness.

2.5.1 Methods based in S-N Curves

Wöhler's curves are the most acknowledged and used method for fatigue calculations. Despite not being the most accurate tool, as long as they are not focused on the physical behaviour modelling, the methods based on this tool are much extended given its simplicity and the direct accounting of the influence parameters.

There are many Wöhler's curves formulations on reinforced concrete available. Among them stand out the ones result of the work of authors like Aas-Jakobsen, Petkovic, Holmen, Hsu or Zhang; apart from the formulation included on the Eurocode or the Swiss Regulation. The curves are all similar, with different important behaviour on the zones regarding low and high number of cycles. All of them have been calibrated through experimental tests and show good reliability levels, checked by experience.

The most accepted ones on reinforced concrete are the ones proposed by Hsu, valid for compressive stresses are omitted.

These S-N curves based its calculation procedure on the maximum stress level on the structure. That means that no multiple points are taken into account simultaneously, and therefore, stress redistribution processes are omitted.

In this sense, efforts to elaborate an accurate tool have led to the introduction of numerical corrective coefficients. Model Code [116] includes a reduction coefficient η_c based on the stress distribution of the studied cross-section, trying to emulate the beneficial effects of the stress redistribution. Opie and Husbos [117] work resulted in the proposal of a θ parameter, which took into account the variation of the stresses in the compressed material zone, and included it as a third design variable on his S-N diagram.

In order to obtain real fatigue results, Wöhler's curves cannot be applied alone, as long as they are only valid for a specific stress range. A damage accumulation tool is therefore needed. In this regard, Palmgren-Miner linear hypothesis is the most extended and used on, providing simple but effective results. However, given the importance of nonlinearities and the complex material evolution, caution must be taken when applying it to reinforced concrete, not being valid in most of the cases.

2.5.2 Continuous Damage Models

The methods based on S-N curves, treated on the previous section, are only referred to the failure instant and do not take into account the damage process of the material, which can result into important material properties variations and durability reduction, important in the study of non-linear materials such as concrete. In this sense, the continuous damage models appear as a solution to take into account this material evolution when designing against fatigue.

Nowadays, continuous damage models are the most reliable solution to perform fatigue calculations. Fatigue damage evolution is considered, obtained from computations on time instants which take into account current material properties.

First proposal of damage evolution calculation procedure dates back to 1981, when Mazars [118] published a simple model based on the deformation and young modulus influence over the stress. The same Mazars [119], developed his model in the next years. In 1986 he took into account the influence of microcracking processes, leading to a difference between tensile and compressive damage.

Nevertheless, Mazars' model did not include the direct calculation of damage from stress ranges caused by load cycles. It was Papa [120] [121] in 1993 who took Mazars' model and developed it to include the calculation of fatigue loads. He used a parameter n, calibrated from experimental results and dependent on the relative stress range and the minimum relative

stress.

A more developed model was presented by Pfanner [122] in 2002. Introduced as a uniaxial fatigue damage model, it includes the nonlinear material behaviour by dividing the strain on an elastic and a plastic part. At the same time, elastic strain is divided on two parts, regarding the presence or non-presence of damage. The influence of fatigue loads is introduced through a so called energetic damage model, which equalizes the energy given by the fatigue loads (in terms of stress and number of cycles on a given damage basis) into an equivalent static energy (dependant on a damage and stress levels. The model included implicitly the redistribution of stresses on the concrete section.

In 2004, Alliche [123] introduced a new model, capable of reproducing the three-dimensional fatigue behaviour of concrete, which was based in a previous formulation by Dragon [124] that took profit of thermodynamics potential. Damage was defined on an effective resisted cross-section area which took into account crack surfaces and stress concentrations. Performed numerical simulations showed the good properties of the model regarding the progressive reduction of stiffness, the three stage strain velocity differentiation, and the plastic strains accumulation.

Further models with different interesting contributions where later published. Among them stand out the results of Zanuy's research in 2008, and the one of Mai's in 2011 model. Zanuy [43] proposed a compression plain concrete model, which was based in all the previous existing studies and calibrated through experimental tests in reinforced concrete beams. Apart from its model, it must be pointed out as well the proposal of stress redistribution reduction factor [125], based on the bending characteristics of the problem, which is nowadays prescribed by the Model Code. Mai's [126] publication consisted of a three dimensional model based on a previous fatigue formulation by Marigo [127]. Experimental and numerical tests showed a good behaviour of the model and a good representation of the softening and ductile properties of concrete.

2.5.3 Final Remarks

Many concepts regarding the fatigue process behaviour of concrete have been commented and discussed. The main points are detailed next, along with notes on its importance and influence.

The physical fatigue damage process of concrete is a complex phenomenon which high levels of related uncertainty. Nevertheless, it is clear that is closely linked to an internal micro

cracking development, which can be divided into three phases. Moreover, it is accepted that a complete description the process needs to include the loss of stiffness and resistance due to material deterioration.

The actual methods to study fatigue behaviour of materials in concrete can be divided on the ones based on S-N curves, and the ones on continuous damage models.

S-N curves models are based on simple relation between parameters which reflect the loading processes and the material properties, and are valued through calibration on experimental results. They only provide information about the failure conditions and do not reflect the physical damage temporal evolution process and its consequences. In this regard, efforts have made to include parameters which try take into account the effects of such evolution. It is worth mentioning the different proposals of section stress redistribution parameters.

Continuous damage models try to give a holistic perspective of the fatigue process. Actual state of the art research results into very complex models which cannot be used to solve engineering problems, as long as is very difficult to implement on them real conditions and properties without recalling on high levels of uncertainty, and in expenses of using a big amount of resources.

Given this knowledge scenario, S-N curves are the most employed tool on engineering design and verification procedures. Despite lacking of the inclusion of the material evolution process, and the parameters which are influenced by it, it has proven to be an acceptable solution, as long as the uncertainty levels are known and fatigue failure does not represent a major problem on the great majority of structures.

2.6 Fatigue Codes

The different relevant constructive codes which nowadays present a procedure for the verification of the fatigue limits state, including the computation of fatigue damage for a given stress history, are presented in this section.

2.6.1 Eurocode 2: Design of Concrete Structures (EN 1992)

2.6.1.1 Introduction

Eurocode 2: Design of Concrete Structures [19] is the concrete related series of documents that form a part of the Eurocodes (EN harmonized rules), the European standards which rule over the structural design. Eurocodes, developed by the European Committee for Standardisation as requested by the European Commission, are to be considered and followed on all the European public works, in substitution of the national construction codes, although nowadays they coexist in some countries.

Eurocode 2: Design of Concrete Structures defines technical compulsory guidelines for the design and construction of concrete, reinforced concrete and pre-stressed concrete; by means of the limit state design philosophy.

EN 1992 includes the next documents as parts of it:

- Part 1-1: General rules, and rules for buildings
- Part 1-2: Structural Fire Design
- Part 1-3: Precast Concrete Elements and Structures
- Part 1-4: Lightweight Aggregate Concrete with Closed Structure
- Part 1-5: Structures with unbonded and external Prestressing Tendons
- Part 1-6: Plain Concrete Structures
- Part 2: Reinforced and Prestressed Concrete Bridges
- Part 3: Liquid Retaining and Containing Structures

As interest of this thesis' topic, not specific document of the Eurocode 2 is dedicated to offshore structures. Therefore, the prescriptions which will be applied on this thesis will be taken from the documents which present relevant related contents.

2.6.1.2 Fatigue Design

The first and most general document of *Eurocode 2* is the *Part 1-1: General rules, and rules for buildings*. It includes superficial and general prescription for the verification of fatigue resistance. Reference is made to it on the chapters related to materials, and on the section of the ultimate limit states chapter dedicated to the fatigue limit state.

According to it, the FLS shall be accounted for those structural components subjected to regular load cycles, without further specifications. It separates the verification on the single check of each of the materials, including concrete, reinforced steel and prestressed steel. The procedure which must be followed for the computation of stresses and the combinations of loads are indicated.

S-N curves are provided for the computation of fatigue effects on steel, while only general check formulas are stated for its verification on concrete. In this sense, the *Part 1-1* of the *Eurocode 2*, does not account for the concept of damage, presenting only simplified verification methods which do not account for cycles with varying stress ranges.

Regarding the other documents contained in the *Eurocode 2*, some interesting information can be found on its *Part 2: Reinforced and Prestressed Concrete Bridges*. Given the important cyclical nature of some of the loads which act on a bridge, it presents a series of prescriptions for the verification of fatigue resistance on those types of structure, including S-N curves and a linear damage addition method which can account for different stress range cycles.

The Part 2 of the *Eurocode 2* defines the need for a fatigue verification on those structural components subjected to regular load cycles. In the same sense as the Part 1, this is a qualitative description, without further specification on which constructions shall be verified and which not. A separated verification for concrete and steel is prescribed.

The computation of fatigue resistance must account for the verification of compression and shear. In the case of compression, the possibility of selecting between the curves prescribed on the national annexes of the Eurocode (documents which include prescriptions and specifications which each member country is free to define), and a simple S-N curve and. The basic Palmgren-Miner hypothesis formula for linear damage addition is presented as the accumulation solution for every possible selected case. The equations relating to this simple curve and the addition rule, as presented in the code, are next included.

Miner's rule for damage accumulation is presented in the next form.

$$\sum_{i=1}^{m} \frac{n_i}{N_i} \leq 1$$

Where m defined the total number of cycles classes on the same amplitude, n_i is the number of cycles for the class cycle i; and N_i is the ultimate number of class i cycles that the structural component can support before failure, as computed by one of the methods before mentioned. On the right side of the inequality, a maximum value of 1 accounts for the maximum allowable value of damage that the code prescribes.

The S-N curve follows the next expression, in which the resisted number of cycles can be directly computed.

$$N_i = 10^{\left(14 \cdot \frac{1-E_{cd,max,i}}{\sqrt{1-R_i}}\right)}$$

Being,

$$R_i = \frac{E_{cd,min,i}}{E_{cd,max,i}}$$

$$E_{cd,min,i} = \frac{\sigma_{cd,min,i}}{f_{cd,fat}}$$

$$E_{cd,max,i} = \frac{\sigma_{cd,max,i}}{f_{cd,fat}}$$

Where the index i refers to one of the to be considered stress cycles, R_i is the stress ratio, $E_{cd,min,i}$ and $E_{cd,max,i}$ are respectively the minimum and the maximum compressive stress level, $f_{cd.fat}$ is the design fatigue strength of concrete, and $\sigma_{cd,max,i}$ and $\sigma_{cd,min,i}$ are respectively the upper and lower stress.

The computation of the design fatigue strength of concrete shall be performed with the next formula.

$$f_{cd,fat} = k_1 \cdot \beta_{cc}(t_0) \cdot f_{cd} \cdot \left(1 - \frac{f_{ck}}{250}\right)$$

Where k_1 value can be found on the correspondent national annex of the Eurocode, $\beta_{cc}(t_0)$ accounts for the concrete's strength at first load application time in days t_0 and f_{cd} is the design resistance of concrete, computed as the characteristic strength f_{ck} divided over the

partial safety coefficient for fatigue $\gamma_{m,f}$, which is prescribed in this code with a value of 1.5. Further reference to these values can be found on the general document and the corresponding annexes.

2.6.2 FIB Model Code for Concrete Structures

The fib Model Code for Concrete Structures [116] is the document resulting of the work of the pre-normative organization International Federation for Structural Concrete, an international non-profit group which tries to promote the use, research and development of concrete by settling the basis of constructive codes on concrete structures and actualising the concrete knowledge.

The fib Model Code for Concrete Structures is formed by a single document which normalizes the whole life cycle of the concrete structures, considering all types of concrete structures.

Extensive reference is made to the fatigue phenomena from a general point of view, without further specifications on the particularities of maritime nor offshore structures. Again, a separated verification for steel and concrete is defined.

In the *Model* Code, fatigue reference can be found on the chapter relating to material properties, in which the behaviour of concrete and steel is accounted on the basis of parametrised equations and comments; and in the chapter for the ULS verification on non-static loading, in which an analysis methodology is proposed.

It is in this verification chapter, in which a broader range of interesting prescriptions can be found. *Model Code* proposes four different methods for the verifications of the fatigue limit state, on an increased refinement progression.

The *Level I approximation* states that if a qualitative valuation can assure that no variable load can produce fatigue effects, no further check is needed. Otherwise, a further level method must be employed.

The *Level II approximation* proposes a simple verification procedure, consisting on the definition of the maximum stress ranges which respectively steel, concrete under compression, and concrete under tension cannot exceed. A limit of 10^8 cycles over the structure is defined for the employment of this approach.

The *Level III approximation* refers to the consideration of a single load level. The representation of the variable dominant load, which is associated to number of repetitions during the required design life, must be taken to term. It will be associated to a load level, which will define the correspondent to be verified stress ranges.

Finally, the *Level IV approximation* takes into account the fatigue damage caused by variable loads of different magnitudes and the addition on the basis of the Palmgren-Miner summation.

As for the interest of the structure analysed in this Master Thesis, in which the loads and the environment make fatigue resistance a critical factor, this more refined level has resulted of special interest in order to properly characterize fatigue resistance.

Model Code's fatigue verification *Level IV approximation* prescribes the definition of a load spectrum containing all the information regarding its variations. Resulting load cycles on similar properties can be divided into blocks, in order to categorize its effect level.

A total fatigue damage value is defined to be computed, as the result of the addition of the total fatigue effects of the cycles categorized in those load blocks. Palmgren-Miner summation is proposed for that purpose, whose equation, as presented in the code, is stated next.

$$D = \sum_{i=1}^{j} \frac{n_{E_i}}{N_{R_i}}$$

Where D is fatigue damage, i accounts for the index of the stress block, j is the index defining the total number of defined stress blocks, n_{E_i} is the number of acting stress cycles for the block i, and N_{R_i} denotes the number of resisiting cycles for the stress level associated to the block i.

The maximum value of fatigue damage is defined through the next formula.

$$D \leq D_{lim}$$

Where D_{lim} result to be the limit damage resisted by the studied structural component, which, according to the specification, must adopt an adequate value, without specific values. A comment in this regard is included, detailing that its value shall account for the stress time history as proposed by Zhang [128].

In the case of the verification of the structural concrete components, the *Model Code* introduces a more complex analysis than the one presented for the *Eurocode 2*. The possibility

of analysing compressive and/or tensile stresses is introduced, leading to an analysis proposal which provides a deeper description of the fatigue phenomena.

Given the highly prestressed state of the offshore structures, needed for guaranteeing its durability, the analysis proposed by the *Model Code* for cyclic compressive stresses results of special interest.

A methodology is proposed in that case for the computation of the resisted cycles N_i of each consant amplitude stress block i. On a previous stage, the appropriate computation of the representing cycle stress level is defined, which needs of the following parameters.

$$S_{cd,min} = \frac{\gamma_{Ed} \cdot \sigma_{c,min} \cdot \eta_c}{f_{cd,fat}}$$

$$S_{cd,max} = \frac{\gamma_{Ed} \cdot \sigma_{c,max} \cdot \eta_c}{f_{cd,fat}}$$

Where $S_{cd,min}$ and $S_{cd,max}$ are respectively the minimum and the maximum compressive stress level, γ_{Ed} is the design load factor, $\sigma_{c,min}$ and $\sigma_{c,max}$ are respectively the minimum and maximum stress levels, η_c is the in the next paragraph detailed redistribution factor, and $f_{cd.fat}$ is the design fatigue strength of concrete. Further reference to them is made next.

Computed relations where $S_{cd,min} > 0.8$, will need to be accounted with a value of $S_{cd,min} = 0.8$.

Model Code is the only document of the presented in this thesis which proposes the use of a design load factor γ_{Ed} different than $\gamma_{Ed} = 1.0$. In this case, a general value of $\gamma_{Ed} = 1.1$ is proposed, which might be reduced to the unity in the case of accurate or conservative stress analysis verified by in-situ observations.

The redistribution factor η_c accounts for the stress redistribution on the compression zone of a concrete section subjected to cyclical stresses, which proves to reduce the fatigue damage. Its effect is evaluated through the averaging of the stresses values. The expressions proposed by the code to compute it are presented next. Further reference to the physical background of this phenomena can be found on Chapter 2.

$$\eta_c = \frac{1}{1.5 - 0.5\frac{|\sigma_{c1}|}{|\sigma_{c2}|}}$$

Where σ_{c1} is the minim value of the compressive stress within a distance of 300 mm from

the surface under the relevant load combination of actions, and σ_{c2} is the maximum value for the same 300 mm area and load combination for which σ_{c1} was computed.

The computation of $f_{cd,fat}$ must be made following the next formula, whose parameters and construction follows the same scheme as the one presented for the *Eurocode 2* fatigue computations.

$$f_{cd,fat} = 0.85 \cdot \beta_{cc}(t) \cdot f_{ck} \cdot \left(1 - \frac{f_{ck}}{400}\right) \cdot \frac{1}{\gamma_{c,fat}}$$

Where the partial safety load factor for material concrete under fatigue $\gamma_{c,fat}$ takes a value of $\gamma_{c,fat} = 1.5$.

Once computed the minimal and maximal stress levels, the resisted number of cycles is defined by *Model Code* through the employment of a S-N curve, which is based on two different parametrised curves and a frontier point which separate them. Both curves must be computed using the so called parameter Y, defined as follows.

$$Y = \frac{0.45 + 1.8 \cdot S_{cd,min}}{1 + 1.8 \cdot S_{cd,min} - 0.3 \cdot S_{cd,min}^2}$$

A first piece of the curve, which applies for high stress levels, is constructed through the next expression.

$$\log_{10} N_1 = \frac{8}{Y - 1} \cdot \left(S_{cd,max} - 1\right)$$

Where $\log_{10} N_1$ is the base ten logarithm of the number of resisted cycles for $S_{cd.max}$ and $S_{cd.max}$, and which will apply, according to the code, for values of $\log N_1 \leq 8$.

When higher values are obtained, the stress levels of the cycles will be sufficiently low to use the second defined curve, which will result into higher values of the number of resisted cycles N. In that case, the expression to be used takes the next form.

$$\log_{10} N_2 = 8 + \frac{8 \cdot \ln(10)}{Y - 1} \cdot \left(Y - S_{cd,min}\right) \cdot \log\left(\frac{S_{cd,max} - S_{cd,min}}{Y - S_{cd,min}}\right)$$

For which N_2 will result into the resisted number of cycles.

2.6.3 DNV Rules and Standards

Det Norske Veritas (DNV) is an international certification body and classification society whose origins date back to the 19th century, when it was created as the main Norwegian competent authority for the inspection and evaluation of merchant vessels. It is now the largest classification society, besides having expanded its enterprise to energy related areas, including, for example, wind or oil and gas. It bases his business on the capacity to offer expertise (technical, business, etc.) in several industries.

Among his activities, in which for example technical assessment, risk management or consultancy can be found, the publication of public standards and regulations stand out. Given his knowledge-based business and its huge efforts on research and technological developing, these publications tend to be cutting-edge when it comes to standardized procedures and methods. Among them, many regulations which are offshore related can be found, including topics such as the general design of wind turbine structures, the determination of environmental loads or the design on offshore concrete.

The DNV constructive codes stand out for its specialization on maritime and offshore structures and for the state of the art contents when it comes to design procedures and knowledge deepness. A wide range of publications of interest can be found, which cover different kinds of applications (from wind turbines to multi use barges) or construction techniques (from normal steel to special concrete types).

As for the purposes of the fatigue design research of this Master Thesis, the so called DNV-OS-C502 Offshore Concrete Structures has been selected, which provides a complete and deep set of prescriptions and indications on the design and calculation of offshore concrete structures [129]. Other available DNV codes that focus on wind turbine design, mostly refer to this concrete specific code when it comes to the particularities of this material.

The DNV-OS-C502 Offshore Concrete Structures includes extensive references to the fatigue design, acknowledging its problematic for offshore environments. Besides the common reference to material fatigue properties and stress calculation recommendations, further relation is made to fatigue load determination and structural details verification.

Regarding the specifics its verification of the fatigue limit state, the same schematic as in the other codes, formed by the Palmgren-Miner hypothesis and a S-N curve is given. Nevertheless, its proposal stands out by limiting the total fatigue damage to a value which could be inferior to 1, given certain states of maintainability. As stated in the code, the Miner’s rule

follows the next equation.

$$D = \sum_{i=1}^{k} \frac{n_i}{N_i} \leq \eta$$

Where, the different parameters follow the common nomenclature for linear fatigue

Limit of **Cumulative Damage Ratios**	No Inspection/Repair Access	Below or in the Splash Zone*	Above Splash Zone*
η	0.33	0.5	1.0

**: Further Reference in Text*

Table 2 Pros and cons trade-off of the three main floating platform types [08].

damage addition, and η is the variable representing the total allowable fatigue damage. This value will take one of the values stated in Table 2.

Limit values of the cumulative damage ratios, as stated in Table 2, depend on the severity of the durability aggressive conditions on each material's zone and on the possibility on accessing them for repair. For those harsh environments in which the normal sea state severity denies the possibility of accessing the splash zone for repair, a value of 0.33 shall be taken. For reinforcement the same values will be taken, except for the above splash zone regions, in which it will be reduced to 0.5 given the impossibility of reparation.

In this case, the computation of the maximum resisted load cycles N is also accounted by means of a S-N curve, with the particularities of some extra parameter which accounts for the properties of the specific offshore environment in which the structure is located. Its expression is stated next.

$$\log_{10} N = C_1 \cdot \frac{1 - \frac{\sigma_{max}}{f_{rd}}}{1 - \frac{\sigma_{min}}{f_{rd}}}$$

Where N is the maximum number of resisted cycles, σ_{max} and σ_{min} are, respectively, the numerically largest and least compressive stress, C_1 is a factor accounting for the structure's placement and f_{rd} is the compression strength.

The factor C_1 can take one of the next values (listed from more to less fatigue resistance).

- $C_1 = 12$ for structures in air

- $C_1 = 10$ for structures in water and stresses in the compression range
- $C_1 = 8$ for structures in water and stresses in the compression-tension range

As it can be seen, despite being able of accounting for tensile stresses, the DNV code does not propose any special S-N curve or methodology for this finality, proposing a reduction of the parameter C_1 and the selection of a null value when tensions occurs.

The compression strength f_{rd} takes into account the redistribution stress (Chapter 2), determined by the mean stress effect on the concrete compression zone. In this code, it is defined by means of the α parameter which must be employed and computed according to the next expressions.

$$f_{rd} = \alpha \cdot f_{cd}$$

$$\alpha = 1.3 - 0.3 \cdot \beta \geq 0.1$$

Where β is the ratio between the numerically smallest and largest stresses on the concrete compression zone, calculated in a distance between points less than 300 mm.

The partial fatigue material factor $\gamma_{m,fat}$ for the computation of f_{cd} might use a value of $\gamma_{m,fat} = 1.35$, when the design is bases on dimensional data that accounts for tolerances and imperfections, and $\gamma_{m,fat} = 1.5$, when no control in this terms exists.

In a similar concept as the two pieced S-N curve proposed by the Model Code (Section 2.6.2), the DNV code allows an increase of the resisted cycles N for enough low stress values, or, in other words, for sufficient high values of the N value obtained on the first curve piece.

In this sense, the code states an increase for values of $\log_{10} N > X$, where the expression defining X is detailed next.

$$X = \frac{C_1}{1 - \frac{\sigma_{min}}{C_5 \cdot f_{rd}} + 0.1 \cdot C_1}$$

The increase will be made effective through the multiplication of $\log_{10} N$ by the factor C_2, which is defined next.

$$C_2 = \left(1 + 0.2 \cdot (\log_{10} N - X)\right) > 1.0$$

Which must be greater than the unity to maintain its increasing factor nature.

Material Load Factors, Concrete in Compression	**Model Code**	**Eurocode 2**	**DNV-OS-C502**
$\gamma_{c,fat}$	1.5	1.5	1.5*
Partial Load Factors			
$\gamma_{E_d,fat}$	1.1*	1.0	1.0

**: Further Reference in Text*

Table 3 Pros and cons trade-off of the three main floating platform types [08].

2.6.4 Code Comparison

A general joint view on the main characteristics and prescriptions of the three presented codes can be interesting to compare them, obtain conclusions, and evaluate the results that will be obtained with them and to build the fundaments of a theoretical base in case further research on its behavior is needed.

On a previous phase, it is interesting to compare how each of them treats the partial factors for load and material resistance, given that those will have a very high influence on the final results extracted from them. The values proposed by each code are detailed on Table 3.

As it can be seen in Table 3, almost all the codes define a value of the partial load factor $\gamma_{E_d,fat}$ equal or very close to the unity, which implies the no application of a safety magnification on the loads. The determination of the fatigue loads, which is described by frequent and measurable processes, shall be enough reliable to avoid the necessity of adding uncertainty factors to it. A slightly bigger value of $\gamma_{E_d,fat} = 1.1$ is prescribed by the Model Code, for those cases in which the stress determination presents a lack of accuracy.

Regarding the material safety coefficients no huge disagreement is seen, presenting all the codes the value of $\gamma_{c,fat} = 1.5$, which coincides with the used in almost all the ultimate limit states. The DNV code allows the reduction of this value to $\gamma_{c,fat} = 1.35$ for those cases in which a high control is exercised on the construction process and the design is sufficiently accurate.

All three codes take to term the fatigue damage computation on the basis of the S-N curves and the Miner's hypothesis of linear damage addition, introducing different parametrizations of it and considerations on its use. As stated in Chapter 2, this procedure is the more adequate for the computation of fatigue effects on real structures.

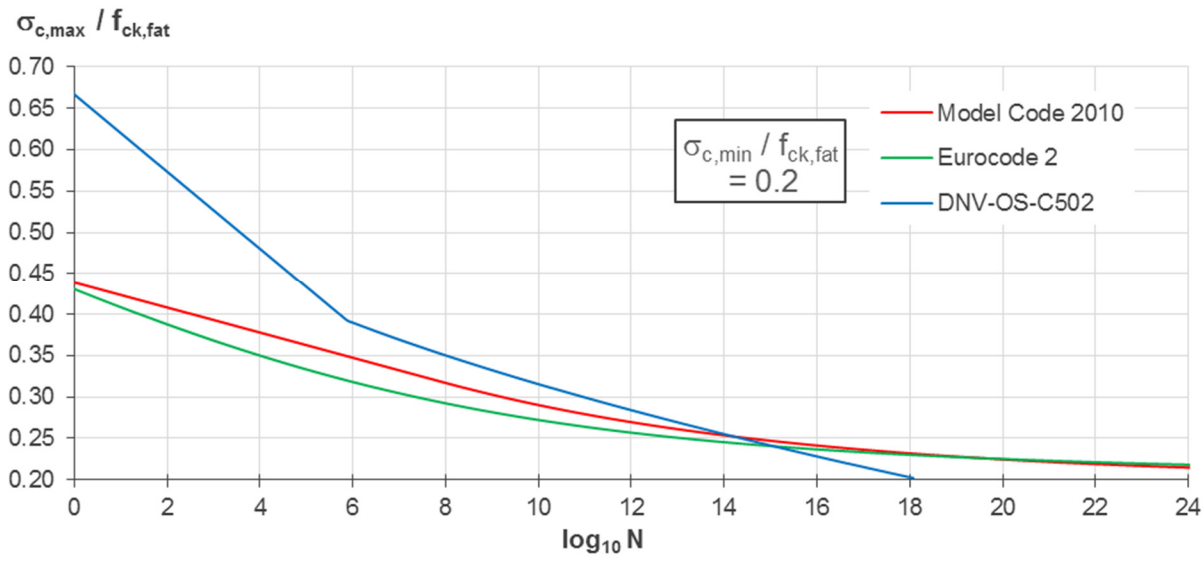

Figure 11 S-N curves for a minimum stress level of 0.2, based on the parametrisation and procedure of different codes.

As remarkable aspects, the use of different values of the limit damage by the DNV results of special interest, which introduces the maintenance as a factor which can increment fatigue life; and the application of the redistribution factor, introduced through different methods on the Model Code and the DNV, phenomena widely known which can have a high influence on the concrete's fatigue life.

In Figure 11 a sample of the S-N curves which will result from prescribing a minimum stress level of $S_{cd,min} = \frac{\sigma_{c,max}}{f_{ck,fat}} = 0.2$ are detailed. The resisted total number of cycles N is plotted on a logarithmic base 10 scale, given its exponential character.

The three curves show similar tendential shapes, being possible to differentiate the two different straight stretches on the DNV code curve (blue), and an approximately straight one followed by a curve on the Model Code curve (red).

It is worth mentioning the differences between the DNV curve and the other ones. The DNV curve presents a limit value of the maximal stress level of approximately $\frac{\sigma_{c,max}}{f_{ck,fat}} = 0.66$, for which the number of resisted cycles is $N = 0$. The Model Code and the Eurocode provide it around the value of $\frac{\sigma_{c,max}}{f_{ck,fat}} = 0.43$, which represents a much lower fraction of the total characteristic resistance.

This behavior is attributed to the prescription of each code, for which different reduction parameters are to be applied to Model Code and Eurocode material strength in order to increase

the safety of the process, while the DNV code will define variations on the limit damage. Even so, a much greater resistance can be expected on the DNV calculations given the linear character of the fatigue damage addition and the logarithmic one of the S-N curves output.

2.7 FOWT Concrete Structure Fatigue Design

2.7.1 Introduction

On the previous sections, the state of the art regarding the areas of knowledge which relate to the fatigue processes on concrete floating offshore structures have been presented. Different considerations have been made separately, regarding, on a first part, the mechanical modelling possibilities of an offshore floating structure; and, on a second one, the current methods used for concrete fatigue evaluation on real engineering problems.

When it comes to the combination of both of them, in other words, the fatigue design of concrete FOWT, no other information than superficial approaches on non-specific documents can be found. Most of these documentation presents a theoretical base obtained from the experience on fixed bottom concrete structures and floating offshore steel structures. The specific characteristics of its application on concrete FOWT are regarded with superficial comments and considerations, which generally indicate the existence of differences without further detail.

The state of the art knowledge regarding the design of this type of structures is presented in this chapter. A global approach to this procedure is therefore introduced, given the lack of specific documentation and the non-availability of referenced past experiences.

A good apprehension and understanding of all this knowledge is considered to be essential, given that it is the only known theoretical concepts in which the process of fatigue design on a concrete FOWT which is performed as objective of this thesis can be based.

2.7.2 Design Codes on FOWT

Some codes published by independent agencies on the design of floating offshore wind turbines have aroused in the last years. They try to give general guidelines about its design and construction, a broad view of the factors influencing the design process and references to it. Usually they are on a primarily stage, prescribing few procedures, offering different computation possibilities, and referring themselves to other guides. Despite it, they are a useful tool to know the state of the art of the subject, and start working on the engineering work planning.

Two major sets of codes, published by relevant agencies on the matter, stand out. On one side the DNV offshore standard DNV-OS-J103 Design of Floating Wind Turbine Structures [25]

and the related offshore wind constructive codes [129] [130] [131] [132] [133]. On the other the codes of the American Bureau of Shipping (ABS) including among others, the Global Performance Analysis for Floating Offshore Wind Turbines Installations [134].

Those have been analysed and worked for the fatigue design purposes of this thesis. Some of the most important conclusions extracted from them are here presented.

The DNV-OS-J103 defines the aspect its authors consider to be fundamental on the process of structural design. It is based on the IEC 61400-3, the guide on design of offshore floating structures published by the International Electric Commission [135]. It contains guidelines with different levels of deepness, including the establishment of a general design principle based on limit states and partial safety coefficients; the definition of the to be considered environmental conditions, general loads and load effects; and the prescription of the characteristics to be considered on the material, and recommendations about the limit states calculations. Additionally, referenced is made to constructive aspects and design of especial components, such as mooring system or components; and transport and installation processes.

Its reference on concrete are limited, providing general information and, for structures using concrete as the main material, referring to the DNV-OS-J101 (Design of Offshore Wind Turbine Structures) [130], which at the same time makes reference to the DNV-OS-C502 (Offshore Concrete Structures) [129].

The ABS guide contains a little foreword describing floating offshore wind structures. Further reference is made to general design requirements, material properties and environmental conditions and loads. Chapters are dedicated too to the design of the mooring systems or industrial components.

Both guides treat the design problem of FOWT in a very similar way, being identical in the general prescriptions and recommendations. In the both of them, the influence of the shipping industry is present, given that both author agencies have the ship certification as its core business. In this sense, little reference is made to constructive aspects which treat on concrete, such as its fatigue calculation, which is mostly extern referenced.

2.7.3 Fatigue Design Process

The aim of fatigue design is to ensure a planned structure with a sufficient resistance against fatigue failure. This means that the construction must resist the effects of all the loads

that will be acting onto it during the service life for which the structure is planned. The fatigue life of the designed structure must be adequate.

A verification method is used to ensure the correct fatigue design of the structure. Given the resistance characteristics of a floating offshore structure, the external conditions that will determine its loads, and the minimum required fatigue life; a value of fatigue damage is computed. A result which surpasses the maximum allowable fatigue damage will imply the fatigue collapse of the structure during its service life and therefore the no verification of the fatigue resistance. In this case, the realization of modification on the structure resisting properties will be necessary until the fatigue resistance is verified.

In the next sections, the different parts of this verification process are explained. First, a deeper insight on the peculiarities verification process, which is based on the limit states procedure, is given. Following it, aspects of the different parts of the verification process are detailed in different sections, including considerations on the treatment of the external climatic conditions, the obtaining of the structural response and the verification procedure.

2.7.3.1 Fatigue Limit State (FLS) Verification

The verification of the fatigue life is based on the philosophy of the limit states, being it subjected to the accomplishment of the so called Fatigue Limit State (FLS). Design following these principle is the state of the art procedure, as corroborated by the general structure design standards [19], and more specifically the ones referred to floating offshore wind turbines [25] [134].

The verification of the FLS is more intricate than the other limit states. For instance, the verification of the ultimate limit state needs of the determination of the ultimate loads on the structure, which appears to be a not complex task. A maximum load is probabilistically determined, and a level of reliability to that computation is obtained as well. In case of doubt, sensitivity and reliability studies will not be difficult to perform. It is in the case of fatigue limit state in which the load determination process takes a whole new dimension, being it necessary to compute all the loads at which the structure will be subjected during its design life.

Therefore, a first objective on the verification process is the determination of the loads that will be acting on the structures along its service life, in this case, fatigue loads. The definition of the fatigue loads values is commonly not an easy task, as long as its dynamic behaviour is implicitly variable and hard to quantify. On an offshore environment like the one which occupies

us, this valuation is even more complicated, given the extremely stochastic character of the environmental actions that the structure suffers, which are highly variable and difficult to be measured with precision. Other factors, like the continuous variation of the structure position or the interaction between actions, make it even more difficult to assess correctly this step.

A simulation accounting for a complete mechanical model of the structure and its environment along time must be therefore employed. It is the only method that can account for all these difficulties, given its ability to model all the conditions affecting the structural resistance at each time instant.

The loads that will be applied on that structural model will basically consist on the action of environmental processes on the structure and its system, mainly the effect of wind waves. Its variability conditions the irregularity of the loads which will act on the structure. There are many methods which describe the physical magnitudes and physical behaviour of these phenomena. These procedures include the determination of the loads which are generated when interacting with physical bodies. Therefore, the problem of determination of loads is transformed into the determination of the environmental actions magnitude which acts on the structure.

Fatigue processes are caused by the stress variation on the structure during its service life, caused by the continuous loading variations. A complete determination of loads, environmental actions parameters in this case, during all the life of the structure presents itself as an unreasonable endeavour. Of course, it is impossible to determine the precise variations of these environmental actions during such a long span design life such as the one projected for an offshore structure. Moreover, it would be imprudent to focus on it as long as the description and calculation on the fatigue processes content a huge inherently uncertainty.

The variation process of the wave and wind magnitudes are known to be stochastic procedures, widely and deeply studied and documented. The value determination process used takes profit of this property, transforming the loads to be determined into stochastic loads, which will be necessary to take into account as so on the analysis.

The verification through the FLS needs therefore of an adequate fatigue load representation method. The expected load history, which is mainly determined by the wind and wave environment, shall be represented by a number of discrete conditions. This method allows a practical way to represent the environmental conditions which will cause the loading. Discretization must ensure a good representation of the load variability. Nevertheless, fine discretization is not necessary, given the uncertainties involved in the magnitude measuring and variability determination.

Each condition that will be taken into account consists of a reference wind direction, a reference wave direction; a reference sea state, including wave height, period, current; and a wind state including defined mean wind speed and standard deviation.

The range of the values included in each discretized condition and the total number of cases considered can influence the fatigue damage determination. Literature proposes orders of magnitude for each of them in this sense. 10 to 50 cases considering 8 to 12 reference directions are considered to be a good refinement. Sensitivity studies can be necessary in this regard.

All the significant stress ranges caused by each of these discretized conditions shall be accounted. The stresses caused by wind and wave should be established by time domain analysis under due consideration of the highly nonlinear motion characteristics of the floater and its interaction with the control system. It is necessary to use site specific environmental data to compute them.

The fatigue damage originated by each must be computed and valued according to the portion of the verified service life time in which they occur, given that it will be the time in which those processes will affect the structure. A probabilistic study is commonly made to determine the expected portion of time that those conditions will have to be accounted.

Moreover, the discretized environmental conditions which will determine the loading on the structure must be categorized in the so called design load cases (DLC). Each of these accounts for the temporary situations corresponding to some ranges of the environmental parameters values which modify the wind turbine service state, and therefore the loads and responses of the turbine control system.

The resulting load effects, which are obtained in form of stresses, produce the fatigue damage which must be carefully computed. The used method are the S-N curves, which provide information about the resistance of the structure to a repeated action. More information in this regard can be found on Section 2.5.1.

A final addition of the damage associated to each design load case shall account for all the required time in the defined fatigue life that has been taken into account in the computations. The comparison of this damage to the maximum allowable fatigue will provide the information regarding the verification of the structure. A result implying the no verification of the structure, and therefore the necessity for a design modification, will mean the repetition of the whole verification process for the new defined structure.

2.7.3.2 Site-Specific External Conditions Determination

The design process of a floating offshore wind turbine is highly determined by the so called site conditions, defined as all the site-specific conditions which may influence the structural design. The most important of the site conditions on a FOWT are the environmental conditions, given its importance over the magnitude and variation of loads.

The consideration of these environmental conditions on the calculation needs of a representation system, which takes into account its magnitudes and properties, along with the physical processes behind them, in order to adapt them into real variables and parameters useful for the future description of its affectation on the floating structure, in other words, the loads determination.

Environmental conditions studied and considered for the calculation of fatigue loads are wind, wave, currents and water levels.

2.7.3.2.1 Wind Climate

The wind climate represents the behaviour of wind for a given geographical location.

Distinctions are made between extreme wind conditions (EWC) and normal wind conditions (NWC). Normal wind conditions refer to the representation of recurrent structural loading conditions. The extreme ones are used to model rare conditions which might happen over the design life, conditioning its resistance. Both are correlated, being possible to extrapolate EWC from NWC.

The details of the normal wind conditions representation system are the ones of interest in the context of fatigue research. Possible extreme conditions are disregarded in this sense, given that the damage caused by them can be neglected.

Therefore only NWC have been treated in this work, which will be explained in detail next.

Representation of normal wind conditions includes the introduction of different parameters. Wind is a stochastic process, and therefore needs to be described probabilistically. A short term and a long term description are defined.

The short term description of the wind climate can be divided on 10 minute periods, for which constant wind states are assumed to prevail. Those states are commonly described by two main parameters: the 10-minute mean wind speed U_{10} and the standard deviation of the

wind speed σ_U. The 10 minute mean wind speed parameter is the mean of the wind velocities measured on that 10 minute period. The deviation of wind speed measure the variability of the registered velocities over the mean. Each of the 10 minute wind states will be then described by an arbitrary stochastically varying set of wind velocities, in consistence with U_{10} and σ_U parameters.

A magnitude of interest is the wind turbulence. It is defined as the natural variability of the wind speed about the 10 minute mean wind speed U_{10} which is characterized by the before mentioned standard deviation σ_U. It informs about the variability of the wind velocity for each short term state. The variability of the wind velocity on the 10 minute period is adequately modelled through a normal distribution.

The long term description consists on the characterization of the stochastic variation of the main values of the short term states along time, without constrictions. Probability distributions for both of the parameters are used. The long term characterization of U_{10} results indispensable. Unless data indicates otherwise, a 2 parameter Weibull distribution can be assumed for the 10 minute mean wind speed U_{10}.

The long term calibration of the wind deviation can also be performed. Usually it is performed via a conditional distribution of σ_U on U_{10} based on a lognormal function.

Calibrations on the function for the obtaining of the long term distribution must be done on the basis of wind data, which is necessary to accomplish some characteristics. The use wind data can be formed of series of empirical statistical data, covering a sufficient long period of time. In this regard, the sensibility of the results depends on the parameter of interest. Codes set 10 years as a minimum. It is of interest to work on data without temporal gaps.

Velocity determination should take profit of all possible information, including measurements, hindcast data, meteorological models and correlation with other available data.

The influence of height on wind data measurements is a decisive parameter. Wind is very sensitive height variations. In this sense, wind speed data at the hub height is of interest. In case of no information available at that point, empirical conversion methods exist, for which it is very important to know the distance at which wind was measured.

A further concept of interest are the reference wind conditions. Those describe a series of values referring long term wind velocity and/or deviation which are to be used for the representation of certain conditions.

Among them, it is interesting to remark the Normal Turbulence Model (NTM), used for the representation of long lasting conditions such as the ones necessary for fatigue design. It represents turbulent wind speeds in terms of a characteristic deviation of wind speed $\sigma_{U,c}$, which is defined as the 90% quantile in the probability distribution of the standard deviation σ_U conditioned on the 10 minute mean wind speed at hub height.

The Normal Wind Profile (NWP) stands out as well. It simply represented the average wind speed as a function of height about sea level, without further characterization. An adequate power law for the vertical distribution of wind must be chosen.

Other reference wind conditions referring to extreme wind conditions exist.

2.7.3.2.2 Wave Climate

Wave climate describes the wave conditions and properties of a specific sea site. It includes the consideration of parameters such as wave height, period and direction.

There are many different parameters which describe these variables. The next statements will refer to them generally, and further reference will be made to them further on this thesis.

Wave climate is characterized in short term by describing the wave height, wave period and direction of origin of a set of waves of an appropriate duration so it can be considered to have stationary conditions. Such a duration is usually framed between 30 minutes and 3 to 6 hours. A shorter muster will imply a lack of enough data to characterize adequately the stationary conditions, and a longer one will imply a loss of them.

The short and long term calibration of the wind climate must be based on specific wave data. Empirical statistical data is normally used as a basis for design. In order to obtain good calibrations, the covered period must be long enough, preferably 10 years or more for long term characterizations.

For the collection of good quality wave data, measurements and hindcast models are considered to be the best methods. The use of hindcast data should be accompanied by calibrations against measured data to ensure its quality. When no on site specific data is available, transformations must be done to adapt the accessible registers to the location of interest. Water depths or topographies, among others, shall be taken into account.

The long term wave climate is described through different probabilistic distributions of the

parameters which define it. Long term distribution of wave height is usually good calibrated with a 3 parameter Weibull function. Wave period usually follows a lognormal distribution conditioned on the wave height. In regard of the direction of origin, it is common to group them on sectors and take probabilities directly from the occurrences on each sector. Other methods of representation consider the use of scatter diagrams.

It must be stand out as well that wave and wave climate are correlated, especially for sea states which are mainly wind originated. A 2 parameter Weibull distribution for the wind velocity conditioned on wave height is often a good calibration.

In the same sense as for wind, reference sea states including characterizations of the values also exist. For the fatigue study, the Normal Sea State (NSS) takes special relevance. A Normal Sea State is characterized by the definition of a wave height representative value, a period representative value and a direction. A wind mean speed is as well statistically associated. Its application on fatigue design requires of the consideration of a series of them, associated with different mean speeds. The number of considered NSSs must be large enough to predict adequately the fatigue life. Some disclosures in this regard are given in further chapters.

The Normal Wave Height (NWH) is the expected value of the significant wave height conditioned on the concurrent 10 minute mean wind speed. The range of wave periods should be based on the possible correlated ones, selecting the ones with the highest loads or load effects in the structure.

2.7.3.2.3 Sea Currents

Sea currents are continuous directed movement of sea water. Despite they might vary within space, are often represented as horizontally uniform flow field of constant velocity and direction, with magnitude dependant on depth.

Currents influence the hydrodynamic system by varying its added mass coefficients, among others. Despite it, for fatigue damage calculation, are considered to be of little importance given inertia dominated wave and small velocities, reason why are ignored

In this sense no further specifications on sea currents modelling is made, but plenty of references can be found on literature.

2.7.3.2.4 Water Levels

For the calculation of the hydrodynamic loading and system response, it is necessary to take into account the water level variation if significant.

There are many characterized water levels. Among them, the Normal Water Level Range results of interest of the fatigue design. It is assumed to be the variation of water level with recurrence period of one year.

2.7.3.3 Design Situations, Load Cases

The determination of loads for fatigue design must take into account the load histories at which the structure is subjected during specific operation conditions that might be necessary to be faced by the structure during its necessary life. The correspondent characteristic load history on each of them is often taken as the load history which is expected to happen, without factorization.

The possible operation conditions are classified into the so called load cases. Each load case defines the loads to be considered for a design situation on a limit state to be proofed. In this sense the groups of load cases sharing design situation will account for the same group of loads, but in different magnitudes depending on which limit state is checked.

The fatigue limit state design load cases will account for the design life of those possible design situation in which significant damage can be produced, including fault conditions. The loads to be considered should be defined such that it is ensured to capture all contributions to fatigue damage.

Of course, the effect of all the environmental loads shall be taken into account, including the combined effect of wave, current, water level, wind or rotor loads.

The here defined load cases have been extracted from the IEC 61400-3, normative which refers to offshore structures, without further details on the floating type ones [135]. The specific codes on floating offshore structures, such as the DNV-OS-J103 [25], do not include an own design load case list, referring themselves to the before mentioned normative, and adding some considerations which might be attended.

As defined in the code IEC 61400-3 the DLC which refer to fatigue are defined next:

- Design Load Case (DLC) 1.2, Power Production

  - Wind Condition (WinC): NTM, $v_{in} < U_{10,hub} < v_{out}$
  - Wave Condition (WavC): NSS, H_S according to joint probability distribution of H_S, T_P and $U_{10,hub}$
  - Wind and Wave Directionality (Dir): Codirectional in multiple directions
  - Current (Cur): No currents
  - Water level (WL): Normal water level range, or above mean still water level

- DLC 2.4, Power Production plus occurrence of fault
  - WinC: NTM, $v_{in} < U_{10,hub} < v_{out}$
  - Wavc: NSS, $H_s = E[H_s|V_{hub}]$
  - Dir: Codirectional, in one direction
  - Cur: No currents
  - WL: Normal water level range, or above mean still water level
  - Other: Control, protection, or electrical system faults including loss of electrical network.

- DLC 3.1, Start up
  - WinC: NWP, $v_{in} < U_{10,hub} < v_{out}$
  - Wavc: NSS (or NWH), $H_s = E[H_s|V_{hub}]$
  - Dir: Codirectional, in one direction
  - Cur: No currents
  - WL: Normal water level range, or above mean still water level

- DLC 4.1, Normal shut down
  - WinC: NWP, $v_{in} < U_{10,hub} < v_{out}$
  - Wavc: NSS (or NWH), $H_s = E[H_s|V_{hub}]$
  - Dir: Codirectional, in one direction
  - Cur: No currents
  - WL: Normal water level range, or above mean still water level

- DLC 6.4, Parked (standing still or idling)
  - WinC: NTM, $V_{hub} < 0.7 \cdot V_{ref}$

  - WavC: NSS, H_S according to joint probability distribution of H_S, T_P and $U_{10,hub}$
  - Dir: Codirectional in multiple directions
  - Cur: No currents
  - WL: Normal water level range, or above mean still water level

- DLC 7.2, Parked and fault conditions
  - WinC: NTM, $V_{hub} < 0.7 \cdot V_{ref}$
  - WavC: NSS, H_S according to joint probability distribution of H_S, T_P and $U_{10,hub}$
  - Dir: Codirectional in multiple directions
  - Cur: No currents
  - WL: Normal water level range, or above mean still water level

- DLC 8.3, Transport, assembly, maintenance and repair
  - WinC: NTM, $V_{hub} < 0.7 \cdot V_{ref}$
  - WavC: NSS, H_S according to joint probability distribution of H_S, T_P and $U_{10,hub}$
  - Dir: Codirectional in multiple directions
  - Cur: No currents
  - WL: Normal water level range, or above mean still water level
  - Other: No grid during installation period

The fatigue load cases accounts for the design of conditions of power production, start up and shut down, parked, transport conditions, and additionally some of those plus the occurrence of fault.

In the power production design situation, the wind turbine is functioning and connected to the electric grid. The loads corresponding to the operating rotor shall be accounted, including mass and aerodynamic imbalances, which are usually provided by the turbine manufacturer.

DLC 1.2 is the FLS load case on power production. Environmental conditions must account for atmospheric turbulence (NTM) and stochastic sea states (NSS) that may occur during normal operation of the wind turbine. The number and resolution of sea states for each wind speed must be adequately considered, given its influence on fatigue damage results. Those must be associated with the full long term distribution of metocean parameters. Codirectionality of wind and wave loads, considered in multiple directions shall account for a good result. Currents are neglected.

DLC 2.4 accounts for a fault occurrence while at power production condition. This involves a transient event, namely a fault or loss of electrical network connection, while the turbine is producing power. Therefore, the consideration of loads variation due to loss of the control or protection system must be done.

In this design situation, DLC 2.4 account for situations where the fault does not involve an immediate shutdown, and a sufficient long situation with the over described conditions is originated, being the production of fatigue damage possible. The likely duration of this situation must be considered when accounting for this DLC generated fatigue damage.

The foreseeable reduced time of actuation of such a situation, in comparison with other DLCs, allows to use less sea states, being it only necessary the use of the expected sea state for each wind velocity, in substitution of a whole probabilistic determination of possible combinations.

DLC 3.1 refers to start up. This situation includes the events resulting in loads during the transient situations from any parked to power production state. The number of events in this regard and its duration shall be predicted based on the control system behaviour, provided by the turbine manufacturer. For this case, as it happened in the fault on power production condition, the consideration of the expected wave height should be sufficient.

The DLC 4.1 is created for the normal shut down cases, different from the emergency shut down, which does not account for fatigue. Normal shut down takes the same characteristics as the previous defined start up load case, but for the process in contrary direction.

DLC 6.4 represents the design situation of a parked wind turbine (without functioning) for fatigue loads. Wind turbine might be standing still (without movement), or idling (internal motors are on, despite not transmitting its power). It must account for the expected amount of time of non-power production, considering all those wind speed which can imply significant fatigue damage on the turbine. Consideration must be given to the loss of aerodynamic damping given the still rotor. Sea states adequately combined with wind cases, using the probabilities obtained through the long term joint distribution, must be used for the loads calculation. The number of sea states must represent correctly the final caused fatigue damage.

The DLC 7.2 takes into account parked conditions with a fault, resulting of malfunctioning on the electrical network or wind turbine. Similarly to the previous case, the expected number of hours of non-power production due to faults shall be considered. The rest of the considerations of DLC 6.4 apply here as well.

Finally, DLC 8.3 accounts for that time in which the structure is subjected to fatigue damage in conditions which cannot be applied to any of the other defined design load cases. This DLC accounts for the hours in which the structures is submitted to transport, assembly, maintenance and/or repair. The no existence of wind turbine loads, or its partial action, must be taken adequately into account. For the environmental loads, NSS condition shall be assumed, determining as usual through the long term joint probability distribution different values to be considered and computed.

2.7.3.4 Load and Load Effect Calculation

Once the concurrent parameters of the environmental processes and the non-stochastic loads are determined, the total values of the added loads that they generate and ultimately of the load effects, must be duly computed. Proper methods, including simulations along time and accounting for the dynamic structural behaviour must be used.

Dynamic simulations utilizing structural dynamic model are usually employed. The characteristic stochastic behaviour of some of the loads can be considered through the input of variable condition values which follow that probabilistic behaviour. In this cases, simulations period must be sufficiently large to account for complete reliability of the process simulation, without letting loads be out of them. In the case of wind, six 10 minutes simulations are commonly considered as sufficient for each mean hub height wind speed and sea state.

2.7.3.5 Limit State Analyses

The limit states design (LSD) procedures, also known as load and resistance factor design (LRFD), are based on the verification of a series of conditions that the structure must accomplish during its service life [19]. These conditions may refer to resistance (ultimate limit state) or operability (service limit state), among others. Loads and its load effects are computed for the studied structure, given the site and operation conditions. Those are compared adequately to the structure resistance.

Partial safety factor method accounts for the uncertainties and variability in loads and materials, analysis methods and the importance of structural components; ultimately reducing the risk of theoretic malfunction.

In this regard, the safety level of the structure is considered to be accomplished when the so called design load effect S_d does not exceed the design resistance R_d. The mathematical expression, which is called the design criterion, is included next.

$$S_d \leq R_d$$

The obtaining of the design load effect S_d and the design resistance R_d respond to prescribed methods.

On the case of the design load effect S_d, it might correspond to one of two different calculation methods. On one hand, the multiplication of the characteristic load effect S_k times the load factor γ_f, resulting into the next expression.

$$S_d = \gamma_f \cdot S_k$$

Or to the realization of a structural analysis using as input the result of the multiplication of the characteristic load F_k times the load factor γ_f, which is next mathematically stated.

$$Fd = \gamma_f \cdot F_k$$

The load factor γ_f is always larger or equal to 1, resulting on a design value greater than the characteristic one.

The use of one of other method depends on the analysis type. Both of them magnify the load, differing at which point of the analysis this consideration is done, before or after the structural analysis. In this regard dynamic and nonlinear problems will usually take to term the structural analysis first, in order to obtain the best possible modelling of these behaviours, and apply alter the load factor over the analysis' resulting load effects. Other types of analysis tend to use the method where the analysis is performed with the load already magnified.

The design resistance computation is computed on a similar way. For its case, the design resistance is computed through the division of the characteristic material strength f_k over the material factor γ_m. This material factor γ_f is always greater than 1, resulting into a design material resistance smaller than the characteristic one.

Further reference is made on to these procedures on the literature.

In the case of fatigue analysis the parameters on the load effect versus resistance comparison account for the damage obtained for the wind turbine on a specific location during the required service life, and the maximum damage as specified by the codes. The material factors respond to different value proposals that can be found on the codes.

3. WindCrete Fatigue Design Approach

3.1 Introduction

A fatigue resistance analysis, taking into account the related established verification and design recommendations, has been performed on the WindCrete conceptual proposal of floating offshore wind turbine structure.

The literature and past experiences on the analysis of floating offshore wind turbines are limited and scarce, moreover almost inexistent or impossible to access for concrete spar type turbines. In this sense, the resulting work performed for this thesis, as presented in this chapter, can be regarded as a methodology proposal.

Its elaboration introduces some new procedures, which are based on the behaviour of the concept and on existing literature. Each of these methodologies have been properly analysed in terms of adequacy and results reliability. In some cases, decisions between problem approach procedures had to be made. The knowledge used on the possible choices, has resulted most of the times result of proof and error processes. Those are presented and adequately commented, given the experience that different attempts has provided.

This fatigue analysis and verification method proposal has tried to be as close to a real engineering method as likely; describing the reality as best as possible, and trying to be conscious of the reliability of the results obtained. Providing the best possible engineering results which shall be applicable to a real structure has been the final objective. Considerations and hypothesis have been set out in this sense, and reference to them is made along the different explanations regarding the steps followed which are included in this chapter.

The methodology used, along with the numerical result of its calibration and application are presented. The methodology has been used for the analysis of a real service condition of the WindCrete structure.

3.2 The WindCrete Concept

WindCrete is the commercial name given to the concrete floating offshore wind turbine structural concept developed by researchers of the Barcelona Civil Engineering School (*Escola Tècnica Superior d'Enginyers de Camins, Canals i Ports de Barcelona*) of the *Universitat Politécnica de* Catalunya [136] [137].

Based on the flotation principle of a spar buoy, the WindCrete takes profit of the concrete advantages in the offshore environment in order to reduce construction and maintenance costs, and increase its lifetime.

It presents an annular cross section on a monolithic design, combining together substructure and tower. The absence of joints allows to cut down montage costs and simplify the fabrication process; while offering less weak points, in which the durability, especially given the importance of the fatigue processes, of the whole structure could be compromised.

The general dimensions of the structure respond to its resistive behaviour, hydrodynamic properties, movement response on service state, and its constructive costs. The solution adopted accounts for a balance between draft (height below water level), which helps reducing the material cost and the pitch and roll eigenperiods; and the total amount of material needed.

A 217.7 m large structure is designed, presenting a height of 87.7 m above the mean stillwater level (MSL), and a correspondent draft of 130 m. A distance of 25 m has been planned between the lowest position of the wind turbine blades and the MSL, allowing for rotor diameter of up to 130 m.

Three different volumes compose its structural body. A cylinder acting as a floater, a slender cone which takes the function of the tower supporting the turbine, and a short length cone which acts as transition piece between floater and tower.

A cylinder on the lowest part takes the function of supporting floating substructure. It is designed with an external diameter of 13 m, a ring thickness of 50 cm, and a complete length of 113.5 m. The bottom part of this cylinder ends on a semi sphere, which provides advantages on hydrodynamic and resisting terms.

The thickness of 50 cm extends itself on the transition cone, and further on the first meters of the tower. The transition cone, present a lower cross section with diameter 13 m, as correspondent to the cylinder, and a superior one of 10 m, coinciding with the tower base. It allows optimizing the structural response, by reducing prestressing losses and deviation forces.

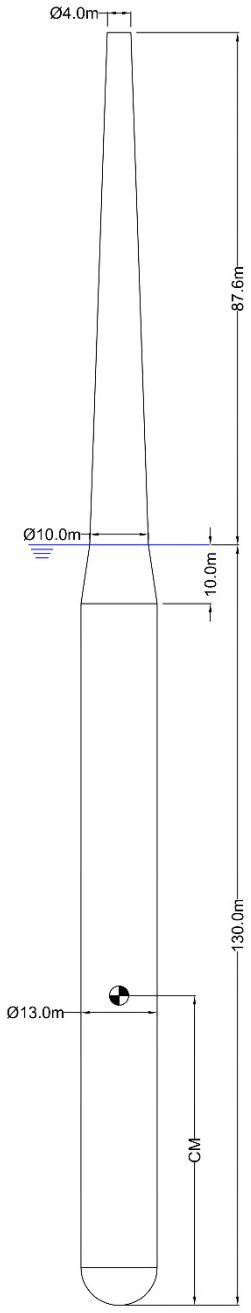

Figure 12 General dimensions of the WindCrete coneptual structure for FOWT *[143]*.

Its total length is 10 m.

The tower is planned on a length of 87.7 m. As correspondent, the diameter at the base of the tower is 10 m, while a 4 m one is presented on its superior part, where the top of the complete takes place. A thickness of 40 cm is defined for the tower walls, except for the first meters after the transition cone where a progressive reduction of it is designed to converse the 50 cm present on it. Figure 12 includes a sketch of the structure along with its dimensions.

Its modelling has accounted for some simplifications in the regard of some complex geometrical details or some concept phase inherent undefined aspects, which are needed for the correct structural analysis. Sizes and dimensions have been taken as detailed on the over description paragraphs, except for bottom part, where no semi sphere or closing has been modelled, considering it as a cross section with the same properties as the cylinder. The thickness transition part is considered to extend itself along the first ten meters of the tower base, on a linear behaviour.

The prestressing modelling of the structure needs of some further specifications and considerations, given that it depends of its spatial location. Further reference to considerations relating its implementation and computation are given in Section 3.5.2.

In the same sense, the definition of a material resistance for the employed concrete will result of the specific design for the proposed location. As for a coherent value which shall serve to obtain coherent results, a value of $f_{ck} = 60\ MPa$ has been used, given the necessity of the concrete to resist high magnitude loads and the large compressive stresses of the prestressing.

3.3 Fatigue Load Determination Approach

3.3.1 Introduction

A method for the verification of concrete floating offshore structures is proposed in this thesis. It treats important and complex aspects such as the determination of the environmental conditions on the structure, for which probabilistic methods are used; and its posterior computation as load effects. Ultimately, the information obtained is used to compute the fatigue damage on the structure.

Solving such a problem requires of the proposal of different conditions. Some hypothesis on the problem have had to be made. WindCrete is at the time of publication of this thesis a concept with much development and growth potential, without any real economic or social conditionings that would appear on a real installation project. In this sense, conditionings as localization have been simply proposed and taken adequately into account. Reference to them is made on Section 3.3.2.

Once an adequate localization is known, an analysis of its environmental conditions has been performed. Real data including registers of the environmental parameters describing the wind and wave conditions has been employed. The particularities of the data used and its implications are detailed on Section 3.3.3.

Finally, the available site real data is used to perform a statistical analysis of the combined wind and wave climate, from which the series of adequately discretized sea states and its probability of occurrence is determined. Those will be used on the upcoming section to perform the load effect and damage computations. Details and considerations employed for the definition of the sea states are included on Section 3.3.4.

3.3.2 Spatial Location

A complete fatigue analysis requires of a full description of the service conditions. In this sense, given the conceptual phase of the WindCrete, a placement for the structure has had to been selected and characterized in order to be able to propose a real approach with all the possible engineering considerations.

This thesis has proposed a location in this regard, ensuring its compatibility with the structure and taking into account potential zones where it could be used and the benefits of this

concept would be greater than other alternatives.

In this regard, a local application of the structure has been seek, by selecting a spot on the Gulf of Lion. This gulf is located on the north part of the Mediterranean Sea, mainly containing the French coast of the Languedoc-Roussillon and Provence regions, with chief port on Marseille. It reaches the northern Catalan coast on the east (north of Spain) and the French city of Toulon in the west.

This gulf is known for its richness on high wind velocities on the Mediterranean Sea, being the best location to make the most profit of a wind turbine.

As commented on Chapter 1 WindCrete is designed to be applied on zones with special oceanic conditions. In this sense, the problem proposal has accounted for this necessities. A minimum water depth of 150 m is needed, which accounts for the structure length and the maximum possible vertical oscillations. Nevertheless, its installation process requires of an extra amount of 50 m. No restrictions are posed on the distance to coast, although some considerations are made. A minimum distance of approximately 30 km is proposed to avoid visual landscape perturbations from the coast. On other sense, large distance will increase the transportation and construction costs, as well as the maintenance ones. The cost of the electrical connection cable will be increased as well. Other factors as maritime navigation or environmental properties shall be also taken into account.

The continental shelf of this wind-rich zone named gulf of Lion is a wide coastal plain, with water depths of 50 m at approximately 15 km of the coast, and an offshore zone starting at 100 m depth at 60 km distance coast distance where the slope rapidly increases to the Mediterranean abyssal plain, reaching the 500 m depth in almost 10 to 20 km.

Nevertheless, the south east limiting zone of the gulf of lion, which extends itself to the northern part of the Girona coast in Catalonia, presents water depths of 200 m at 15 km from the coast, coinciding with the zone where the large slope to the abyssal plain start.

Considering the exposed factors, which include a perfect water depth that allows installations without unnecessary costs; an adequate distance to the coast, which avoids excessive maintenance and installation cost, but eliminates the visual contamination; and enough wind profit; a spot in the mentioned north Catalan coast will be selected for the realization of the practical application of this thesis.

As for a specific location, other conditions that are not object of study of this thesis, such as economic and production optimality, would define it. The calculations performed in the next

chapters have accounted for the environmental data of a specific point, as specified in the next chapter. For practicality reasons, that could be considered the precise location of the wind turbine.

This water zone has been selected for the placement of the wind turbine, and therefore the problem to be faced will consist of the structure placed on this sea zone, and therefore subjected to its environmental conditions.

3.3.3 Environmental Data

Real environmental data has been used for the development of this thesis. Given the, in the over chapter, proposed location for the wind turbine, and taking into account the database requirements specified on chapter CC the best possible source has been used.

The meteorological and physical oceanographic (metocean) parameters necessary for the fatigue design process have been obtained from the *Puertos del Estado* database. *Puertos del Estado* is the public organism in charge of the Spanish port system. Additionally, they develop and manage oceanographic measure and prevision systems, which result into a large database of metocean parameters that is constantly being updated. Other information sources have been as well considered, remaining this one as the best one for the purposes of this thesis, taking into account the relation between quality and facility of access.

For the proposed region on the previous chapter, hindcast models and buoys measurements have been found on different points. A point with related metocean information from a hindcast model has been selected. In this regard, a proposal of wind turbine placement on that spot would make sense when trustworthy data is important. It could be used as well for wind turbine sin its proximities, given that no better information source is available.

Hindcast models are able to produce metocean data of the past years, being able to approach those geographical places or time interval where no measured information was available, and coinciding with the one measured or known.

For the problem faced in this thesis, the output data of a hindcast model has been considered to be better, given the longest span of year covered, a good temporal density of values and a larger geographical cover, approaching to the potential desired installation point of the wind turbine.

Given its predictive characteristics, hindcast models can lead to some error or bias on its

data. In this sense caution shall be taken when using its data. A validation of the metocean parameters with some close measuring point is always desired. No further checks have been made for the used set of data, assuming that the public organisation who manages has taken care of not spreading data with unchecked sources of unreliability levels.

The metocean parameters dataset used responds to the *Puertos del Estado* SIMAR database. It contains simulated time series of a wide of wind and wave parameters. The simulation offers parameters covering the time span between 1958 and the actuality, being actualized every day. Data is presented on from 1 to 3 hours intervals.

Further explanation can be found regarding some details about the specifics of the computation numerical model, like resolutions or input data among others.

The data provider gives as well advice on the use of the data and warning possible loss of reliability of the data for some situation. Those have been considered when using the data.

In this sense the wind model does not take into account geographic height variations extended on less than 50 km, which happen to be 20 on some cases. Convection local processes of wind are as well not taken into account. Despite it, good representation of local winds and sea precedent winds is made. The wave models output must be consider as data on open water with undefined water depths. For both measures, the peak values are normally underestimated. Wind data is given at 10 m height.

The output wave data consists of the spectral parameters of each 1 hour considered sea state, consisting of the next stated variables.

Regarding wave data:

- Hm0: Spectral significant wave height (0.1 m resolution)
- Tp: Spectral peak period (0.1 sec resolution)
- Tm02: Spectral mean period, moments 0 and 2 (0.1 sec resolution)
- DirM: Direction of wave (1º resolution)
- ‘Var’_V: Height and direction of sea waves (same resolution, incomplete set)
- ‘Var’_M1/2: Height, peak period and direction of swell waves on 2 possible different contributions (same resolution, incomplete set)

In relation to wind:

- Mean wind velocity (0.1 m/s resolution)
- Direction of wind (1º resolution)

The exact set of data used corresponds to the SIMAR 2126144 hindcast model point. It corresponds to a location with coordinates 3.50º E 42.00º N, 25 km away of the city of l'Estartit port and 40 km of the Roses city port. It corresponds to a water depth of 200 m.

The dataset includes hourly measures from 1958 to 2016, resulting in a total of 505 044 registers, corresponding to short term characterizations of hourly time periods, from which only the values related to significant wave height, mean period, wind velocity and directions of precedence of both wind and waves. No interest has been found on the direction of the waves given by the sea and swell separation variables. In this regard, wind and wave correlation have been found separately.

3.3.4 Long Term Wave Climate Characterization

3.3.4.1 Introduction

The fatigue analysis procedure needs of the modelling of the environmental circumstances at which the structure will be submitted along its total service life. As stated on previous chapters, these environmental circumstances translate into the long term probabilistic environmental load determination of the structure.

This procedures involves the characterization of the long term wind and wave climate, taking into account the combination of both of them, in order to determine a probabilistic discretization of the possible sets of waves and wind conditions acting together given through its parameters. The procedure applied and considerations taken regarding this computations are detailed in this section.

This proceeding will conclude on the assumption of year probabilities of each set of data considered, for which the long term distribution will be assumed to be representative of the one year behaviour, and rare events with no probabilities of occurring during the year will be disregarded.

The output data of this proceeding will consist of a series of wind and wave variables set,

with the year probability in time that have of acting together. They will represent the time of year with a wind sea state on properties whose short term characterization would results into the parameters defining it. Each set will be represented by a central value, considering the data values on the range between minus half the resolution and plus half the resolution of each parameter. Further reference in this sense will be made on the next chapters.

Therefore, the year load consideration distribution will be performed through the assignation of an actuation time span to each set of variables, obtained from the year probability of actuation of the given set.

The load effect of each of this data will be obtained through the model that will be presented in Section 3.4.1. It is a dynamic rigid body model, with good levels of reliability. Each of the variable set will be introduced as environmental loads or conditions on the model, which will carry a simulation on an adequate period of time. The load effects obtained from this simulation can be then extrapolated to the real time span in which the given set of load acts. The details and considerations which have been taken in this process are later explained.

As an ultimate output of the final phase, fatigue damage can be adequately computed and added for each of the variables set. A year damage will be obtained, from which the resisted fatigue life of the structure will be easily calculated.

These final results will cover the load effects resisted by the structure during its whole life, and will take into account on a reliable manner the influence of the temporal varying environmental loads on it.

A Matlab code has been carefully created to automatize this procedure, resulting into an easy tool to obtain precise results, allowing as well to realize sensitivity analyses in an easy way.

3.3.4.2 Previous Considerations

The long term characterization of the acting set of environmental loads parameters has been performed on a probabilistic basis, fitting adequately different sets of functions to the available data.

The good behaviour of those functions when representing phenomena such wind and waves has been taken into account through the selection of the literature recommended distributions and the validation of its data fit.

The parameters which the dynamic analysis model needs for a correct simulation and the adequate representation of the environmental loads are:

- Wave Height
- Wave Period
- Wind Mean Velocity
- Wave Origin Direction
- Wind Origin Direction

Some adjustments have been made to the original database set in order to adequate it to the type of analysis which carries the model and the relation between result reliability and computational cost. Those adjustments consist basically on the selection of the appropriate sea state description parameters and on the group of data with an excessive resolution.

As mentioned in previous chapters many different parameters can describe the short term characterization of wave state. A variable regarding wave height and wave period has had to be selected. Most of the codes regarding offshore wind turbines design recommend the use of the significant wave height and the peak spectral period. Significant wave height correspond to the mean of the greatest 1/3 of waves registers on a stationary short term wave state. Peak period correspond to the period of the set of waves which contains the most quantity of energy among the different registered short term waves. These are parameters which present values over the mean wave height and wave period values. Its application results into a good representation of the real transmission of wave energy into the analysed structure for irregular waves.

Nevertheless, the model that will be used for the dynamic calculation of the load effects on the turbine does not introduce irregular stochastic wave loading, introducing instead regular deterministic waves. The modelling of each of the combined metocean parameter set will then apply a load resulting of a constant regular wave with constant parameters. In this regard, if these constant wave parameters are the significant height and the peak period, a overestimation of the loads over the structure will be made, given that much more waves with those parameters value will be applied that the ones acting on reality. If irregular wave would be being modelled, introduction of significant wave height and peak period will make sense given that the introduced model waves would be stochastically defined from those parameters.

In this situation, an energetic criterion has been sought to define the parameters that would define the modelled constant wave. The root mean square wave height has been selected for the wave height, and the mean period for the wave period. Root mean square wave height is

computed as the root mean square value of all the wave height acting on a stationary short term sea state. It gives a good approximation on the energetic content of the mean energy content of each of the waves loading the structure, given that the wave energy is proportional to the square of the wave height [138], and results therefore into a good way of modelling the energetic transmission of each wave of the short term stationary sea state when modelling it as a constant wave set. The mean period is computed as the mean of all the periods of the set of waves. On the constant wave model, period will determine the frequency of wave repetition, which results into an important parameter for fatigue design, given that the frequency of load cycles will be critic for fatigue assessment.

As a conclusion, the root mean square wave height and the mean period have been selected, given that are the best parameters to model the energy contained in the waves of a stochastic irregular sea state into a deterministic constant waves set.

3.3.4.3 General Description

A general description of the procedure to be followed is made.

On a previous stage the parameters of interest will be selected, computed and/or transformed, to obtain the best possible configuration of data properties for the modelling.

Once the variables registers are presented on the way of interest, combined probabilities of occurrence for each of them calculations will be performed. This proceeding involves on a first stage the calculation of the probabilities of occurrence of the wind and wave direction, which are directly computed taking into account the number of occurrences for a given direction and the total number of occurrences. On a second phase, for each direction of precedence, the different variables are fitted to continuous statistical distribution functions, alone and combined depending on its behaviour. Discrete probabilities of the desired resolution are then taken for each set of combined variables, which will be valid for each direction. Combinations with extrem low occurrence are disregarded. A multiplication of each discrete probability per the probability of occurrence of its direction will provide the total probability. At the end, a series of values sets, whose probability sum is the unity will be obtained. That probability will then be associated to the yearly probability of occurrence.

Regard on the specific details to all of these procedures chapters is made on the different next sections.

3.3.4.4 Data Processing

It is necessary to set an adequate format of the metocean registers in order to obtain properly results. This involves some computations, transformations and groupings.

The resolution of the presented data is analysed. Regarding the one of wave height, wave period, and wind velocity resolution, is not a problem, given that it will be fitted to a continuous distribution. Nevertheless, for procedure directions of both wind and waves, the probability distribution is made directly on a discrete basis.

Therefore, the 1 degree resolution results excessive, given that it would imply 360 directions of precedence. This would result inviable in terms of capacity computation and result reliability.

A 16 section distribution of possible directions of precedence has been performed on the available data. Sectors including 22.5º ranges are in consequence created. As for its reference, they have been numbered from 1 to 16. Number 1 sector is centred on the north direction of precedence, including values from -11º (349º) to 11º. Number 2 includes value from 12 º to 34º, being centred at 22.5º (NNE). The rest of the section include the different origins in clockwise direction.

Information about the wave height register is provided on terms of the significant wave height. Being of interest the computation in root mean square wave height, a transformation must be done. Significant and root mean square height are spectrally related, when describing the same short term stationary set of waves. Many approximations can be found on the literature, depending on different parameters. The next transformation has been used.

$$H_{RMS} = \frac{H_S}{1.35}$$

This relation is theoretically obtained and valid for not too steep waves in deep water [138], conditions which are accomplished in the problem solved.

Wave period can be directly found as mean period of each short term stationary measured sea state on the database, and will be directly employed as so.

For mean wind speed, the analysis procedures requires the 10 minute mean wind speed at hub height, as explained in Chapter 2. The values contained in the database are 1 hour mean speeds at 10 m of height. A transformation regarding averaging period and height has to be done.

For this objective, a wind profile power law that can account for mean period modifications will be used. The wind profile power law determines the relation between the wind speeds at different heights. Many of them can be found on the literature, accounting for different conditions.

In this resolution process the so called Frøya wind profile has been employed [131]. It is a special version of a logarithmic wind profile, being the best documented profile for offshore locations and maritime conditions. Literature recommend its use for such placements unless data does indicate other way. The expression stated next is used to transform the one hour mean wind speed U_0 at height H above sea level with averaging period $T_0 = 1$, to the mean wind speed U with averaging period T at height z above sea level.

$$U(T,z) = U_0 \cdot \left\{1 + C \cdot \ln\left(\frac{z}{H}\right)\right\} \cdot \left\{1 - 0.41 \cdot I_u(z) \cdot \ln\left(\frac{T}{T_0}\right)\right\}$$

Where $U(T,z)$ is the output wind speed for averaging period T and height above sea level z; U_0 is the output wind speed with averaging period T_0 (being $T < T_0$) on a height above sea level z; and C and I_u are parameters depending on different variables as stated next.

$$C = 5.73 \cdot 10^{-2} \cdot \sqrt{1 + 0.184 \cdot U_0}$$

$$I_u = 0.06 \cdot (1 + 0.043 \cdot U_0) \cdot \left(\frac{z}{H}\right)^{-0.22}$$

For the calculations to transform the database values to the conditions of interest, the next numerical values have been used.

The original conditions parameters are

$$T_0 = 1\ h$$

$$H = 10\ m$$

Which must be transformed into

$$T = 10\ \text{min} = \frac{1}{6}\ h$$

$$z = 100\ m$$

Resulting into the final formula given through the next expression

$$U\left(T = \frac{1}{6}, z = 100\right) = U_0 \cdot \left(1 + 0.132 \cdot \sqrt{1 + 0.184 \cdot U_0}\right) \cdot (1.027 + 0.0012 U_0)$$

3.3.4.5 Direction Classification

The origin direction of wind and wave of each register for the analysis is considered by means of a previous classification. Each origin direction is treated independently, for which the registers are classified depending on the direction group at which they belong.

Two types of analysis can be performed, resulting into two different classifications: a codirectional study and a bidirectional study.

The codirectional analysis assumes collinear wind and waves directions, for each single register. This method is accepted by many codes as long as wind generated sea is predominant. By making this assumption, and solving the problem as so, this previous step classifications results into 16 different groups of values, whose parameters will be fitted individually. The wave direction is disregarded, taking into account the wind direction for this classification.

The bidirectional analysis assumes the possibility of different origin directions for wind and waves. The resulting classification generates a maximum of 256 possible groups of values, being combinations of origin directions of wind and waves. Each shall be fitted individually.

By proposing two different ways of solving the problem it is pretended to analyse the different behaviour of the method for both assumptions. Nevertheless, the modelling of the sea states accounted by a bidirectional description of the joint long term wind and wave environment has resulted to be extremely time consuming in computational terms, for which the use of its results on the context of this Master Thesis has been disregarded.

In this step, additionally, the probability of occurrence of each origin direction has been considered. It is assumed, that the statistical muster is a sufficient large representation of the population, being possible to directly determine the probability of occurrence by dividing the registers on each direction (or direction combination) among the total number of registers. The sum of the probabilities of all the origin directions shall be therefore one.

Once the probabilistic analysis has been performed for the values of each direction, the total probability of occurrence of each of those values will be result of multiplying the probability obtained from the distributions for that direction times the probability of occurrence of that direction.

As an example, the results on probabilities of directions groups for the studied data has been included in Appendix A. It is easy to see, that the greatest number of occurrences happen to come from the northern direction. Adding the three more northern sectors a 40 % of probability is obtained. This fact results to be coherent with the location being studied, known for the

abundance of north origin direction of local winds, which is the so called tramontane. As a further validation step, a quick comparison with the wave rose of measurements in the zone show this tendency as a clear fact.

3.3.4.6 Distribution Data Fit

The long term characterization of the wind and wave joint climate consists on the long term probabilistic definition of each of its parameters, alone and acting together. This definition consists into the fitting of the wave and climate short term defining parameters on probabilistic distributions, from which the long term variation of them will be obtained. This classification is made independently for each classified group of data sets, which could correspond to a origin direction (wind and wave codirectional) or group of origin directions (bidirectional analysis, wind and wave separately).

The short term parameter independently fitted into its long term distribution are wave height, presented as root mean square wave height; and the wind velocity, given as 10 minute mean wind velocity at hub height.

Wind velocity and wave height correlated, reason why it is needed to obtain its joint probability distribution. A bivariable fit of those parameters will be made, based on the conditional distribution of the velocity on the wave height.

Finally, the wave period is taken into account as variable dependant on the wave height. For this reason, it will fitted to a conditional distribution of the wave period based on the wave height distribution.

The fit of the data regarding each parameter to the distribution consists on the determination of the parameters which describe a function that better represents the group of values of the registers. Therefore, so many sets including the same parameters on different values as direction groups will be obtained.

There are many methods to compute these parameters, from which the most common are the Method of Moments (MoM), the Least Squares method (LS), and the Maximum Likelihood Estimation (MLE) [130]. Some of its characteristics have to be attended.

A fit through the MoM the distribution parameters are estimated from two or three first statistical moments of the data sample; namely mean, variance and skewness. The fit at the modes values of the distribution are ensured to be of high quality. LS method ensures the

minimum value of the sum of square errors for each fitted point. It usually gives very good fits on the tails of the distributions. MLE method consists on the maximization of a likelihood function for the obtaining of the fitted point through the function. It presents advantages, but its application is not always feasible.

The fitting of the different parameters to its function has been performed using the least square method. It ensured good quality results on an easy and comfortable implementation, along with better fit on the tails of the function, which results to be really interesting for the Weibull functions defining wind and wave variability.

The parameter determination process has been implemented on the code through the fitting of the cumulative distribution function to the points formed by the values of the cumulative observations.

Mathematically this process involves the next step. A set of observations of the given variable x are given. These observations are classed, meaning that they are measured on an exact adequate resolution, and more than one observation in each class is normally obtained. The number of observations in each class (observations of the same value) is denoted as n_i, where i is the class number index. Each class mid point (the observed value) is represented as x_i. The cumulative observations for each class value are computed, obtain the points that would form a discrete cumulative distribution function. Its mathematical expression results in the next equation.

$$F_i = \frac{\left[\left(1 + \sum_{j=0}^{j=i-1} n_j\right) \cdot \sum_{J=0}^{J=i} n_j\right]^{\frac{1}{2}}}{N+1}$$

Where the points correspondent to the percentage of values equal or under the observed class mid point are computed; being $N = \sum n_i$ and $n_0 = 0$.

Once the set of points including mid class and percentage number of observations is computed the fitting correspond to the parameters of the distribution that minimize the next expression.

$$\sum_{i=1}^{i} \delta_i^2 = \sum_{i}^{i} (F_i - F(x_i; a, b, c))^2$$

Where a, b and c represent up to three possible parameters of the distribution function.

The minimization is taken to term with the Matlab function *lsqcurvefit*, which solves

nonlinear least-squares problems on a comfortable input output scheme for data-fitting problems.

Some other considerations have to be taken into account on the detail fit of each of the variables. Along it, the theoretical background, the details and the results of each of the fit processes are explained in the next chapters. Consideration must be given that the process explained next are referred to each direction or group of origin directions, and therefore will have to be taken to term for each of them.

Obtained results for the fit resulting distributions parameters for each of the considered variables and combinations have been included in Appendix B.

3.3.4.6.1 Wind Velocity Fit

The long term variation distribution of the 10 minute mean wind velocity U_{10} at a height z above sea level can be represented by means of a 2 Parameter Weibull Distribution.

The 2 parameter Weibull distribution takes the next probability density function and cumulative density functions for a given aleatory variable x.

$$f(x;\alpha,\beta) = \frac{\beta}{\alpha}\left(\frac{x}{\alpha}\right)^{\beta-1}\exp\left(-\left(\frac{x}{\alpha}\right)^{\beta}\right)$$

$$F(x;\alpha,\beta) = 1-\exp\left(-\left(\frac{x}{\alpha}\right)^{\beta}\right)$$

Which are valid for $x \geq 0$; and where $\alpha > 0$ is the scale parameter, and $\beta > 0$ is the shape parameter.

The fit is performed for $x = U_{10}$ following the procedure described on the previous section.

Parameters α and β are obtained for each of the directions or group of directions defined.

3.3.4.6.2 Wave Height Fit

The long term variation distribution of the wave height, represented through the root mean square wave height for our purposes, can be represented through a 3 parameter Weibull distribution.

The probability density function and cumulative density functions of the 3 parameter Weibull distribution are given next for an aleatory variable x.

$$f(x;\alpha,\beta,\gamma) = \frac{\beta}{\alpha}\left(\frac{x-\gamma}{\alpha}\right)^{\beta-1}\exp\left(-\left(\frac{x-\gamma}{\alpha}\right)^{\beta}\right)$$

$$F(x;\alpha,\beta) = 1-\exp\left(-\left(\frac{x-\gamma}{\alpha}\right)^{\beta}\right)$$

Which are valid for $x \geq 0$; and where $\alpha > 0$ is the scale parameter, $\beta > 0$ is the shape parameter, and $-\infty < \gamma < \infty$ is the location parameter.

The fit is performed for $x = H_{rms}$ following the procedure described on the previous section.

Nevertheless, some appreciations must be done regarding the fitting of short term wave height data to the 3 parameter Weibull distribution, which relate to the location parameter γ. The distribution allows some of the observations to lie below a threshold, meaning that a computation of probabilities will give null probability to those values. This threshold is controlled by the location parameter γ. For its properly determination, a threshold probability level F' will need to be defined on the fitting process, which will indicate which points will remain excluded.

For the purposes of this thesis, a value of $F' = 0.2$ has been used, as it appears to be the standard suggested value on the literature [139].

Parameters α, β and γ are obtained for each of the directions or group of directions defined.

3.3.4.6.3 Wind Velocity on Wave Height Conditional Fit

The computation of the joint long term distribution of wind and wave parameters, requires to relate statistically both of them. A conditioned distribution of wind velocity on wave height is proposed by the literature and used in this procedure for that matter.

Given a wave height, represented through the root mean square wave height, the variation of wind speed registers follows a 2-parameter Weibull distribution.

The conditioned relation has been performed by means of a method which relates the statistical parameters of the 2-parameter Weibull to the wave height value, which result into the

definition of its parameters α and β as a parametrised function of H_{RMS}. The mathematical expressions of such an approach are stated next, for the regarded variables.

$$f_{U_{10}|H_{RMS}}(u|h) = \frac{\beta}{\alpha}\left(\frac{u}{\alpha}\right)^{\beta-1} \exp\left(-\left(\frac{u}{\alpha}\right)^{\beta}\right)$$

$$F_{U_{10}|H_{RMS}}(u|h) = 1 - \exp\left(-\left(\frac{u}{\alpha}\right)^{\beta}\right)$$

$$\beta = c_1 + c_2 \cdot h^{c_3}$$

$$\alpha = c_4 + c_5 \cdot h^{c_6}$$

Where c_i with $i = 1, \dots, 6$ are the parameters which will need to be calibrated in order to fit the conditioned distribution of wind speed on wave height.

The fitting process has been performed following the general guidelines provided on the previous chapter. Nevertheless, the conditional character of this function requires of some additional computations on different intermediate steps which are worth mentioning and explaining.

The ultimate parameters of interest which are to be obtained are the c parameters, ranging from c_1 to c_6. This implies a different fitting from the one performed in the previous individual calibrations. Here, instead of points x_i of a given variable and its observed F_i, the calibration consists of points x_i, where $x_i = h_i$ for each observed class i of h, and the parameters α_i and β_i, which represent the distribution of the different values of u for each observed class h_i.

Therefore, a previous calibration process has to be performed. So many 2 parameter Weibull distributions as observed classes of h will need to be calibrated. This calibrations have been performed following the Method of Moments instead the Least Squares method, as recommended by literature. This process has consisted on the computation of the mean and the variance of each set of observed wind velocities on the same wave height. Once mean and variance are computed, the values of the parameters α and β of the 2 parameter Weibull distribution of the wind velocity for each observed class of wave height can computed solving the next nonlinear system of equations.

$$E(u) = \alpha \cdot \Gamma\left(1 + \frac{1}{\beta}\right)$$

$$Var(u) = \alpha^2 \cdot \left[\Gamma\left(1+\frac{2}{\beta}\right) - \left(\Gamma\left(1+\frac{1}{\beta}\right)\right)^2\right]$$

Where $E(u)$ is the mean of the wind speed values registered for a given wave height, and $Var(u)$ the variance of them. Γ refers to the gamma function.

The *fsolve* function of Matlab has been employed for the resolution of the different systems.

At this point of the calculation process, the α and β values of the 2 Parameter Weibull distributions of wind velocity for each given observed class of wave height have been computed. This results into a set of 3 variable points (h, α and β) including so much values as observed classes of wave height.

Consideration has been done here to the variations of the register's value. In some cases, the number of registers to be fitted appeared to be very small in comparison with other fits, resulting into a wave measured class with only a little quantity of wind measurements associated, and resulting parameters α and β presenting rare values. Two possible sources for this behaviour have been identified. On one hand, a small availability of data due to the residual character of the studied direction, which only contains a few states each year. On the other, the apparition of extreme value measurements on a random basis, which conditioned significantly the posterior final calibration. As for the purpose of modelling the fatigue life loads, the considerations of one of these extreme measurements on the calibration would suppose a deviation of the final distribution, resulting into average greater values of environmental magnitudes. Therefore, given the small probability of occurrence of those extreme events on a yearly basis, they have been disregarded when selecting the points of h, α and β to be fitted.

Once this refinement has been taken to term, the fit of the c parameters has been taken to term following the least squares method as proposed on the previous section.

This results into the determination of 6 c parameters for each direction or origin direction group, which will define the conditional distribution of wind velocity on wave height.

3.3.4.6.4 Wave Period on Wave Height Conditional Fit

For wave climate characterization, the wave period is known to be approximately linear dependant on the wave height. Therefore the probabilistic long term characterization of wave

period is only sensible if it is conditioned on the wave height.

For this purpose, literature proposes a lognormal distribution of the wave period conditioned on the wave height value. This approach is named Conditional Modelling Approach, for which further information can be found on the references [140]. Given a wave height, represented through the root mean square wave height, the variation of wave period registers follow a lognormal distribution.

On an analogue process to the one performed in the previous section, the mean μ and standard deviation σ of the lognormal distribution of the wave period will vary accordingl with the value of the wave height. This relation will be computed through the calibration of different parameters which relate the wave height to μ and σ. The mathematical expressions on of this approach result as follow for the wave period T_m.

$$f_{T_m|H_{RMS}}(t|h) = \frac{1}{\sigma \cdot t \cdot \sqrt{2\pi}} \cdot \exp\left\{-\frac{(\ln t - \mu)^2}{2 \cdot \sigma^2}\right\}$$

$$F_{T_m|H_{RMS}}(t|h) = \frac{1}{2}\left[1 + \operatorname{erf}\left(\frac{\ln t - \mu}{\sigma\sqrt{2}}\right)\right]$$

$$\mu = a_0 + a_1 \cdot h^{a_2}$$

$$\sigma = b_0 + b_1 \cdot \exp(h \cdot b_2)$$

Where a_i and b_i with $i = 0, 1, 2$ are the parameters which will need to be computed in order to obtain the distribution of wave period on wave height.

A conceptually similar procedure to the one detailed on the section dedicated to the wind speed conditioned distribution on wave height has been followed here.

In similar terms to that process, the ultimate parameters which have to be calibrated here are the a and b parameters, which will fit the functions state over to the points including the mean μ and the standard deviation σ for each class of observed wave height.

The computation of μ and σ values for each class of bserved wave height will follow here as well a calibration of a distribution, in this case a lognormal, for the observed values of T_m on each wave height. Method of moments has been employed here as well, resulting in this occasion a much more direct and simple procedure, involving two independent linear equations. Those equations are stated next.

$$E[\ln T_m] = \mu$$

$$std[\ln T_m] = \sigma$$

The parameters μ and σ result from the direct computation of the mean and standard deviation over the wave period observations for each class of wave height. Natural logarithm of those values are used given the logarithmic character of the equation.

The wave period values found in the database do not show extreme values as the ones appeared for wind speed. In this regard, no refinement has need to be done and the whole set of computed values of h, μ and σ has been used for the final calibration.

The final calibration has followed again the lead of the general method described in the previous section and has used the least squares method. A verification process of the results obtained show the before mentioned linear relation between the mean wave period and the wave height.

The final results of the proceed explained in this section will be the determination of parameters a_0, a_1, a_2, b_0, b_1 and b_2 for each of the directions or group directions.

3.3.4.6.5 Joint Wave and Wind Climate

Once the long term characterizations of the different parameters describing the wind and wave climate have been taken to term, a useful description of the joint wave and wind climate needs to be configured.

As mentioned in the introduction, the interest of the approach presented on this thesis is the representation of the environmental conditions which will act on the structure on the average year. The variables of interest have been defined and its continuous probabilistic characterization has been taken to term. In order to adequately model the different situations produced on that average year and its variations, it is necessary to discretize the computed joint long term distributions.

The discretization must be performed for each of the variables. Each discretized value will be represented by its middle value and will include the situations where the variables takes a value between minus half the resolution and plus half the resolution. This discretization procedure neglects the possible influence on the load effects that a variation of the variables value less than half the resolution has.

Therefore it results of great importance to carefully define the resolution of each of the

variables discretization. Very small resolutions can lead to a computational resources waste, modelling more than once situations which generate the same load effects. On the other side, large resolutions will imply a loss of reliability, given that the same relevance will be given to groups of variables values which generate load effects of different importance.

The resolution used for each of the variables on the study object of this thesis is given in the next table. The different values have been selected after reading the recommendations of different codes on the matter, selecting the most restrictive values found on them. In this sense the realization of a sensibility study has not been found to be of relevance, although it could have worked as a double check process.

- Wave height H_{RMS}: 0.5 m
- Wave period T_m: 0.5 sec
- Wind velocity U_{10}: 2 m/s

Once the appropriate resolution of the variables defining the wind and wave climate have been defined, the representation of the different joint wind and wave sea states which are expected to happen in an average year must be computed. The probabilities of each of them will have to be computed, assuming that the long term probability that will be obtained from the distributions can be associated to the probability of occurrence in the average year. Then, the yearly probabilities of occurrence of each state will be used to determine which time portion of the year will the structure be subjected to these environmental conditions, resulting into the characterization of the importance of such a sea state and into the practical result of the assignation of a total weighted damage level to the structure.

Each joint wind and wave state will be defined by a root mean square wave height H_{RMS}, a mean wind speed U_{10}, and a mean wave period T_m. This sea state will therefore represent all the instants of year in which the structure is submitted to a short term stationary sea state with all of its descriptive variables belonging at the sea state defining variables values. The associated probability will determine the percentage of year time where such sea states occur.

The definition process of the different sea states to be considered and its associated probabilities is explained next.

This proceeding has been based on the joint wave height and wind speed probability computation for each feasible set of variables that might act together. Some adequate computations must be done to obtain a reliable probability representation, which are here developed.

The computations of probabilities implies a change of the analysis concept performed until now. The density and cumulative probability functions computed in the last sections treat the different represented parameters as continuous variables. By definition, probabilities of occurrence cannot be described on continuous variables, given that the probability of a differential value of any variables will tend to null.

Therefore the probabilities computation needs of a discretization of the feasible range of variables, approximating it to a continuous function. For each discretization made, the probability of finding a value included on them will be calculated. In this case very small resolutions are seek.

For a pair of values of two variables the joint probability density function is needed. The volume under the surface determined for the ranges of both of them will define the probability of the values to be found inside those ranges. For the ranges with centres value U_{10} and H_{RMS} and resolutions Δu and Δh respectively, the next equations defines this property.

$$P[u = U_{10}, h = H_{RMS}] = \int_{U_{10}-\frac{\Delta u}{2}}^{U_{10}+\frac{\Delta u}{2}} \int_{H_{RMS}-\frac{\Delta h}{2}}^{H_{RMS}+\frac{\Delta h}{2}} f_{U_{10},H_{RMS}}(u,h)\, du\, dh$$

The joint probability density function must be computed, Bayes applied theorem has been used, represented through the next expression.

$$f_{U_{10},H_{RMS}}(u,h) = f_{U_{10}|H_{RMS}}(u|h) \cdot f_{H_{RMS}}(h)$$

Developing this expression with the different calibrated parameter it results into the next formula.

$$f_{U_{10},H_{RMS}}(u,h) = \left[\frac{c_1 + c_2 \cdot h^{c_3}}{c_4 + c_5 \cdot h^{c_6}}\left(\frac{u}{c_4 + c_5 \cdot h^{c_6}}\right)^{(c_1+c_2\cdot h^{c_3})-1} \exp\left(-\left(\frac{u}{c_4 + c_5 \cdot h^{c_6}}\right)^{(c_1+c_2\cdot h^{c_3})}\right)\right]$$
$$\cdot \left[\frac{\beta}{\alpha}\left(\frac{x-\gamma}{\alpha}\right)^{\beta-1} \exp\left(-\left(\frac{x-\gamma}{\alpha}\right)^{\beta}\right)\right]$$

Where the coefficients from c_1 to c_6 are the result of the conditional calibration of the wind velocity on the wave height; and α, β and γ are the ones correspondent to the 3 parameter Weibull independent distribution for the wave height.

In the resolution process followed, the before mentioned integrals have been approximated to the computation of the volume of discrete parallelepiped with a base determined by the ranges of values on the basis of a very fine discretization and a height times the value of the previous function for the centre points of the range.

A resolution of 0.05 has been used for this endeavour after realising a comparison of the results precision and the computational cost of its variations.

Once the probabilities for each of those small resolution discretized ranges have been computed, the probabilities of the original joint discretization points can be easily computed by adding the correspondent ones on each final presentation range. The probability of finding a value between the range limits, will be the same as the sum of the probabilities of as many smaller ranges contained in the original one.

As a final result, pairs of wind velocity and wave height values correspondent to its respective discretized ranges, will have been computed along with its probability of acting together, of course, for the given direction or group of direction of study. A simple transformation consisting on the multiplication of each of those probabilities times the probability of occurrence of the origin direction for which they are calculated, will provide the global probability of having a sea state with such a wave height, wind speed and origin direction.

At this point, a large number of triads of values will have been obtained, some of them with very small probabilities values, given the continuous character of the function which was originally used for this endeavour. In practical terms the modelling of the sea states with such a reduced probability will mean the assignation of damage for a sea state which happens only a very small quantity of time.

Having selected a year as the modelling time for which fatigue damage will be computed, it is possible that the probability that some of those sea states have to be happening on the average year is null. In this sense a criterion must be selected to decide which of those sea states are excluded from the damage modelling.

For this problem, the solution adopted has consisted on the determination of a minimum probability, which would give the sea state enough importance to consider it on the damage contributions. Because of the proposed framework consists on the determination of fatigue damage for an average year, any sea state whose computed probability lies under the probability of the one year return period sea state probability will be considered to not happen.

That probability of the sea state with one year return period, will correspond to the extreme event happening once a year. Given the original database, which assumed short term sea states of 1 hour duration, the threshold probability has been computed as follows.

$$P_{T_R=1\ year} = \frac{1\ sea\ state}{1\ year \cdot 365 \frac{days}{year} \cdot 24 \frac{hours}{day} \cdot 1 \frac{sea\ state}{hour}} = \frac{1}{8760} = 0.00011$$

Therefore any sea stated discretized from the continuous functions with a resulting probability less than 0.00011 will be considered to not happen on the average year and null probability of occurrence will be assigned to them.

At this point, the probability of the remaining values has been recomputed so that its sum can be equal to the unity. This process assumes that the small periods of time leaved by the rare sea states will be occupied during the average year by the normal sea states. This process has consisted on the division of each of the sea state's probability over the total probability sum of the remaining sea states.

The discretization on sea states defined by a wind speed, a wave height and a direction or group of origin directions has been performed. The complete description of the states needs of the definition of an adequate wave period.

Wave period probability distribution function has been computed conditioned on the wave height. As the main theories state, and as the results of the calibrations have proven, it appears to be approximately linear with the wave height. Moreover the possible values of wave period to occur for each wave height do not show a great variation between extremes, with most of the probability density on the centre points of its lognormal distribution.

In this sense, it has been considered appropriate that the definition of the wave period for each sea state could be made by the expected value of that parameter for the given wave height and the given origin direction of that sea state. Wave period will determine the frequency of incidence of the wave over the structure in the linear modelling, for which considering a central value can be accepted as a way to automatically take into account the prorating of those possible sea states with longer periods in compensation for those with higher frequencies.

These assignment has been done for every single considered sea state employing the next equation.

$$E[T_m|H_{RMS}] = \exp\left(\mu + \frac{1}{2}\sigma^2\right) = \exp\left(a_0 + a_1 \cdot {H_{RMS}}^{a_2} + \frac{1}{2}(b_0 + b_1 \cdot \exp(H_{RMS} \cdot b_2))^2\right)$$

Where the different a and b parameters are the calibrated parameters for each direction on the conditioned distribution of the wave period on the wave height.

3.3.4.7 Design Load Case Consideration

In order to perform a correct service life fatigue analysis of the structure, design load cases

must be taken into account (Section 2.7.3.3). The joint wave and wind climate proposed sea states will have to be distributed among the considered design situations, and computed on the prescriptions (parameters, loads, etc.) that each of them defines.

Given the conceptual phase of the WindCrete development, in which no exact design conditions and details exist, it has been considered reasonable to take into account only two design load cases. Those correspond to the Power Production state (FLS 1.2) and the Parked conditions (FLS 6.4).

The rest of design situations respond to cases such as fault appearance, or start up / shutdown. These conditions affect mainly the loads generated by the rotor, which are specific turbine dependant values provided by its manufacturer, and therefore are difficult to be accounted on a conceptual design phase. The variation of these loads is considered because of its cyclical character. Resonance problems can be generated on those states given the new appearing frequencies, which would not have been accounted for service state on a general dynamic verification, and which shall not have an especially harmful fatigue effect. It can be therefore concluded, that this assumption shall not generate further disturbance on the final obtained results.

The main differences between Power Production and Parked responds to the loads generated by the control system and the turbine rotation, which will be present on the first condition but not in the second. Final total difference between loads on both of them will be considerable.

During the service life of the structure, this conditions will respond to the state of the environmental parameter related to wind velocity. For very high ($U_{10,hub} > v_{out} = 25\ m/s$) and very low ($U_{10,hub} < v_{in} = 3\ m/s$) wind velocities the wind turbine will not be able to operate. Therefore, the Parked design load case shall be considered for those cases, and the Power Production for the rest ones.

The determination of the proposed sea states which will be analysed on the basis of each of them is made in relation with the wind velocity prescribed on them. Those high wind sea states will always act in combination with parked wind turbines, idem. to the low ones. The probabilities for the sea states considered in each DLC will also provide information about the occurrence time of each of them along the year.

As stated in IEC 61400-3 and developed in Section 2.7.3.3, the different fatigue design load cases must be combined in order to represent the influence of each of them over the

structure along its design life. This requirement is guaranteed through the previously explained categorisation and simulation of sea states given its related design load condition.

The final resulting characterized sea states, which discretely describe the joint wind and wave climate, and which will be employed as the sea environmental parameters combination determining the fatigue action, have been included in Appendix C.

3.4 Structural Analysis

3.4.1 Introduction

The environmental loads acting on the structure along its design life have been characterized through the statistical description of its long term combined wind and wave climate. For design purposes, it is presented as different discrete sea states, defined by constant environmental parameters, in which the climate variables values for the structure design life can be grouped.

In order to obtain the fatigue damage generated on the structure during its design life, which will depend on the time stress history of the structure, the determination of the associated load effects for each of them is necessary.

A mechanical model that can simulate the behaviour of the structure under those environmental states is needed. In this section, the characteristics and properties of the in this thesis employed model used for the calculation of the load effects on the structure are presented.

The employed model has been created on the context of the WindCrete development research of the DECA-UPC. It has been validated successfully in different thesis and papers. It is implemented on Matlab programming language, taking profit of the versatility of this software on the parametrization of input data, and the possibility to realise modifications on the calculation parameters and on the results post-processing.

A 3D dynamic model has been selected for the evaluation of the load effects introducing as input the environmental parameters of each sea state on an adequate representation, and the loads correspondent to its design load case. It is based on the introduction of the structure as a rigid body on the mechanical global system where the loads of the different subsystems interact. A time evolutionary analysis is made, being equilibrium guaranteed on each time instant, and obtaining the variations of the structure position and kinematic properties, along with the loads position, allowing to determine almost directly the stresses on the structure. The model can be considered to be aero-hydro-servo-rigid, with some restrictions on the coupling between subsystems.

Phenomena like breaking waves, or flow influence of nearby objects, seabed or coast are disregarded, given the deep sea character of the structure in service conditions. Further research would require of the influence check of nearby turbines, in case of a farm configuration.

The main loads taken into account have been:

- Wind
- Waves
- Wind Turbine Loads

Design codes propose other different types of loads which may or may not have been taken into account. In this sense, water level influence is taken into account automatically by the code, given its dynamic behaviour. Other loads, like currents or ice loads, have not been introduced, given its extraordinary occurrence of the possibility of effect neglecting.

The particularities and its implications of the model selected and its usage are presented in the next section.

3.4.2 Model Characteristics and Implementation Insight

The specifications regarding the conditions that the model simulates and how are those simulated are presented in this sections. Particularities on its implementation procedure are detailed as well.

As a previous step, a reference system is selected for the determination of the spatial variables of the model. In this sense, advantage is taken of the definition of two three dimensional systems: a global fixed one, where absolute displacements will be referred; and a local one placed on the structure centre of gravity, useful for the consistent determination of loads. A third reference system is defined for wave direction, which will be based on the global coordinate and dependent on a plane rotation, which will indicate the wave incidence direction.

Transformation between the coordinate systems, when needed, are implemented through transformation matrix which work on all three space directions.

3.4.2.1 Hydrodynamic Subsystem

The model takes into account the forces interaction with the hydrodynamic system by modelling with the forces as described on the Section 2.3.3. It is worth mentioning the introduction of buoyancy forces. The cylindrical slender geometry of the structure allows to consider that all buoyancy is originated, and therefore applied, on the structure bottom. It takes

into account the standard buoyancy force due to the displace fluid volume, and additionally the pressure variation due to the water profile modification by waves, which is adequately included through an exponential affectation with depth because of the influence of wave kinematics.

The wave environment has been represented in form of regular waves, for which no variations on the dynamic system modelled wave's direction, height or period has been introduced. Given the interest of the energy related effects of the wave train over the structure, the parameters representing this constant wave have been adapted in this regard (Section 3.3.4.4).

The wave loads introduction has been performed introducing the Airy wave theory and the Morison's equations. Airy wave or linear theory allows a simple implementation in front of theories of superior order, but does not provide information on the waves' kinematics above the still water level. Nevertheless, comparisons with the results of scale tests on the structure based on RAOs show that the employment of the linear wave theory produces good output results for the frequency input load ranges in which the structure is being simulated. Therefore, the necessity to apply a higher order theory has not been considered.

Waves parameters are introduced on its own reference system, which as mentioned before is based a rotation, characterized by the angle of incidence of the wave, over the global system of coordinates. Those are computed from the input of properties like wave height and period following the selected theory, in this case, Airy wave theory. A change of coordinates is performed to obtain the kinematics of the waves on the structure. Regular expressions for the obtained velocities and accelerations are transformed into the global axes, and from those into the structure local axes. At the end of the process, coordinates referred on the structure height (local coordinate) will be obtained.

Once the velocities and accelerations of water due to waves over the structure have been obtained, it is necessary to compute the part of those that will generate loads on the structure given that the structure will be in movement. In this sense, it is necessary to compute the relative velocities between water and structure on every height of the body, for which will be necessary to compute the structure's velocities.

Finally the loads at each point of the structure are computed using the Morison's equation.

Morison's equation proves to be an adequate theory for the description of this phenomena. Its applicability is limited by the diffraction characteristics of the system to maximum value of the structure diameter (D) over the wave length (λ) of 0.2. Its mathematical expression is given next.

$$R_{diff} = \frac{D}{\lambda} < 0.2$$

Where R_{diff} is the diffraction parameter, D is the structure diameter and λ is the wav e length.

Given a structural diameter on the submerged zone of 13 m ($D = 13\,m$), the theory applicability will be valid for wave lengths over 65 m ($\lambda > 65\,m$), which will be the case of the wave we are working on.

The hydrodynamic wave force computed on every discretized point of the structure is finally added by its integration along the longitudinal cylinder axis, form which moments can also be obtained. The vertical integration limit will be placed on the sea level at the time instant of computation. It is possible to apply the position equation of the in this case, Airy wave theory.

3.4.2.2 Aerodynamic Subsystem

The introduction of wind loading follows the scheme described on the previous paragraphs for the hydrodynamic loading.

In this case the wind action is given by a wind velocity at the hub height which generates a wind profile over all the tower height in contact with the atmosphere. The wind velocity is computed according to a turbulence mode, for which a different magnitude is applied on every time instant, dependant on a stochastic generation model.

A coordinate transformation into the local system of coordinates is needed. The final wind velocity applied corresponds to its perpendicular component with respect to the structure's longitudinal axis, given the different inclinations of it at each time instant.

The rest of the process is similar to the one of wave loading. Loads are computed following the indications of the *Eurocode 1-4: General actions – Wind Actions (EN 1991 1-4)*, and accounted over the model for each time instant.

3.4.2.3 Control System and Rotor Loads

The wind turbines loads would depend on the rotor's angular velocity and the blades pitch degree. On a real wind turbine, these parameters are adjusted automatically by the control

system when the wind velocity is modified.

As for the model employed, the loads originated on the rotor have been considered to be constant for each modelled sea state, dependent on its wind mean velocity. The relation between rotor loads and wind velocity has been obtained through simulations with the software FAST on a fixed-bottom offshore structure. Therefore, this approach does not account for the effects of wind spatial turbulence or for dynamic effects of the rotor loads. Nevertheless, it is possible to assure that its results are on the safe side, given a check procedure realized in a comparison with the results of a more advanced code, based on AeroDyn and implemented on test variations models with coupled subsystems.

Loads of the rotor for load cases where it is parked will be duly accounted.

3.4.2.4 Mooring Lines

The effect of the mooring lines introduction has been based on a quasi-static response. An extern Matlab code created at the DECA UPC has been used for this requirement. The mooring takes the form of a catenary of fixed total length. A range of horizontal displacements is imposed to it, and the corresponding forces for each of them are computed. The data obtained is used to calibrate a stiffness equation in vertical and horizontal directions, which will be used to model the reaction force of the mooring system on the anchorage points.

3.4.2.5 Subsystems Coupling and Resolution Procedure

Once all the actions have been introduced on the model, the temporal evolution of motions on the structure is computed. Movement equations are defined considering a mass point corresponding to the whole mass of the structure on the centre of gravity. The dynamic global system (dynamic inertia mass, damping…) is solved for each time step. The expression of motions is made in global coordinates in all six degrees of freedom.

In this procedure, the dynamic masses for each degree of freedom are computed, considering the adequate added masses. Dynamic Inertias are then computed by defining small roll and pitch angles, which is a simplification that allows the consideration of constant inertias.

The equations for each of the degrees of freedom are coupled, resulting into a non-linear system of second order differential equations, which is solved using the Runge-Kutta method.

Initial conditions on the position of the structure can be given to the solver.

After obtaining the position of the structure on each time step, it is easy to obtain the internal forces which it is submitted to. The principle of d'Alembert [141] is applied, for which the forces, external, internal and inertial (acceleration), should be at equilibrium at every time step. Given the computed geometrical position, the process is simple.

After its computation, the integral of the forces are integrated along each direction, obtaining the correspondent shear force. Moment is later obtained by numerically integrating the obtained shear.

3.4.3 Simulation Procedure

The particularities of the simulation process on the model which has been described in the previous section are presented in this section.

Mechanical simulations have been performed on the dynamic model of the structure for each of the environmental parameters combinations (sea state) that have been proposed on Section 3.3.4.6.

Input data has consisted on the definition of a wave height, a wave period, a mean wind speed, and the origin directions of wind action (codirectional case) in respect to north origin direction.

Following the indications of the different codes, simulations with a real time duration of 550 seconds have been taken to term. This duration is considered to be sufficient to account for all the effects of the dynamic and coupled processes on the three-dimensional system which lead to a non-regular response of the structure, presenting different evolution trajectories of parameters such as displacements or forces along time, appearing to be aleatory. The results, as showed in the next sections, show an approximate scheme which is repeated during the 550 seconds of output data. It has proven that a longer simulation would not provide further information on the structural behavior for the environmental input conditions modelled.

The simulation for each sea state starts on a progressive increment along time of the input magnitudes, which takes about 100 real time seconds, which are not included into the necessary 550 seconds, and whose mechanical results are not of interest for the necessary analysis. This sloped application of the input loads avoids the effects that the sudden application of large loads would have on the simulation model. Those would produce results which do not happen in reality

given that the real structure is constantly subjected to loads. A progressive increment guarantees that only real conditions will be modelled. The exclusive employment of the results regarding the application of the total magnitudes is at any case needed.

In this sense, each simulation will be composed of the time of load preparation, determined to be 100 seconds, and the next 550 second in which loads based on the total value of the environmental conditions are applied. The code provides automatically the values of the required output variables for the 10 minute simulation period with constant inputs and disregards the rest.

The output of each sea state simulation is presented in a set of different numerical Matlab arrays, including vectors and matrixes among others. Many different variables and parameters can be obtained from them. A differentiation can be made between the ones which provide simulation results, and the ones that contain information or references about those results.

The ones selected, which have been used for the resolution of the problem, include both references and calculation results. As for the results, the matrixes including the forces have been selected. Those consist of:

- Moment in X direction
- Moment in Y direction
- Axial Force

In total, those sum 5 matrixes per simulated sea state that are available for the upcoming computations. Each of them provides the evolution along time of the correspondent force (matrix' columns) in various cross sections of the structure (matrix' rows), distributed along its height. The selected output arrays regarding results references include a vector which determines the simulation real time instants for which the values on each column of the forces matrix accounts, and a vector that indicates the height of the different cross sections in the case of the rows. It is worth mentioning that the time vector starts on the second 100, given that, as stated before, the previous ones account for a progressive loading intensity up to the values that define the load case to avoid un real behaviour, and the simulation results only contain the output obtained for these necessary values, which happen to start at that time instant.

The 5 resulting forces matrixes have been systematically selected and stored according to the environmental input parameters at which they refer. In the case of the reference vectors, it is not necessary to extract and save all of them, given that the simulation output points and time instants conditions had been defined equally for all the sea states. Therefore only the one

of a simulation has been kept as reference, being only necessary to check the others in order to maintain the computations coherence.

Further output parameters, regarding kinematics and other variables, have not been automatically disregarded, given its possible interest on the verification of the simulation process and results coherence in further steps of the problem resolution.

Resolution selected for the simulations output results has consisted on values obtained every half second, leading to a total of 1101 effective time instants (550 second simulation) with associated values. For every single instant of these 1101, values are obtained for 871 cross sections along the structure longitudinal axis, which is obtained after defining a resolution of 0.25 m between the bottom of the spar and the height 130 m (corresponding to the second cone part), from which a vertical separation between section of 0.5 m is defined. In this sense, and regarding the row (cross section) and column (time instant) distribution, the size of each force matrix is 871 x 1101.

3.4.3.1 Forces Results Validation

Values obtained have been verified, checking on its numerical values, on order of magnitude coherence on the oscillations for each sea state, and on the differences between sea states defined by different intensity environmental conditions; as well as a consistency on the distribution of values along the tower length.

A global analysis has been performed on all the output values provided by all the performed analysis, without discerning between those selected for power production and parked conditions. Consideration on the possible disparity between both could be performed if the precision necessity of the model complexity was too high.

A Matlab code has been created in order to analyse the magnitudes and its variations of the structural analysis forces output values. As stated before, for each analysed sea state output matrixes show the time evolution of each output force on every programmed cross section. As for the interest of fatigue analysis, moments and axial forces output have been taken into account. The available moment information is given on the two components correspondent to each rotation axis on the cross section plane. A simple transformation of the data in order to obtain the total moment through the addition of both is needed, for what the next formula has been employed.

$$MOMENT = \sqrt{MOMENT_X^2 + MOMENT_Y^2}$$

At this step, the total moment and the axial force evolution on each section is available. As for the objectives of globally analysing the correctness of the data, maximum and mean values computation of its time evolution have been considered to be adequate.

The results obtained show a coherent order of magnitude and value variation of the different forces.

Axial force values show small variations along time, which is a coherent behaviour given the properties of the performed simulation. The only loads acting along the longitudinal axis of the structure are its own weight, which is equilibrated through the buoyancy force applied at the bottom of the structure; and the inertial variations of it correspondent to its heave (vertical movement), which given the small vertical displacements shall be negligible.

Regarding the variation of the axial force along the structure length, the expected values according to the own weight of the structure have been obtained. The logical decrease of this force along its height given the area reduction has been checked. Its values on the structure bottom and the structure head section, correspondent respectively to the total weight of the structure and point with zero own weight, have been carefully checked and accepted.

Both behaviours, along time and height, can be clearly observed on Figure 13. On this diagram, the values obtained for each cross section are plotted in the vertical axis,

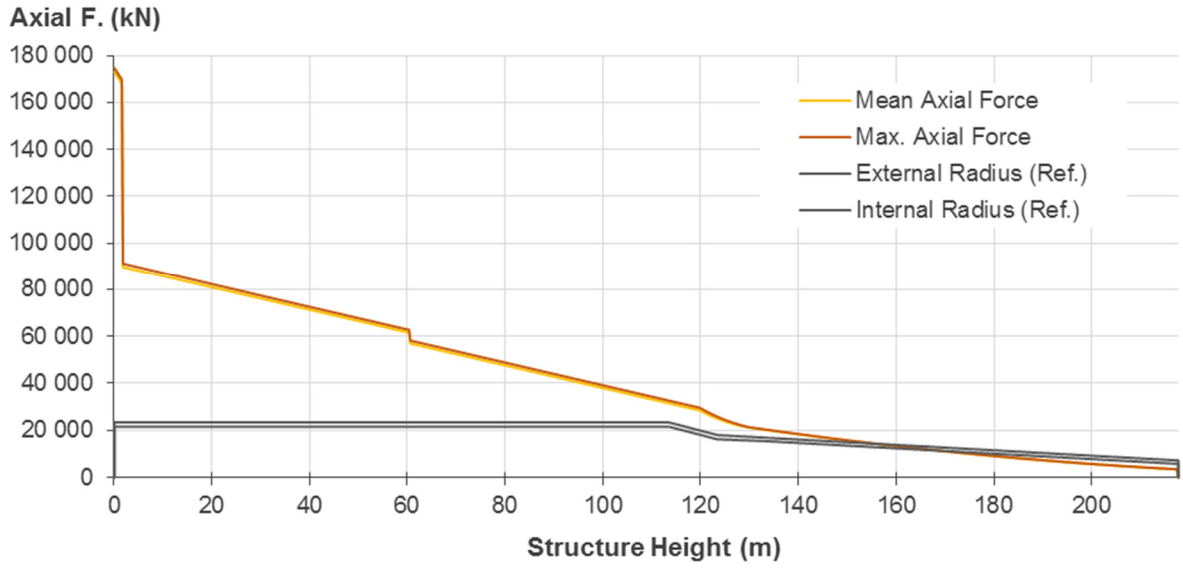

Figure 13 Mean and maximal axial force of the analysis output for each cross section along the structure.

corresponding to the axial force in kilonewtons. Each cross section is referenced on the horizontal axis with its height, taking the bottom of the structure as the zero value. In the bottom part of the plot and in grey colour, the external and internal surface lines of the structure have been inserted as a non-dimensional and visual reference. The mean values of the time evolution have been computed and stored for each sea state and cross section. Of those, the mean values of the different output sea stated for each cross section have been computed again, which are shown plotted in yellow.

Axial force variation can be clearly seen along structure height. A mean value of approximately 175 000 kN (17 000 t) is obtained on the bottom part of the structure which corresponds to the total weight of the structure and the added ballast, which is applied as a load on that correspondent surface. Axial force decreases linearly with height on the cylinder (constant area) and non-linearly on the tower, where the diameter is linearly reduced. Changes of slope can be seen on the transition cone (~120 m) and on the thickness reduction stretch (~130 m). The dynamic and floating properties of the structural system modify slightly these values, reason why the slope change is not exactly coincident with the diameter change section of the tower. The value on the top of the structure approximates to zero force. Around the 60 m height, an abrupt value variation can be seen. It corresponds to the vertical force performed by the mooring lines, which are implemented on that position.

The small time variations of the axial force can be observed on the plotted line in red. It corresponds to the maximal values of axial force for each cross section among all the simulated sea stated and all its time variations. The same length behaviour as for the mean values is observed. As expected, practically no magnitude alterations are obtained, even when absolute maximal values (time maximum of maximal output sea state) are being compared to mean time values of mean sea state values. Therefore, it can be concluded that the employed model performs a good simulation on the axial forces.

As for the moment behaviour, different analysis have been performed. In this case, a more depth is needed, given that, differing from axial force behaviour, moment is expected to vary substantially on each simulated time instant and each modelled sea state.

On a first stage, the evolution along the structure height of the obtained moment has been checked. A previous qualitative plot on Matlab including the time mean and maximal values on each cross section for all the evaluated sea states shows a similar relative evolution on the structure length for all of these, differing on the correspondent magnitude to each section, which depends on the sea state’s defining parameters value.

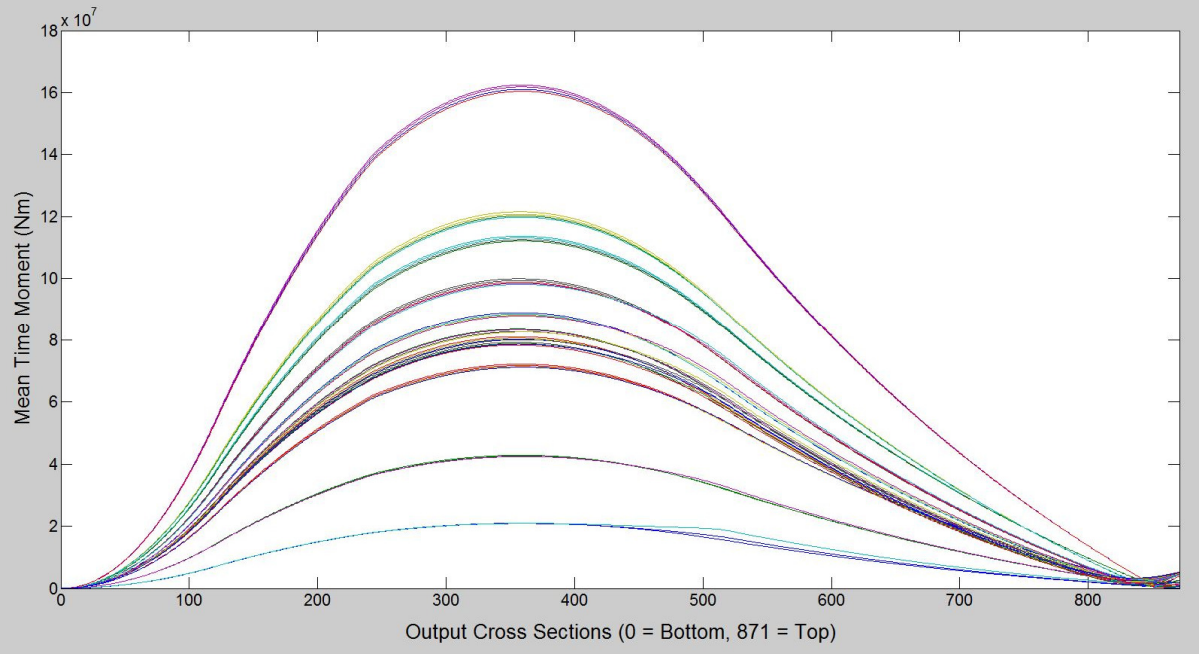

Figure 14 Mean time history values along the structure length for the sea state with north direction origin

As an example, the mean time moment values on each section for the set of sea states corresponding to the north direction is included in Figure 14. Each plotted line corresponds to a sea state. It is easy to see the same variation on all of them. Further checks performed with the rest of sea states show the same behaviours.

The pattern form which all the sea states follow is coherent with the aspect of the results of previous phases of the conceptual design, which were validated through the results comparison with different structural analysis software. The maximum moment point corresponds to approximately 3/4 of the draft height of the structure (~90 m height over the 130 m draft, section ~521), showing a steeper descend of the moment value on the submerged part (left) than in the tower stretch (right).

On Figure 23, some moment increases appear to exist for some of the simulated sea states on the sections close to the tower top. The expected behaviour in this regard, given the theoretical behaviour of the structure, is to descend down to a value of zero at the structural top, which is presented in the great majority of computed sea states. The misbehaviour on this stretch appeared of them, has been to found to be related to numerical problems of the solving code, which have not been possible to solve. In this regard, it will not be possible to consider as reliable the resulting forces values on the sections in which this moment increase exist, and therefore it will not be possible to perform fatigue evaluation on those section given the lack of

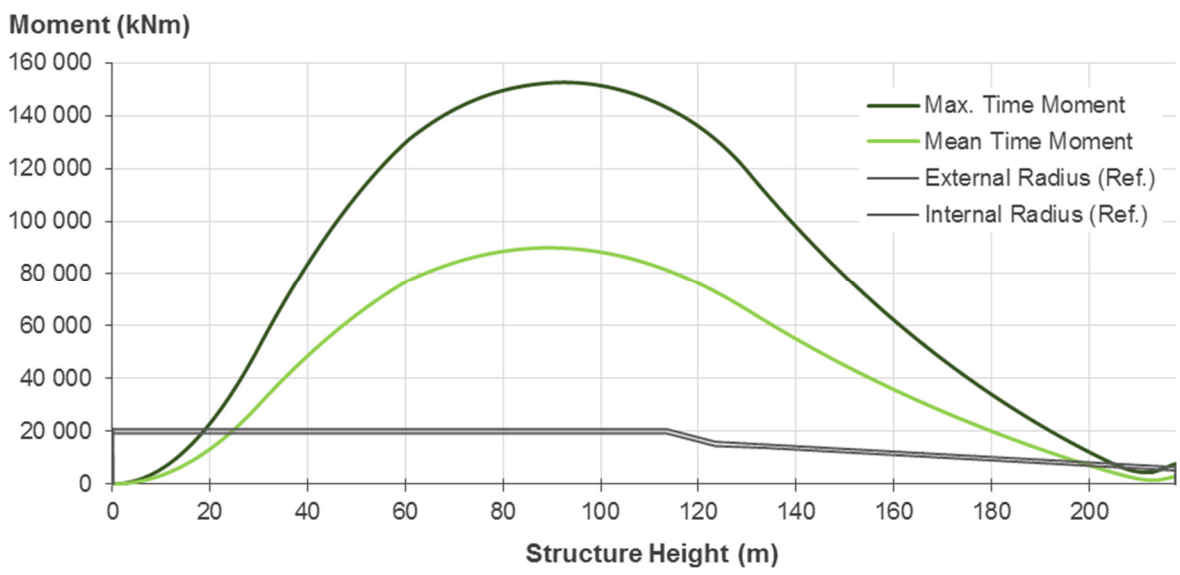

Figure 15 Mean of the maximal and mean time history bending moment for each sea state along the structure.

information regarding its real mechanical behaviour. Further reference to the precise consideration to this lack of data and the affected sections will be made on the fatigue evaluation section, for what can be advanced that no major inconvenience on the fatigue assessment will be produced as long as the in comparison small forces on that section will avoid the possibility of its critical character.

Regarding the magnitude values of the obtained moment outputs, different analyses have been performed.

As a first view, the order of magnitude of the output values has been obtained. The mean among sea states for the time evolution mean and maximal values of moment in each cross section has been plotted and analysed. In Figure 15 the results can be seen. The same shape as the one described in the previous paragraph can be directly observed, with the maximum value present on the approximately the same cross section. A maximal value of ~150 000 kNm for the mean of the time evolution peak values is there observed, together with a maximal one of ~90 000 kNm for the mean of the time evolution mean values. These output magnitudes correspond to the order of magnitude correspondent to the conceptual design of Windcrete (Order of 100 000 kNm as maximal moment).

Additionally the values obtained on the simulation of the sea state which causes the biggest forces on the structure have been plotted and checked, in order to guarantee that the maximal service loads of the structure are inside the range of expected values for which the

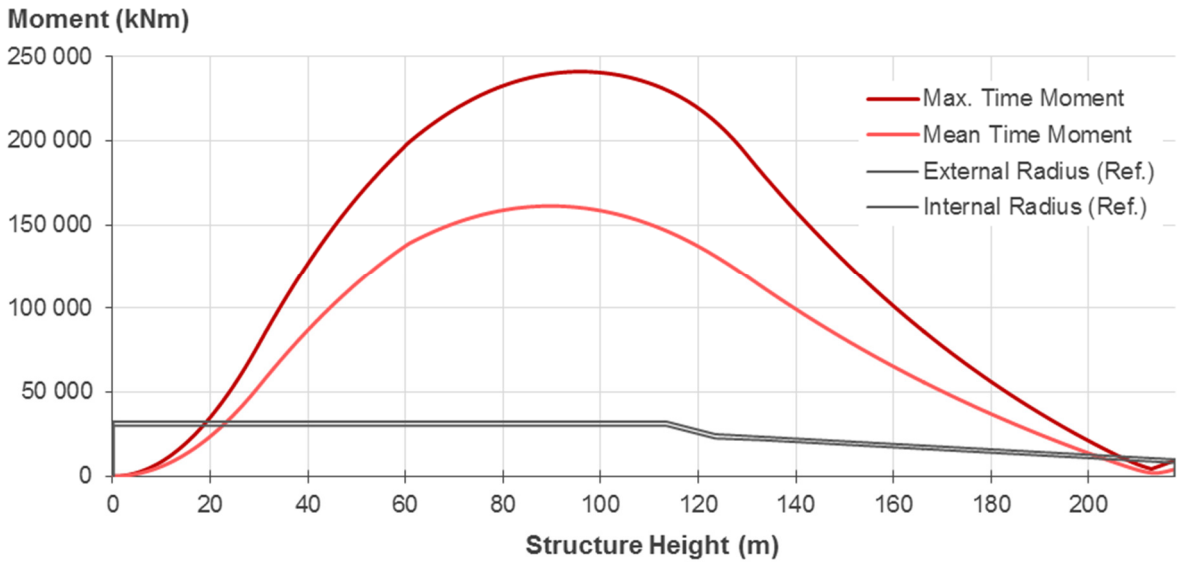

Figure 16 Mean and maximal time history bending moment along the structure for the highest intensity simulated sea state.

conceptual design phases of the structure has accounted. For that case, reference with the number 192 and corresponding to a wave height of 2.25 m and a wind speed of 11 m/s, the time evolution mean and maximal values for each cross section have been plotted in Figure 16. Beside the coherence showed by the form of the values along the structure, a peak value of approximately 240 000 kNm appears. The ultimate limit state design performed on the conceptual design phase of the structure allows this moment on the range of resisted forces, which presents coherence when comparing the magnitude of the sea states in each of them and

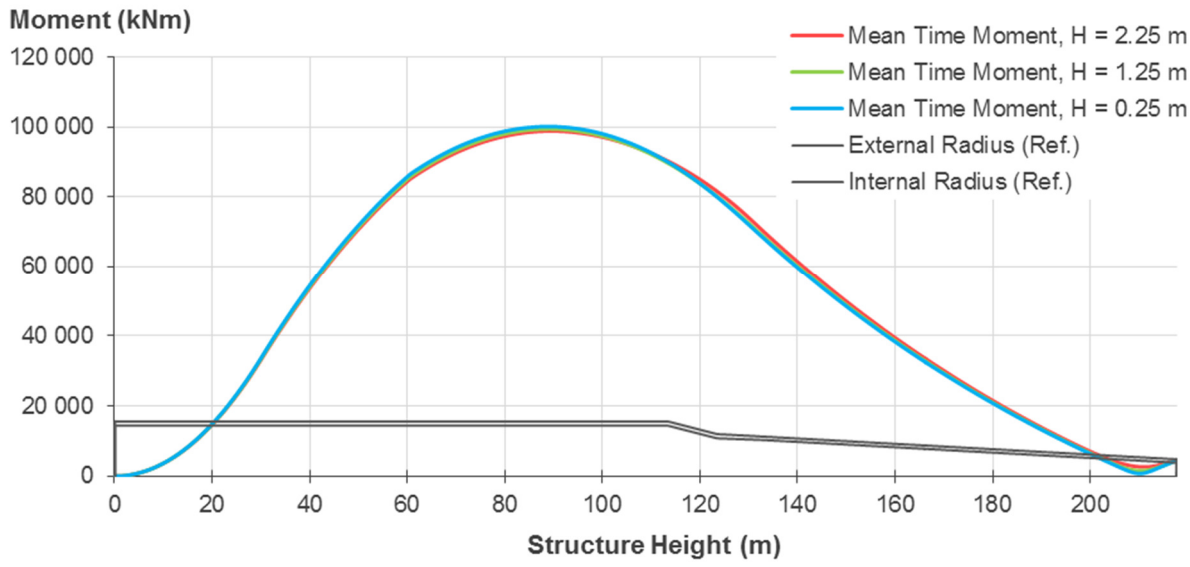

Figure 17 Mean time history bending moments for sea states on the same wind spped and varying wave height

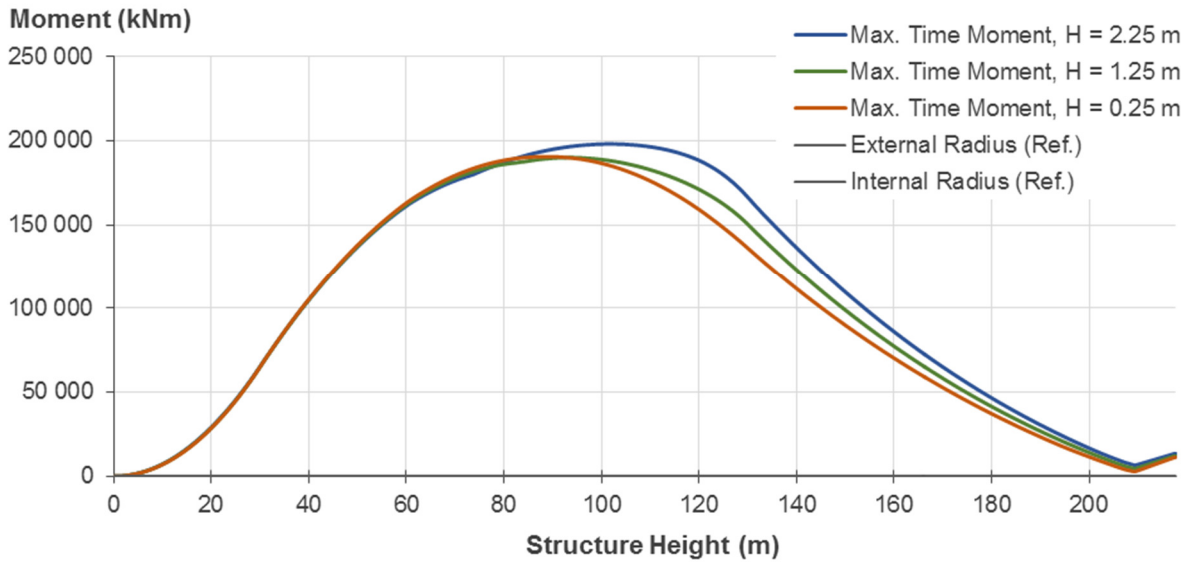

Figure 18 Maximal time history bending moments for sea states on the same wind spped and varying wave height

the output peak moment.

An expanded comparison analysis on the results of simulation made for different sea states provides information about the importance of each of the environmental parameters over the forces magnitude. Studying the global moment variations for individually increasing or decreasing wind velocity and wave height, while leaving the other unaltered, shows in an easy way the influence of each of them on the structural behaviour. No further checks have been taken to term on wave periods, since they vary according to the wave height and do not affect force magnitude as long as, directly, they only define the wave frequency.

Wind velocity has been fixed while increasing the defining wave height value. In Figure 17 three different sets of moment values can be observed, correspondent to the time mean values of the moment along the structure height originated by each of the three sea states. Sea states with reference numbers 379, 394 and 409 have been selected to exemplify the check process; which correspond to the NNW origin direction. All three of them are characterized by a wind mean velocity of 15 m/s, and wave heights of values 0.25 m, 1.25 m, and 2.25 m respectively. No practical difference on the mean output values can be seen, being the maximal relative variation of a 2 %. The maximal mean values results to be around 100 000 kNm.

A further analysis has been performed on the same cases as explained in the previous paragraph by comparing the maximal time values of each of them along the structure height. Results have been included in Figure 18. In this case, the output value similarity of the previously

analysed mean moment is only maintained on the left slope, reaching considerable differences on its right side. The values relation on this part appear coherent with the different magnitudes of the wave height, increasing with it. The maximum values along the cross sections in this case appears close to the 200 000 kNm.

After analysing the results of the performed analysis together, many direct conclusion can be obtained. The simulated system model provides good and coherent results. The diverse range of moment magnitudes is clear (Figure 14). Variations along the structure length and its magnitudes have been proven to be adequate (Figure 15 and Figure 16). It can be assured that the main influence on the moment change relies on the wind velocity variation, given that as it has been stated on Figure 17 and Figure 18 wave height has almost no influence on it. Regarding the influence of wave height a possible increase of the fatigue effects can be obtained on the middle superior part of the structure for increasing wave height values, given the maximal values increase on that stretch and its corresponding influence over the fatigue ranges.

3.5 Fatigue Analysis

3.5.1 Introduction

Given the long term combined wind and wave climate, represented in form of discrete sea states with constant environmental parameters, the evolution over time of the load effects for each of them has been obtained through the dynamical simulation. Each of those states will have an inherent probability of occurrence and an associated design load case.

Fatigue life computation of the structure can be then performed by adequately taken into account and combining the damage produced by those load effects, given the probability of occurrence of the sea state which generates them and the load case in which they act. On this section the process proposed and followed for its calculation over the WindCrete structure is presented.

The S-N Curves method has been employed for the computation of the fatigue damage, following linear addition as stated in the Palmgren-Miner rule. It is considered to be the state of the art method due to its suitability for a complex problem like fatigue computation (see Section 2.5). Moreover, on an offshore dynamic structural problem, further developed methods would be computationally too expensive, not applicable to all the specifications on this case, and unnecessary given the associated minimum inherent unreliability levels generated by the stochastic and complex nature of the problem.

The complexity of the fatigue process, especially in concrete, makes it necessary to focus its design on damage computation methods based on empirical research. This leads to different procedures which take advantage of many different equations, parameters and assumptions. In this regard, there is not a definitive calculation process widely accepted in front of the others (see Section 2.7).

In order to take to term a study with real and applicable conclusions, the fatigue calculation realized in this thesis for the WindCrete concrete structure is based on the procedures and indications of three different constructive codes, all of them relevant, well established and widely used. The codes used for this purpose have been the Model Code 2010, the Eurocode 2, and the DNV-OS-C502. Further reference to them can be found in Section 2.6. It is the intention of this thesis to analyze the hypothesis and considerations of each of them, with the purpose of extracting coherent conclusions on its behavior and outcome reliability, after realizing a comparison on the results obtained for each.

The steps followed in the development of the fatigue analysis of the structure and the details of its implementation on a Matlab code are stated in the next sections.

3.5.2 Stress Computation

Fatigue damage computation needs of the time stress history on the structure in order to be computed. Therefore, the obtaining of trustworthy series of stress evolution over time has been the first step on the performed fatigue calculation process. The aspects of this procedure are explained in this section.

As stated in the codes, fatigue damage is related to, and must be computed on, a discrete point inside the structure. Stress variations and its magnitudes on that point will provide the resultant damage on that position, making it necessary to compute it on the number of significant points which allows to obtain a complete description of the structure fatigue behaviour. The point with the biggest computed damage value will determine the structure fatigue resistance.

3.5.2.1 Computation Process Considerations

Some previous considerations have been performed on which steps will follow the applied numerical resolution method selected for the problem, in order to optimize the global process of computation.

Given the extreme computational waste that would suppose a discretization small enough to represent all the structure volume in which the stress evolution and damage computation should be computed, a set of candidate points which could present the biggest damage values have to be selected.

The created Matlab code for the assessment of fatigue life includes a subroutine for the determination of the time evolution of stresses, given the correspondent time evolution of forces outputted by the simulation model. That subroutine must account for the points where fatigue damage will be higher, given that those will condition the ultimate fatigue resistance of the structure, and that calculations on noncritical points will only suppose a computational waste.

The predefinition of those points has been made in base of the next criterion. It is necessary to compute the candidate points on the basis of structural cross sections; given that the affecting forces are defined on each cross section, and that a univocally relation between

forces and stresses exist. On each cross section to be computed, the largest variations of stresses will appear on the outer rand of the section, where the related moment stresses will be higher because of the large leverage distance as the moment application axis are centred. Therefore, the designed code will have to account for the stress time history and fatigue damage computation on cross section perimeter placed points.

The damage fatigue calculation will be therefore reduced to a set of selected discretized point, corresponding to the candidate cross sections, i.e. the ones where the highest stress levels and variations are expected to happen. The computation code has been programmed on the basis of this procedure. It will possible to easily select the cross sections and the number of perimeter points to be computed.

Further selections must be taken to term in order to decide which will be the minimum necessary number of cross sections and perimeter points on each of them that may determine the fatigue life, allowing to reduce the computational waste again. Reference will be made to them on Section 3.5.3, where the damage calculation procedure through the output of the in this section described code is detailed.

3.5.2.2 Matlab Code Implemented Procedure

Once the definition procedure of the number and position of the to be computed points is done, the Matlab script for stress computation has been coded.

The produced Matlab codes includes a programmed redundant procedure which works on each single discretized point and on each single time instant, as defined by the output of the structural analysis code. The associated defining properties of the point and the correspondent forces to that time instant will serve as input data for each computation. Ultimately, the problem consists on computing a static stress on a cross section’s coordinates for the forces acting upon it on a given time step.

It has been possible to introduce some simplifications on this process which do not make it completely redundant, allowing to save computational cost for some of its steps. The Matlab matrix structure of the input data is leveraged in order to obtain a simple and cost effective algorithm which can provide fast results, by reducing the total number of loop structures.

Details on the programming of the computation of each of these time step static stresses and its physical background is given on the next paragraphs.

The final total contributions consist of the moment over both horizontal axes, axial force, and a prestressing force, which are taken into account as the forces contributing to the stress of each cross section.

It has been possible to make a very important assumption which conditions this step and the upcoming ones. WindCrete is designed to guarantee an almost null maintenance necessity. For concrete, that means ensuring that no cracks will appear, given that those are the main way in which the durability reduction agents can breakthrough and attack the structure. In order to warrant that no fissures will appear during its design life, the structure must be subjected to a full compressed state, with no tensile stresses affecting it. The addition of a complete prestressing system is used for this purpose.

Assuming no tensile stresses allows to consider that no cross section of the structure will be cracked, for which the stress distribution is uniform and lineal over all the concrete section. No need for computation of deformation compatibility, stress distribution, crack depth or other related concepts exist.

By defining a Cartesian reference system with origin on the centre point of each cross section the sections, and perpendicular axis X and Y, the stress computation will therefore correspond to the next expression.

$$\sigma_{i,j} = \frac{M_{X\,i}}{I_i} \cdot y_j + \frac{M_{Y\,i}}{I_i} \cdot x_j + \frac{N_i}{A_i} + \frac{P_i}{A_i}$$

Where i is the index which determines the section where the variable is computed and j the related point in that section. In regard of the included parameters, $\sigma_{i,j}$ refers to the normal stress, M_X and M_Y the moments over each of the axis, I is the moment of inertia of the correspondent section, y and x are the coordinates of the point of interest in the section plane, N is the normal force, and σ_P is the prestressing stress (equal along all the structure length).

The geometrical properties of each section have been computed following the next expressions. The cross sections are considered to be rings, and the measures employed are the ones that follow the scheme of magnitudes given in the description of the WindCrete concept (Section 3.5).

$$I_i = \frac{\pi}{64}\left(D_{ext_i}^4 - \left(D_{ext_i} - 2 \cdot t_i\right)^4\right)$$

$$A_i = \frac{\pi}{4}\left(D_{ext_i}^2 - \left(D_{ext_i} - 2 \cdot t_i\right)^2\right)$$

Where D_{ext_i} is the external diameter of cross section i and t_i the correspondent wall thickness.

The value of prestressing P_i will correspond to the one acting on that cross section, as introduced by the corresponding planned tendons. In this problem a simple but conceptually adequate determination of the prestressing forces along the structure has been performed. It has consisted on the definition of enough length stretches with constant prestressing forces, simulating what would be the distribution of prestressing quantities along the structure in order to guarantee compression but avoid unnecessary large stress levels. This value should account for the real stress transmitted from the tendons into the concrete structure; taking into account, concrete deformation, possible fluctuations due to cable elongation and shortage, and prestressing losses both instantaneous and distributed along the structure service life.

The selected distribution of prestressing forces for the present fatigue assessment performed and its obtaining procedure along the hypotheses made are detailed further in this section. It has been considered to be constant on each defined stretch corresponding to a tendons quantity. Value alterations have been neglected as well. The assumptions inherent to the modelling and the forces obtaining procedure make it unnecessary to refine that much the result precision. A final fatigue assessment would need of an accurate valuation of and the corresponding precise simulation.

The reference coordinates of the points, along a graphical representation of its position can be found in Figure 19. On it, a graphical representation of a standard cross section of the structure can be seen. The sixteen origin directions, as prescribed on the start of the problem approach, are defined. In the cross section middle point, the origin of the system of coordinates representing the moment loading is included. Axis X and Y as plotted will serve as rotation axis of its reference momentums.

The different points on the cross section perimeter will be defined on polar coordinates accounting for a θ angle starting on the north origin direction and rotating clockwise. Given the desired quantity of discretized points, its separation and polar coordinate will be automatically computed.

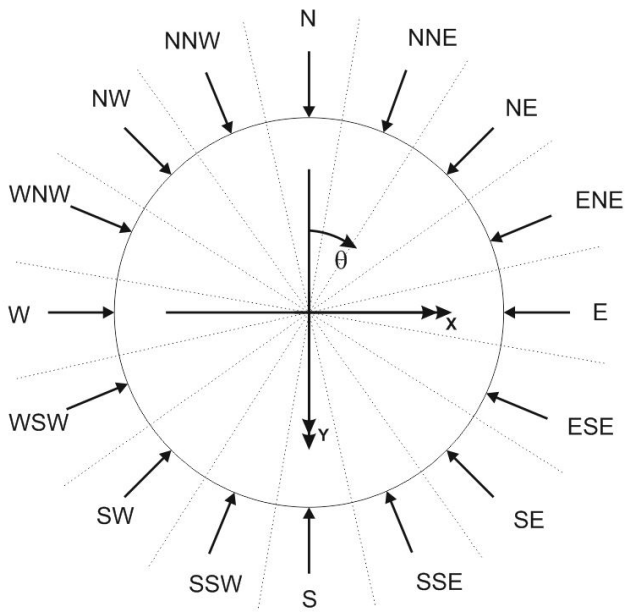

Figure 19 Nomenclature of the degrees of freedom of a floating structure.

Moment stress generated on each of them will be duly accounted in basis of this rotation degree. Adequately sinus and cosinus functions will account for the leverage arm for the stress calculation on that point for the acting moment, and for the compressive or tensile character of the stress given the moment direction. Compression is considered to generate positive stresses and tension negative ones. The equations used are next stated.

$$\sigma_{M_X} = \frac{M_X}{I_{secc}} \cdot y_{point} = \frac{M_X}{I_{secc}} \cdot (-\cos(\theta))$$

$$\sigma_{M_Y} = \frac{M_Y}{I_{secc}} \cdot x_{point} = \frac{M_Y}{I_{secc}} \cdot (-\sin(\theta))$$

Where σ_{M_X} and σ_{M_Y} are the respectively stresses generated by moments rotating over the X and Y axis, namely M_X and M_Y; I_{secc} is the section inertia, indetical for both axis given the symmetry; and y_{point} and x_{point} are respectively the x and y coordinates of the to be computed perimeter point, as determined by the reference system of Figure 19.

On a previous computation step the geometrical properties of all the sections are defined. A Matlab function has been implemented including the generation of vectors which define the exterior diameter and wall thickness for each cross section. The output vector of the simulation process which includes the height of each section where results had been produced is introduced as input. Given the conical form of the tower, only a few key parameters and the

correspondent formulas are need to produce the exact properties of each section by introducing its position in height. Having external diameter and wall thickness accounted, the computation of inertia and area following the over stated formulas becomes automatic.

Given all the previous computed parameters, the stress computation implementation results to be a simple task. For each sea state the correspondent output forces matrixes are loaded. Given the cross section to be computed, geometrical properties vector adequate value and correspondent row of the forces matrix are taken. An empty column vector is created, sized with as much rows as time instants accounted on the forces output matrixes. Each row of the vector is filled with the stress generated from that time instant forces according to the expression given on this section.

The repetition of this procedure for each selected perimeter point, cross section of interest and sea state has been implemented through a system of loops. The results for each computed point do not need to be stored, as the correspondent fatigue computation, whose process is explained in the next section, is implemented to be performed next, avoiding the necessity of saving middle values.

The contribution of each considered sea state must be accounted, for which the process of stress calculation has to be taken to term for all the necessary simulated combinations of environmental properties.

3.5.2.3 Stress Results Validation

A verification process on the functioning of the implemented code has been performed using that created subroutines which contain the stress calculation process. It has consisted on its employment to compute the stresses, on each cross section and time instant, generated by the moment, by the axial force, and, finally, by its sum. This last value is of special interest as long as both will be acting combined.

In the case of the moment generated stress, moments on *x* and *y* have been adequately added, and the radius of the correspondent cross section has been used as leverage arm to compute the related stress, leading to the maximum moment generated stress that will appear on that cross section. For each cross section and load case, mean and maximal values of the time evolution of the obtained stresses have been produced and are available to verify them.

These outputs have been globally checked, on the basis of the verification of key and

indicative parameters referring to maximal and minimal time evolution values, which can be compared in order to check if they reflect its good functioning. It has tried to ensure that no coding mistake has been committed on the program producing those results, which sometimes appear as a consequence of the code complexity and the multiple factors affecting the process.

3.5.2.3.1 Axial Force Stress Validation

The values of the axil generated stress show a good behaviour, and are coherent with the axil forces values analysed in Section 3.4.3.1.

The mean and maximal values of the time evolution on each cross section and sea state of the axial force generated stress had been computed. Of those time evolution maximal values, the maximal sea states stresses have been selected for each cross section. Of the time evolution mean values, the mean among sea states have been computed for each cross section. These results have been plotted in Figure 20.

Regarding the results presented in Figure 20, it is direct to see the oneness between the two plots, both in general shape and in values. The small time variations obtained and verified for the axial forces in Section 3.4.3.1 appear here again, where the maximum sea states stress over the maximum time evolution stress are practically identical to the mean sea states values of the mean time evolution values. Given the linear relation between axial force and axial force

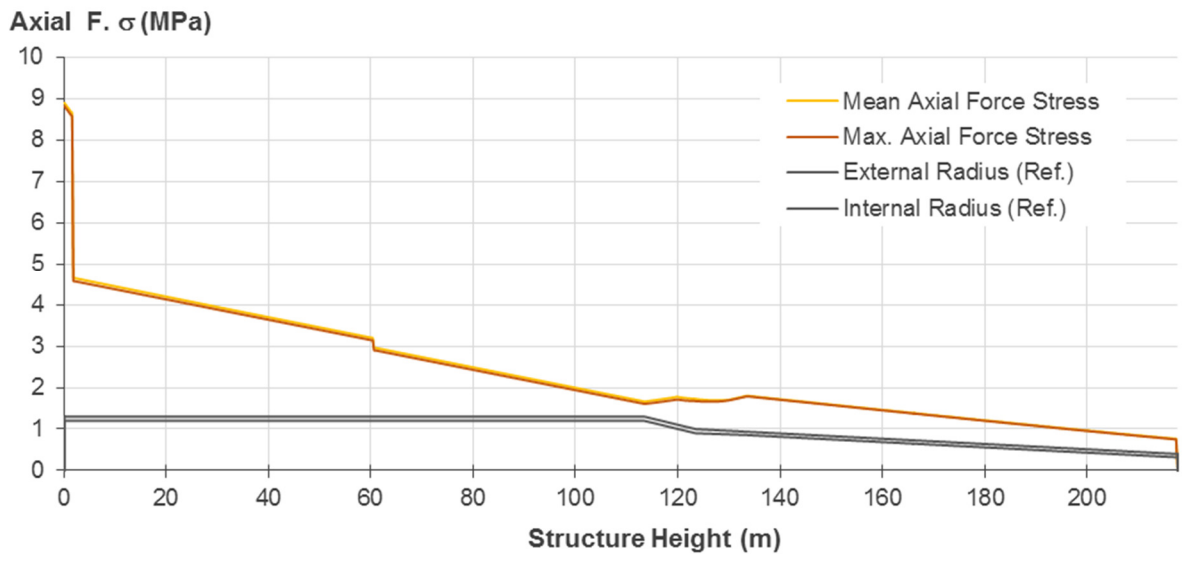

Figure 20 Mean and maximal axial force stress of the analysis output for each cross section along the structure.

stress on each cross section through its area, coherency of the obtained results is ensured.

Some further remarks can be done on the in Figure 20 obtained shape of the axial force stress evolution, which can ultimately ensure the good behaviour of the code in the calculation of the axial forces stresses. As expected, the bigger stresses are located in the bottom of the structure, there where axial force where larger. From that greater values, axial force stress values descends linearly in direction to the structure head. Changes of slope can be seen on its trajectory. It is worth remarking the abrupt value change at height ~60 m, corresponding to the change of axial force due to the mooring lines; and the irregular curve on the transition cone section, where different tendencies of increasing and decreasing axial forces and area values combine.

3.5.2.3.2 Bending Moment Force Stress Validation

Varied analysis for the moment stress output have been made. On a first stage, work has been done over the mean time evolution for each cross section and each sea state, in order to obtain a first view of the regular moment stress behaviour. Over those mean time moment values, the maximal and mean values among sea states for each cross section have been computed and plotted on Figure 21.

From the results presented in Figure 21, a good functioning of the moment stress

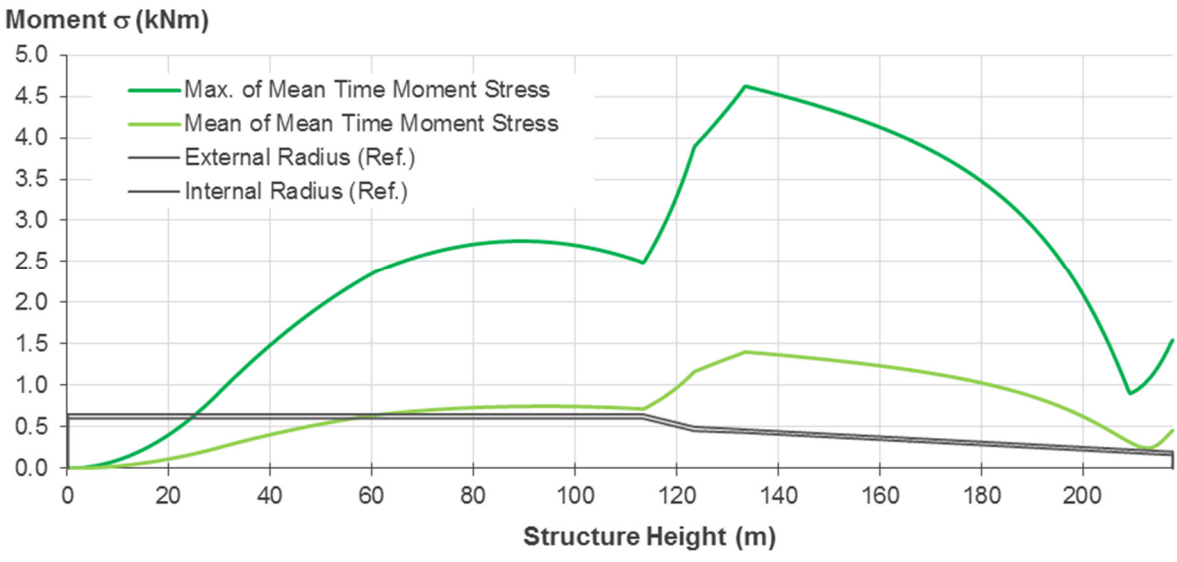

Figure 21 Mean and maximal sea state values for the moment time stress history mean value on each cross section.

computation code can be guaranteed. Mean and maximal cross section plotted curves show the same form, with the correspondent value increase of the maximal over the mean value. Two differenced sectors can be seen on the behaviour of the plotted values along the structure height. On the bottom part, mainly corresponding to the cylinder, moment stress increase corresponds to the tendency showed by the moment force on Section 3.4.3.1. A steep slope takes the moment stress value from zero at the structure bottom to a maximum value at approximately ~90 m height, where it descends again until the cylinder ends at ~110 m height. The constant inertia and radius along the cylinder cross sections guarantees a linear relation between force and stress.

It is where the conical stretches begin (transition cone and tower), when the moment stress stops being linear with the moment force. The progressive reduction of cross section diameter on this sectors affects the inertia moment and the leverage arm of the stress calculation point, for which a highly nonlinear relation is expected. Nevertheless, a qualitative analysis guarantees the correct relation between force and stress.

In order to obtain an impression of the influence of diameter reduction over inertia, Figure 22 has been included, where the absolute value of inertia for the different cross section can be seen. Four section can be seen on it. A constant inertia on the stretch corresponding to the cylinder (from 0 m to ~110 m height); a very steep descend on the transition cone (from ~110m to ~120 m), which corresponds to the fast descend of the diameter on that zone as can be seen on the indicative reference plot of the structure contour in grey; a reduction of the inertia

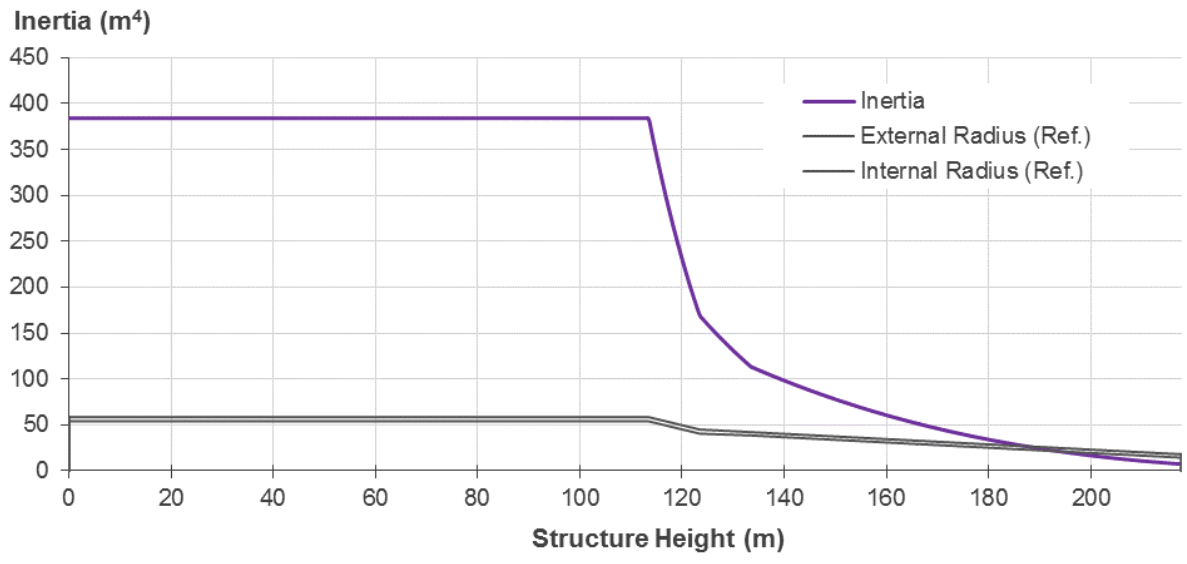

Figure 22 Inertia Evolution along the structure cross sections.

descend slope where the tower starts (~120 m), which extends in the thickness reduction zone of the tower base (up to ~130 m); and finally a small sloped inertia reduction on the rest of the tower (from ~130 m to 217.7 m), corresponding to a constant diameter reduction on fixed thickness.

Given the small and convex slope of the moment force descend on the length corresponding to the transition cone (~110 m to 120 m) that can be observed on Figure 15, and the rapid inertia descend on the transition cone, the fast increase of the moment stress as seen in Figure 21 for that stretch is logical. This increase extends itself a little more in the first sections of the tower bottom (~120 m to ~130 m), where the inertia still descends steeply due to the thickness reduction. The moment corresponding to the rest of the tower shows a concave reduction, which combined with the very small sloped inertia descend produces the descending moment stress values on that sector.

As observed in Figure 23, the moment force increase due to the numerical difficulties of the simulation code for the structure's top shows in Figure 21 by producing high levels of moment stress, given the small inertia and leverage arm on that top section. Once again, it is clear that stress results in that area will not be applicable. Further reference to the dealing with this problem will be made next.

Finally, maximal values of moment stress have been computed and plotted. A coherency check has been performed on them, once in order of magnitude in comparison with the results of the other WindCrete concept development phases, and once in direct relation with the maximum moment force obtained in Section 3.4.3.1.

In Figure 23 the maximal sea state moment stress and the mean sea state moment stress for the maximal moment stress of the time evolution on each cross section can be seen. The maximal contour correspond to the behaviour described in the previous paragraph. A maximal time value for the maximal sea state appears on approximately height ~135 m, leading to maximal stress on that cross section of 7.5 MPa, adequate for the structure values.

A comparison with hand computed values has been done in comparison with the maximal values of moment force presented in Figure 16. Sections of maximum moment force (~95 m height) and maximum moment stress (~135 m) have been quantitatively compared.

- Section 384: h = 95.875 m, I = 384 m4, D = 13 m, M = 240 991 kNm, sigma = 4.07 MPa

$$\sigma_{max} = \frac{M_{TOT}}{I} \cdot \frac{D}{2}$$

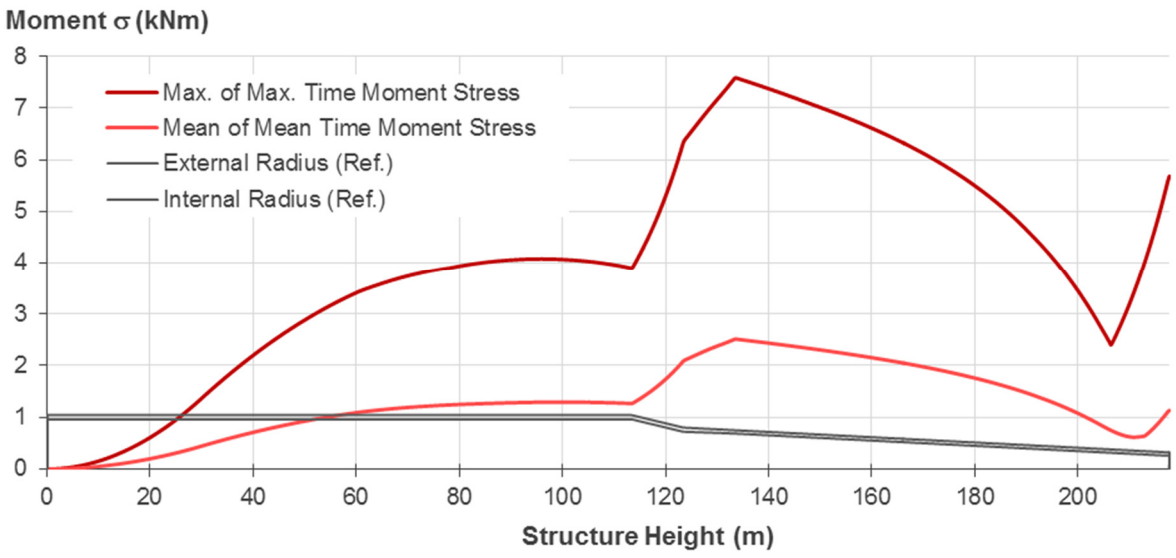

Figure 23 Maximal and mean state, respectively, of maximal and mean time moment stress history along the structure.

$$4.07\ MPa = 4.07 \cdot 10^6 \frac{N}{m^2} = \frac{240\,991 \cdot 10^3\ Nm}{384\ m^4} \cdot \frac{13\ m}{2} = 4.08\ MPa$$

$$\varepsilon_r = 0.2\ \%\ \checkmark$$

- Section 535: h = 133.625 m, I = 113 m4, D = 9.35 m, M = 183 284 kNm, sigma = 7.58 MPa

$$\sigma_{max} = \frac{M_{TOT}}{I} \cdot \frac{D}{2}$$

$$7.85\ MPa = 7.85 \cdot 10^6 \frac{N}{m^2} = \frac{183\,284 \cdot 10^3\ Nm}{113\ m^4} \cdot \frac{9.35\ m}{2} = 7.58 \cdot 10^6 \frac{N}{m^2}$$

$$\varepsilon_r = 3\ \%\ \checkmark$$

After comparing the hand computed values and the code output, the relative error values can be accepted, as long as they are attributed to numerical precision differences. Therefore, it can be concluded that the programmed modulus for the computation of axil and moment forces stresses is adequate.

A small commentary is here previously made about the treatment of the in Section 3.4.3.1 and previously in this section code malfunction of the mechanical simulation tool in the top cross sections for the output moment. The modelled system assumes for null moment on the top section of the tower, which is not reached in the simulation of some sea states due to numerical problems on that area for the solving of the coupled equations. For each simulated time instant

his leads to the in some cases increasing moments which appear on the superior part of the tower, where they would be supposed to decrease.

In order to guarantee the reliability of the results of the fatigue assessment, it will not be possible to consider those sections in the design process, implying the disregard of the output values obtained for them and consequently the impossibility of computing its associated damage. Therefore, it must be ensured that those sections will not be critical ones. Otherwise, the fatigue assessment would be incomplete as long as the determined fatigue life would be associated to the incorrect section which determines the fatigue resistance of the structure.

A small programmed tool on Matlab has analysed all the simulated instants output moments forces along the structures length. The section in which the moment trajectory changes upwards has been stored. The lowest of these section has been determined as the one which will determine the lower border of the disregarded sections. Results obtained after the analysis through the program define that section on a height of approximately 180 m, corresponding to the internal referenced section number 827. Further steps of the fatigue assessment process will only account for the sections under this height, guaranteeing that its disregard does not affect the structure's fatigue life.

3.5.2.4 Prestressing Modelling

Prestressing force along a structural element structural axis must correspond the tensile stresses it will face in design life; in order to reduce them and increase structure durability, rigidity and strength. In the case of WindCrete a total prestressing system has been conceptually planned, for which its force must counteract all the possible tensile stresses which might appear on the structure's service life, leading to a permanent compressive state which guarantees no cracks on the structure and avoids durability problems.

Prestressing force will depend, on one hand, on the structure's localization, whose environmental parameters and its generated forces will determine the maximum possible tensile stresses to be countered; and, on the other, the cross section of the structure, given that great variations on the tensile stress generating forces will appear depending on which height of the structure is being analyzed.

This fact has two major implications. First, different localization will need of different prestressing designs. Not enough compression can suppose structure failure on durability

problems; while an excess can significantly reduce the fatigue life of the structure by determining the mean stress levels of the cycles. Second, coherent and economic prestressing stretches on the structure height will have to be designed. The possibilities of tendon addition and anchoring have to be studied according to the structure geometrical details in order to define the most optimal system which allows the fully compressive state in all the structure length.

A complete and thorough design of the WindCrete concept for its real application will need of a deep study in this regard. Localization, economic and contractual conditions would determine the final prestressing system characteristics. Moreover, modelling the technical properties of the final planned design would need of the consideration of variations on each sections prestressing force along the structure's service life, according to deformations of the concrete structure and the tendons; and prestressing losses, which will have to be duly accounted on its varations along structure height and along the design life, given the affectation of the non-instant losses.

For the purposes of the research on design presented in this master thesis, and given the lack of further information in the regard of what would be the definitive prestressing design system, some simplifications but realistic have been made on the consideration of the prestressing force.

First, the distribution of the prestressing force along the structure's height has been qualitatively performed by defining stretches which have been introduced by previous conceptual design phases of the WindCrete, which would probably differ from what would be a definitive detail project design, given its lack of optimization.

Second, the prestressing force on each of those stretches has been computed employing some qualitative considerations. Given the global and cautious approach that is being used on the whole fatigue assessment that is being presented, prestressing values will result in an indicative factor of its importance, and its influence will be duly studied by checking how variations on it affect the fatigue life.

Finally, no instantaneous losses nor differed have been considered, leading to a section's prestressing force which is maintained constant along all the studied service life of the structure.

3.5.2.4.1 Prestressing Definition

The determination process of the prestressing force on each of the defined stretches is

here presented.

On a previous phase, the maximum possible tensile stresses that could act on the structure's cross sections have been computed. Given the force information available, maximum possible tensile stresses have been computed and stored for each simulated time instant, cross section and sea state as follows.

$$Max(\sigma_t) \rightarrow \sigma_{i,j,k} = \frac{M_{TOT\,i,j,k}}{I_j} \cdot \frac{D_j}{2} - \frac{N_{i,j,k}}{A_j}$$

Where i is the index for the simulation time instant, j for the studied cross section, and k for the sea state. M_{TOT} refers to the total moment, I to the inertia, D to the diameter, N to the axil force and A to the area.

The maximum tensile stress generated by the moment will correspond to the point in the outer perimeter, perpendicular placed from the total moment axis of actuation, in opposition to the maximum which will present the same value on the opposite direction and therefore sign. That maximum tensile stress will be countered by the axial force stress of the section, always generating compression equally distributed on the cross section.

For each cross section, maximum values of the computed resulting tensile stress are selected among all the contributions of the cross sections and time instants. The resulting values in this regard along the structure length have been plotted in Figure 24.

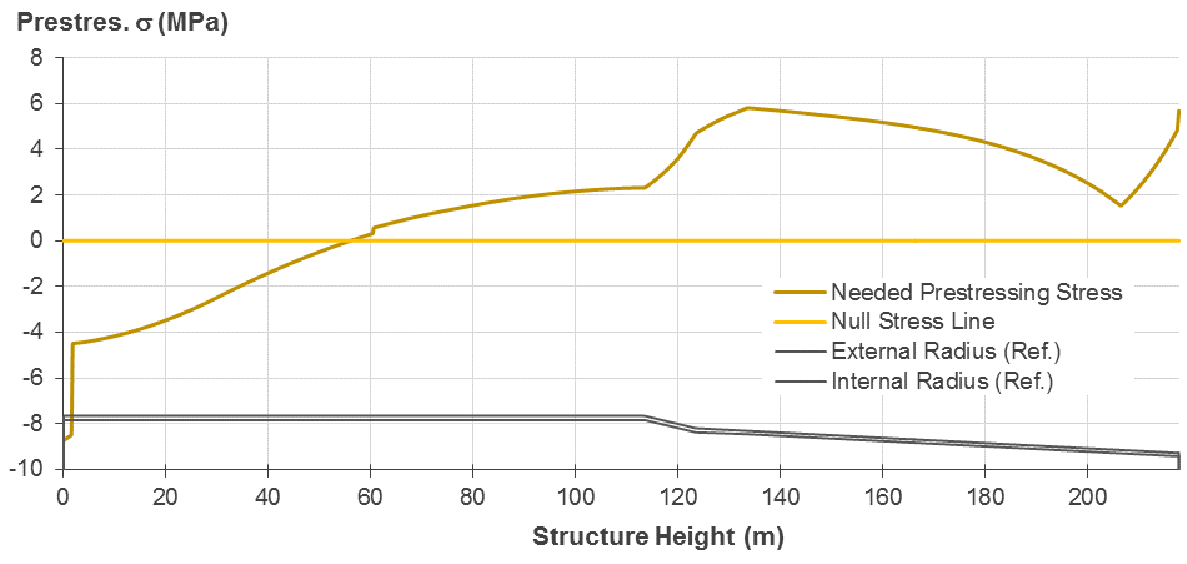

Figure 24 Maximum sea state and stress time history tensile stresses, for each cross section.

The obtained curve shows a form that would correspond to the shape resulting of subtracting the values on a data series for the moment, like the ones showed on Figure 15, to the results of the axial stress, as had been, for example, obtained for Figure 13. The final form resembles the one of the moment, in which the different height values have suffered a reduction of a magnitude which decreases linearly as the cross section corresponds to a greater length.

A further analysis on the results obtained show negative values of the needed prestressing stress for the sections under the approximately 60 m height. This behaviour answers to larger axial stresses than moment tensile stresses, resulting into a naturally permanent compressed set of sections. The decreasing moments forces on that stretch of the structure, along with the large inertia and the great own weight values justify this behaviour.

Moreover, on the right hand side of the Figure 24, corresponding to the top sections of the tower, an increase on the needed prestressing values can be seen, which again corresponds to the larger moments caused by the numerical problems of the output simulation code, combined with almost null axial forces. As stated before, those sections have to be disregarded.

In order to obtain a clearer and more useful distribution of the needed prestressing stress on each cross section, those heights presenting negative values of necessary prestressing have been substituted with a null value; and the information regarding the upper cross sections (> ~180 m, Section 3.5.2.3.2) has been deleted. The resulting curve is detailed on Figure 25.

Finally, the obtained distribution of the necessary prestressing stress level has been

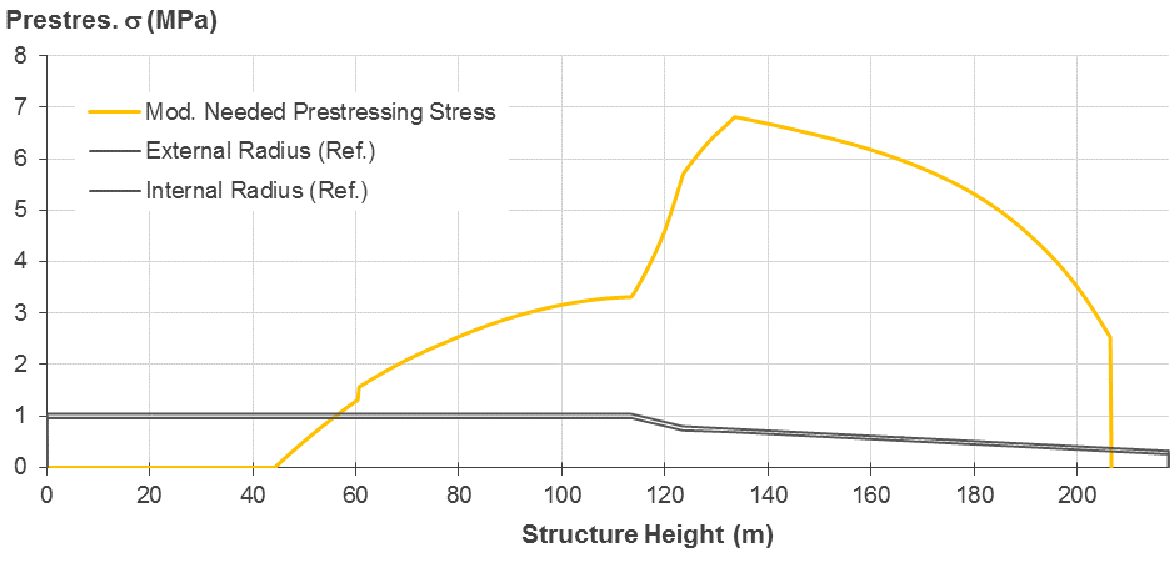

Figure 25 Needed prestressing stress on each cross section.

employed for the definition of the prestressing stretches. The introduction of prestressing is made through tendons which are considered to apply the same force on all the cross sections in which they act. Therefore each defined stretch with the same quantity of tendons will apply an equal prestressing force, whose resulting stress on that stretch will depend on the area of each cross section.

Each prestressing stretch will be characterized by its comprehended cross sections and a constant prestressing axial force. That force will correspond to the one that guarantees that the level of prestressing required by all the cross section of the stretch are satisfied, taking into account the variations on the requires prestressing stress of each section and its area. In most occasions, it will correspond to the force that would be applied on the cross section with the highest prestressing stress need to ensure that its required stress level is reached. If a non-regular relation of the prestressing need and the cross section area do not assure that this method ensures the minimum needed prestressing stress on all the cross sections, further forces corresponding to more demanding sections will have to be used.

Each stretch will therefore probably present many cross sections with a real applied prestressing stress much larger than the one needed. In this sense, a smart stretch distribution definition is key to not overload with compression stresses the cross section which do not needed.

As for the WindCrete fatigue assessment presented, the stretch definition has been based on the distribution of stress levels requirement previously detailed on Figure 25. Two major zones can be seen. On the left side, and for the cross sections corresponding to the cylinder, a general lower stress level requirement, with values up to approximately 3 MPa. On the right side, for the sector of the transition cylinder and the tower, a much larger stress is needed, which is placed between values of 3 and 7 MPa.

In this context, a first prestressing stretch has been defined for the whole cylinder length. Given the lower levels of prestressing stress requirement, the large areas on its cross sections and the small values of the fluctuating moments acting on it; an excess of prestressing level will no suppose a threat for the fatigue life of the structure.

The rest of the structure, corresponding to the transition cone and the tower, presents the exact opposite behaviour. A higher prestressing stress requirements, very small area cross sections and the maximum time variations of stresses caused by the action will make it indispensable to define more than one prestressing stretches. Otherwise, the possibility of over soliciting the compressive stress of some of its cross sections and substantially reducing the

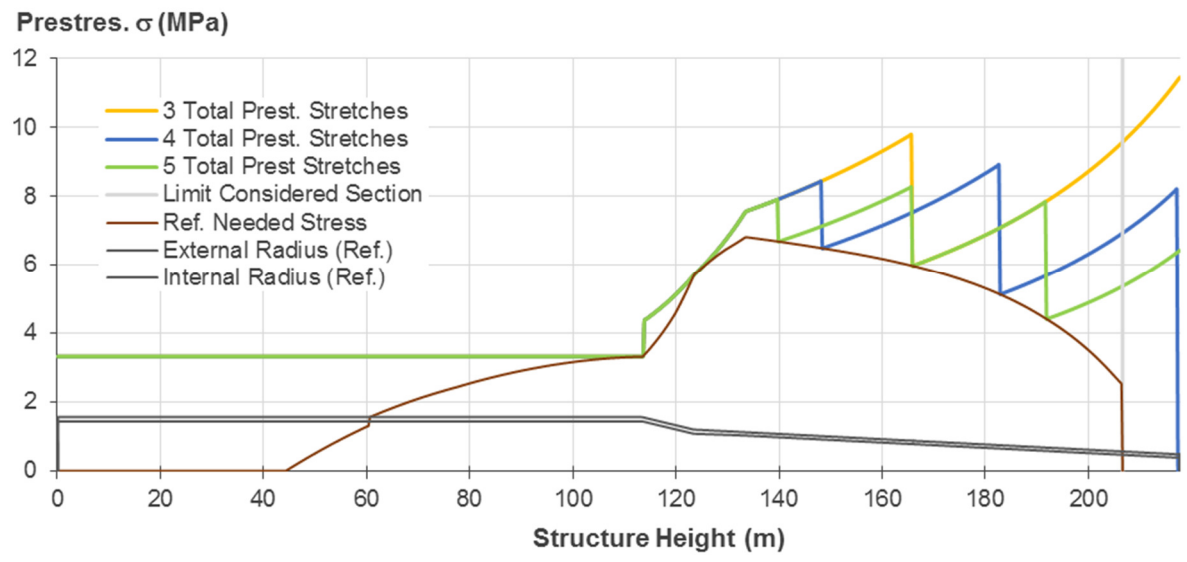

Figure 26 Resulting stresses generated by the forces correspondent to different number of tendon stretches on the tower.

fatigue life can be produced.

Three different possibilities have been studied for the definition of the prestressing stretches; including respectively 2, 3 or 4 equal length stretches on the transition cone and tower sectors.

A Matlab tool has been programmed for the computation of the required prestressing forces on the stretches proposed by each of the three approaches and the computation of the consequent stresses on all the cross sections. Obtained results are presented in Figure 26.

In Figure 26, the plain horizontal line on the left which coincides for the three cases is the resulting prestressing stress applied for the cylinder, equal given its constant area property. On the transition cone and tower sectors, three different plotted lines can be seen. The yellow line, as plotted on the background, accounts for the two stretches definition (3 total stretches). It is easy to see the separation between both on them on height ~165 m. A deeper analysis leads to the sections whose requirements have defined the prestressing force on each of them. On the right side stretch, it corresponds to the section ~165 m. The increase of the correspondent stress applied by the prestressing force on the rest of the sections is then attributed to the area reduction on that direction. As for the middle stretch, a slope change can be appreciated on height ~135 m, which corresponds to the determinant cross section. Its resultant needed stretch prestressing force results in a lower stress to the right of it, given the area increase, and a bigger one on its right, due to the lowest presented areas. A similar behaviour can be observed after

the analysis of the other curves.

As for a final inclusion on the fatigue assessment model, the 4 total prestressing stretches distribution (1 for the cylinder and three for the rest of the structure), corresponding to the blue line on Figure 26, has been selected as the one which would be considered on a real design application of the structure. The maximum prestressing stress level generated by it, which are harmful for fatigue resistance as they increase the mean stress level, are significantly lower as the ones of the 3 total prestressing stretches (yellow line). A further number of divisions would suppose an economic disadvantage on the structure construction as the expenditure on equipment and control procedure would be higher, while no significant advantages on the maximum stress levels would be obtained.

3.5.2.5 Total Time History Stress Values

Once the prestressing stresses that will have to be accounted on the structure sections have been defined, an evaluation of the total stresses magnitude that will be considered on the different cross sections for the fatigue assessments has been made. It is pretended to know the approximate mean and maximum values, which will be taken into account in the fatigue assessment along the structure. It will allow establishing qualitative relations on the damage results that will be obtained along the structure.

Mean values for each sea state of the mean and time history values on each cross section have been computed. The results can be seen on Figure 27.

In Figure 27 the upper line, plotted on a darker blue, represents the mean sea state of the time evolution maximal total stresses for each cross section. On an inferior part, in a light blue, the same mean sea state for the in this case time evolution mean total stresses.

Many interesting information can be taken from this graph. On a first sight the mean maximal stress on the structure will be produced on its base with a value of ~12 MPa , although with no variation as the maximal and mean values are very similar. Therefore a critical fatigue damage is not expected on that bottom cross section.

Further sections with high values of stress and large varaitions (difference between maximal and mean curve) can be seen on the cross sections between a height of ~135 m and ~180 m, where mean values of around ~11 MPa and maximal of ~12 MPa are seen. In this sense, it will be expected for the critical section to be placed on this heights.

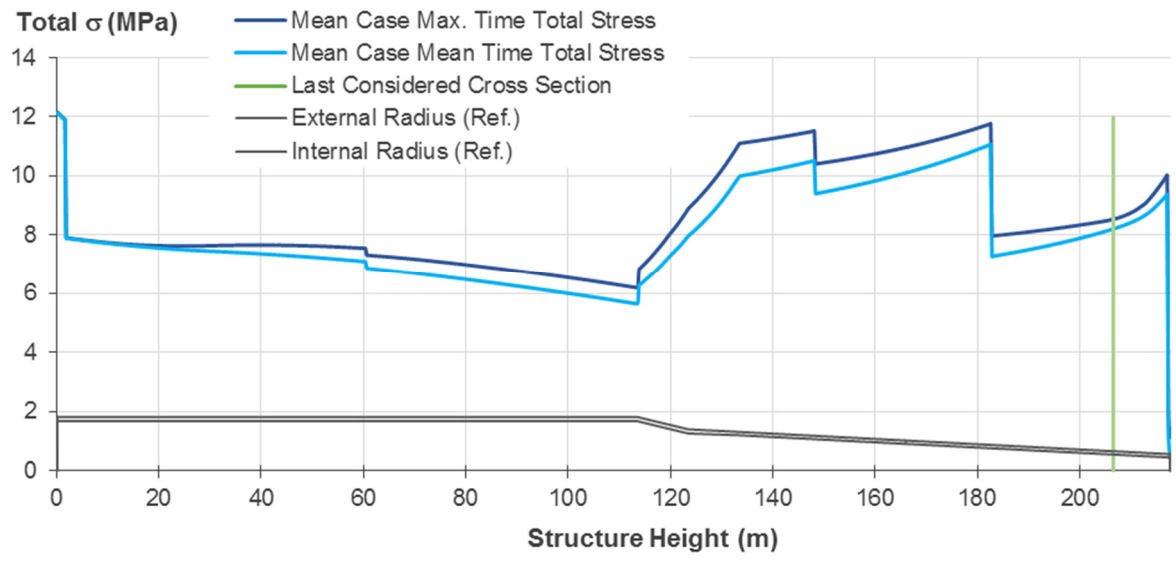

Figure 27 Mean sea state on each cross section for the maximum and mean time stress history values, inclduing all loads.

Nevertheless the here described indicators plotted on Figure 27 are only global parameters which do not account for the real variation of stresses, the time of influence of each sea state, its direction (which determines the point on the cross section with maximal stress) or the number of cycles generated on each of them. In this sense, the critical section on this problem can only be determined after the damage has been computed in all the possible sections and that presenting the critical one is identified.

As a las remark, in Figure 27 the height for which no further cross sections shall be considered has been plotted. As it can be seen the cross sections with large maximal and minimal stress values do not lie above it, for what it is expected that it will not cause any major problems on the reliability of the fatigue assessment. At any case, only the extensive damage mentioned in the previous paragraph will guarantee that this lack of information does not affect the fatigue design.

3.5.3 Damage Computation

The stress computation tool detailed on Section 3.5.2 accounts for the stress variations on each of the selected cross sections defined points of interested. This temporal variations of stresses on each discretized location will cause a fatigue damage associated to it, which can lead to the failure of that point, and the consequently structure collapse, for high values.

Fatigue damage is influenced by the number of stress cycles affecting that point, the magnitude of that cycles and the mean stress level of each of them. The more cycles, the higher the stress range, or the larger the average stress of each of them, a greater fatigue damage will be obtained.

Fatigue damage must be computed on all of the defined candidate points of the structure for the stress variations that will be produced on them along its service life. This service life has been divided in years (Section 3.3) which are considered to contain the same distribution of different sea states. Each of these sea states which are expected to happen on that mean year have an associated probability of occurrence, summing the unity all together. This yearly occurrence of probability is transformed into expected time of actuation, for what the real duration of the effects of that sea state over the structure are known.

Damage computation will consist therefore on the adequate addition of all the contributions to damage by the stress variations caused by all the considered sea states on the point in which is being studied. This computation will have to be made for all the candidate points, which will account for the same influence of sea states but for different stress variations caused by each of them from point to point.

The implementation of a Matlab tool for the realization of this process is explained in this chapter, detailing the hypothesis assumed by the code and the process particularities.

3.5.3.1 Computation Process General Considerations

The created Matlab program follows the recursive scheme employed for the stress calculation, in which right after the stress evolution calculation on a point, the associated fatigue damage is computed. The fatigue damage value will therefore be associated to the real simulation time for which the series of stresses on that point has been computed, obtaining a relation between time of actuation of that sea state and a caused fatigue damage quantity on that discrete point. The complete year damage calculation will consist on the proportional addition on each studied point of the damage caused by each actuating sea state.

The critical point, and consequently the critical section, will be that with a higher one year produced fatigue damage value. Knowing that the obtained damage account for a year of service of the structure, the fatigue life of the structure will be computed as the division of the maximum allowed damage over that produced in one year for the critical point.

The special part of this process, which is the main objective of fatigue analysis research, is the establishment of the relation between stress variations and resulting fatigue damage. For the purposes of this master thesis, this transformation process has been done following separately the indications for fatigue damage calculation over concrete of three different public constructive codes (Chapter 2), which are widely established and used. It has been the objective of this study to produce real applicable results for the WindCrete structural concept, for which the employment of the methods defined by the constructive codes which regulate its design and construction is crucial. It is expected from those to produce different fatigue damage values, as long as the methods they propose are not identical. Its methodology differences and results generated will be for the objectives of this work accounted and compared.

All of the three codes employ the methods of the S-N curves and the linear damage addition of the Palmgren-Miner rule. Further reference on the theoretical background of these methods can be found on Chapter 2. S-N curves work on the concept of cycles, defined as a variation of the stress level on that point which ends and starts on the same value. Each cycle will have defining maximum and minimum stress values, along with a mean stress level corresponding to its mean. The S-N curve defines the maximum number of cycles with constant characteristics that the material will resist on the point that suffers that cycle.

Each of the codes works on S-N curve which follow this principle but are subjected to different numerically calibrations, for which its results are not equal, despite presenting a similar behavior. Besides it, each of the codes makes further assumptions and defines different parameters which much be duly accounted when working, following his prescriptions. Those respond to the physical background of the fatigue phenomena. Further reference to its particularities can be found on Chapter 2.

3.5.3.2 Cycle Counting Method

Nevertheless, the real stress series which are applied on the structure rarely can be distributed on cycles with constant maximum and minimum values, showing a distribution on multiple irregular different value changes, which do not tend to respond to any stablished pattern, and presenting varying properties and even different duration time.

Two major problems, key for the understanding of the fatigue damage computation procedures arise here. On one hand, the transformation of that irregular series of values to cycles. On the other the computation of the total damage produced by that set of cycles, which

will likely be based on a large quantity of cycles defined by different characteristics of maximal, minimal and mean values.

A problem in the context of the fatigue damage computation which has to be accounted is the definition of the cycles which appear on a series of time varying stresses on a given point. The transformation of a time series of a parameter in the cycles constitutes a problem itself which has been widely researched, and which is named as counting problem. Many different methods exist, standing out procedures like the range and peak count methods, the TNO count method and the Rainflow methods [142]. Each of them present its own characteristics and applicability ranges. As for the purposes of the analysis performed in this thesis, the Rainflow methods has been selected given its universality and its inclusion on the Model Code 2010 as recommended method [116].

The Rainflow method accounts for the different cycles found on the stress time history depending on the previous cycles value. It is often also named as the Chinese pagoda method, given the analogy with water drop falling down the roofs of a pagoda, which might not slide itself through all of them (cycles) when the horizontal length of the next roof is smaller than the directly previous ones (small and big range cycles). Further references on its functioning, requirements and assumptions can be found on [116]. For the purpose of this thesis, an external Matlab tool, which has been tested and verified, has been used for its implementation on the code.

The counting method will provide the significant distribution of the stress time evolution on a significant and representative number of defined cycles, each of them with an associated characteristics defined, including stress mean value and value range.

3.5.3.3 Damage Addition

Finally, an approach is then needed to compute the resultant damage generated by such a set of cycles. This is commonly made through a linear damage addition rule, like the Palmgren-Miner rule, which considers that the damage generated by each cycle type can be linearly added.

The final damage calculation will result therefore on the computation of the damage generated by each cycle type. Damage calculation on the linear addition basis turns out to be a simple procedure, which is based on the next equation.

$$D_{TOT} = \sum_{i=1}^{i=m} \frac{n_i}{N_i}$$

Where m is the number of different cycles present on the fatigue damage contribution n_i the number of type i cycles present, and N_i the maximum number of type i cycles that the structure could resist given its properties (maximum, mean and mean value) as obtained from the employed S-N curves.

Classical fatigue calculation on simple static structure take often into account only a few different types of cycles, which are estimated from the simple variations of the loads acting on it along with its number of repetitions. In this sense the problem here presented will account for a large quantity of cycles with different characteristics which hardly will present more than one repetition.

Nevertheless, the consideration of the hypothesis of the linear damage addition theory and its employment, guarantees that the total fatigue damage, whether it its computed for many repetition of an identical cycle, or for a single repetition of many different cycles, will guarantee a good description of the fatigue resistance of the structure. The employment of many different significant figures which Matlab automatically performs will not disturb the final results, as long as the computational cost increase is not harmful and the unreliability inherent to the hypothesis of the problem resolution process account for an objective use of the final results obtained from them.

3.5.3.4 Damage Determination

Given the output of the counting tool, which will consist of the counted number of cycles and its properties, given in form of a mean level and the range of values, fatigue damage generated for each of them is computed and added through the correspondent code S-N curves and prescriptions.

For each cycle defined with a maximum stress level σ_{max} (correspondent to the mean stress level plus half the stress range) and a minimum stress level σ_{min} (computed as the mean stress level minus half the range), a value of total resisted cycles N will be obtained. The damage resulting of that cycle will then be the division between the number of cycles n (most likely one) over the total resisted cycles. The fatigue damage computed for each cycle obtained of the stress series can be then simply added to the total damage count.

The programmed Matlab tool, after computing the stress time history on the selected discrete points for a given case, transform that stress time history into the correspondent number of cycles. The associated damage to each cycle is computed using the desired method S-N curve and considerations, which are later linearly added. The yearly damage rate of that sea state for that point is obtained on the basis of the damage obtained for the simulation output results and the real time in which that simulation has consisted. The final damage contribution of that sea state to that point on a year will be the result of multiplying the yearly damage rate times the probability of year occurrence of that load case. This process is repeated on a first stage for all the sea states, computing the total year damage after adding its contribution. On a second stage, the same process is repeated for the rest of selected points, finally obtaining the year damage at which the structure will be subjected, and, with it the critical section and the fatigue life of the structure.

3.6 Fatigue Strength

3.6.1 Introduction

The fatigue analysis method proposed on the previous sections, which has been implemented on a Matlab code as presented, has been employed for the estimation of the fatigue life of the WindCrete structure, given a proposed spatial location (Section 3.3.2) and the hypothesis about its final design, related to its geometry (Section 3.2) and prestressing (Section 3.5.2.4).

The redundant scheme in which the code is based implies a high computational cost. The necessity to study the structure as a set of discretized points makes it impossible to approach its computation another way which does not consist on the repetition of computations for each of the possible combinations of sea state, cross section, perimetral point and outputted stress cycle.

Given the excessive time that would suppose an extensive computation of the fatigue damage on all the possible points of the structure, the characteristics of its stress behavior and resisting properties are taken into account to work over a set of candidate sections in which the maximal fatigue damage will be most likely produced. An approach like this needs of the verification of the hypothesis made on the selection of critical cross sections in order to guarantee the results reliability, which has been duly accounted.

The approach employed to take to term a cost effective and reliable characterization of the fatigue life is here presented.

3.6.2 Calculation Process

The fatigue damage has been obtained for points placed on the critical sections of the structures. Candidate sections have been selected given the intensity of the moments on its corresponding height and the resisting properties of that section, mainly consisting on inertia. In the sections where the biggest stresses appear greater fatigue damage will be produced. The candidate selected sections must correspond to the ones with results attached, as given in the simulation output (Section 3.5.2.3.2).

Once the candidate critical cross sections are selected, the perimeter discrete points on each of them where fatigue is expected to happen must be selected. The selection of points

where fatigue damage will be computed, and therefore where the stress time evolution needs to be evaluated, has been performed. The specific points on that curve have been selected according to the considered origin directions of the environmental actions. Those cause the biggest loads on the structure, which result into bending moments. Given the origin direction discretization in which the analysis has been based, the moments can only take the direction defined by the central axis of each origin section. Its directions determine the points where the stresses caused by this moments will be higher, which will be the ones placed at the further possible distance from the coordinate centre along the perpendicular direction to the moment axis.

In conclusion, the points whose fatigue damage will need to be studied are the ones correspondent to the sections perimeter and the medium axis of each origin direction section.

3.6.2.1 Candidate Critical Cross Sections Selection

As stated on Section 3.5.2.5, the bigger the mean stress level and/or the stress range on a given cross section, the bigger the damage that will be generated on it. As computed in that same section and presented in Figure 27, where the tendency among different sea states of the mean and maximal total stress values is plotted, the bigger stress levels are obtained in sections between ~130 m and ~170 m height, with mean values around 10 MPa and maximal values on 11 MPa level.

In this sense, it can be expected from the cross section which will cause the structure collapse to be placed on that stretch, but, no singular cross section can be selected as critical with only this information. The total fatigue damage calculation will account for each single variation of the stress range and the mean stress on all of the sections. It is therefore possible that the main values there presented do not represent correctly the influence of each of the modelled sea states on the stress behaviour, being possible too the existence of difference between design cases or design codes.

As a practical and reliable way to optimize computations and avoid the resource waste on the production of recursive information for cross sections without interest, the critical cross section has been seek by computing the damage caused by independent sea states alone. On all of them, the obtained critical cross section responded for the internal number 535, correspondent to a ~133.6 m height. This results into a logical position given the curves of Figure 27, where mean and maximal total stresses where computed as mean sea states values.

A thorough global analysis and verification of the structure would need of the obtaining of the to be computed final damage on all the possible section, in order to disregard what could be effects of rare sea states on the critical section position.

3.6.3 Results Presentation and Discussion

Whole fatigue damage calculation processes over the environmental data, procedures and programmed tools detailed in the past sections have been performed.

Final yearly damage results for the determinant discretized point of the critical sections provided by each code computation prescription are presented in the Table 4.

Yearly Fatigue Damage	Model Code	Eurocode 2	DNV-OS-C502
D_{year}	8.422E-06	2.437E-04	5.706E-07

Table 4 Standard year damage on the critical point of the structure as obtained from the three different codes.

All the in Table 4 presented results have been obtained for what has been proved to be the critical cross section as obtained in Section 3.6.2. The perimeter point of that cross section in which the maximum damage is produced correspond to the one placed 164º from the north direction clockwise. This point coincides with the direction line of most of the obtained sea states, namely, North North-West direction, for what it can be considered to be coherent.

Results observed appear as very low levels of damage which vary substantially (from one to three orders of magnitude) from applied code to code. These damage values can be considered to be neglectable, given that the number of years in which the maximum level damage will be reached is far bigger than a normal required service life.

Even when the most restrictive DNV-OS-C502 damage limit value is used, $D_{lim} = 0.3$, on the most restrictive obtained code, $D_{year}^{EC2} = 2.437 \cdot 10^{-4}$, the fatigue life appears to be sufficient enough to disregard any possible fatigue collapse.

$$FatigueLife = \frac{0.3}{2.437 \cdot 10^{-4} \frac{1}{year}} = 1231\ years$$

3.6.3.1 Results Validation

The validation of this results is a complicated task as long as no previous available experiences on similar problems has been found. Many are the conditions that make it senseless to compare them with other similar fatigue analysis. Previous solved problems do not account for all the features that the presented procedure includes, such as the characterization of the wind climate including directionality, a dynamical simulation on the floating body or the concrete fatigue resistance characteristics. The mechanical simulation procedure influence, or the fundaments of each of the fatigue design codes used, could be accounted in the research of validations and verification of the results. Nevertheless, some efforts have been made on the try to understand better the behaviour of the process and the damage results.

In a previous phase, coherency has been seek on the results obtained by comparing the produced results for each code for defined standard cycle case

A standard singular cycle has been defined in order to compute its damage effects over the structure with the different codes. As seen on Figure 27 mean values for cross section at height ~133.6 m would correspond to a mean value of 10 MPa and a maximal of approximately 11.2 MPa, resulting into a maximal range of 2.4 MPa. Probability pondered mean time period on all the defined sea states, has resulted into a value of ~3,5”.

The S-N curves on all three models for the considered values of the proposed cycle have been plotted on Figure 28. Those correspond to the relation between maximal stress level and

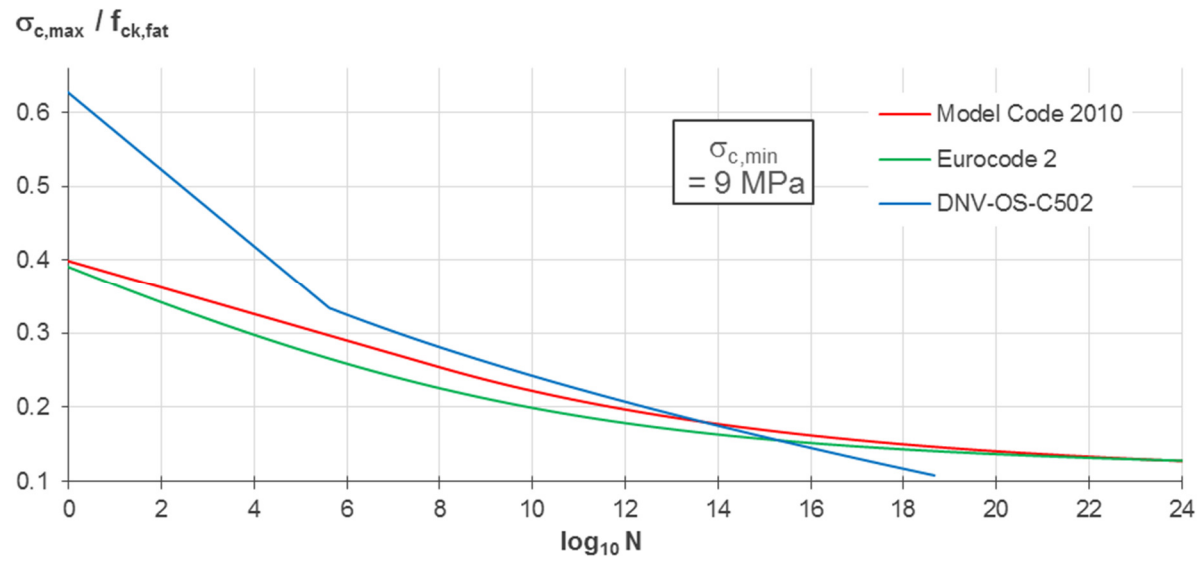

Figure 28 S-N curves for a minimum stress of 9 MPa, as defined by the different codes

the base 10 logarithm of the resisted number of cycles, given the minimal stress of 9 MPa. Considering a stress range of approximately 2 MPa, it would suppose a maximal stress of 11 MPa which corresponds to a maximum stress level of ~0.2.

By entering the Figure 28 diagram vertical axis with a value of the maximum stress level of 0.2, the next values of $\log_{10}N$ are obtained:

- Model Code : ~11.5
- Eurocode 2: ~9.5
- DNV-OS-C502: ~12

The total number of cycles in a year can be estimated by the wave period. The total number would be the 31 449 600 seconds in a year divided over the main wave period obtained of 3.5 seconds which provides a total number of cycles of 8 985 600, corresponding in this single cycle validation to the parameter n of acting cycles.

With this input value of the n and the N value obtained from Figure 28, yearly damages have been computed for each code, as supposing that the cycle will be constant along all the year that no directionality will be accounted, focusing always on the same point.

- Model Code : 2.84E-5 1/year
- Eurocode 2: 2.84E-3 1/year
- DNV-OS-C502: 8.99E-6 1/year

As expected, the levels of yearly damage have been superior to those of Table 4, given the singular direction of the cyclic load considered and the large stress range, as it was defined in relation to the maximal value.

Nevertheless the coherence on the order of magnitude relation between each of the computed codes is maintained. In this sense Model Code has stepped from 10^{-6} to 10^{-5} damage/year, Eurocode from 10^{-4} to 10^{-3}, and DNV from 10^{-7} to 10^{-6}, maintaining the relation between them as outputted from the total number of resisted cycles of the S-N curve and for which the combined sea sate fatigue damage computation also responds.

A good behaviour of the damage computation and addition code, and of S-N curves themselves, can be then expected, as the relation in order of magnitudes between the different codes is maintained for simple cases.

3.6.3.2 Prestressing influence

In a further step, the influence of prestressing stress over the fatigue behaviour of the structure has been checked. It is known that mean stress level, which is mainly determined by prestressing, has a big influence on the fatigue damage produced. Moreover, it is very possible that a change of the spatial location of the wind turbine can lead to higher forces and higher prestressing stresses, for which the obtaining of its influence becomes a crucial part of this previous conceptual phase that will affect completely future designs. The increment of prestressing stress can also be accounted as a general increment of the mean stress, as could be produced by other factors such as area reduction

Yearly Fatigue Damage	P + 0 MPa	P + 1 MPa	P + 2 MPa	P + 3 MPa	P + 4 MPa	P + 5 MPa
Model Code	8.422E-06	2.733E-05	1.183E-04	7.058E-04	6.098E-03	1.630E-01
Eurocode 2	2.437E-04	1.117E-03	6.369E-03	4.587E-02	4.329E-01	1.000E+1
DNV-OS-C502	5.706E-07	1.621E-06	4.824E-06	1.511E-05	5.016E-05	2.316E-04

Table 5 Standard year damage on the critical point of the structure from the three different codes with prest. increment

The resulting values have been included in Table 5. Each value obtained has been computed for the same cross section as the values in Table 4, and obtained in an approximately 164º clockwise from north origin direction (+-1º error).

It is easy to see an increment on the yearly damage when the mean stress level is grows. For each extra 1 MPa of prestressing added, the relation between different codes in order of magnitudes is maintained.

For the increment case of 2 MPa a critical fatigue life of 47 years when taking into account Eurocode 2 and limit damage of 0.3 (0.3/0.00637=~47). For an increment of 1 MPa more (3 MPa added in total) and the same limit damage, Eurocode 2 will provide a fatigue life of only 7 years.

In regard of the other codes, longer fatigue life would be provided by them. As for the ones critical, as they could interference the planned design life, Model Code provides a fatigue life of 50 years with a D_{lim} of 0.3 for the addition of 4 MPa. In the case of the DNV code, even with the maximum computed addition of 5 MPa a large fatigue life of 1295 is obtained.

3.6.4 Fatigue Behaviour Conclusions

A complete fatigue analysis, following the prescriptions and procedures detailed by different constructive codes, has been taken to term. Its final results lead to some conclusions which are here presented.

A first observation on the different yearly damage rate values obtained shows a clear difference between the results provided by the different codes. *Model Code* procedures produce damage values which two orders of magnitude below the ones of *Eurocode 2*; and one orders of magnitude above the DNV code for offshore concrete structures. In this regard, *Eurocode 2* proceed appears as the most limiting one, and the one that would produce the maximal levels of safety. In this terms, it would be close followed by the *Model Code*, and much further would be placed the DNV, which would not be so limiting.

Given the disparity of the results obtained, verifications and validations over the damage computation steps and over all the general mechanical analysis, both conceptually and referred to the computational tools created, have been taken to term and presented. Coherence has been observed in all them (Section 3.4.3.1, Section 3.5.2.3 and Section 3.6.3.1), for which errors on the final results have been disregarded.

A closest look on the obtaining process of the final results has stated the correlation in order of magnitude between the damage results and the values of the S-N curves employed for its determination. For the values adjacent to the S-N curve points representing the mean cycle properties on the critical sections, the corresponding number of resisted cycles for each curve presents as well this order of magnitude relation.

The difference between the damage values obtained for the different codes state once again the complexity of the fatigue phenomena and the empirical character of the approaches that try to describe it, both on the resolution process and on the final form of the S-N curves.

As it can be seen in Figure 28 all three curves follow the same shape, with differences of varying intensity among the three of them. *Model Code* and *Eurocode 2* present similar values, while the DNV code show much larger values of maximal stress level for values of the resisted cycles number logarithm below 6. This behaviour has been attributed to the different parameter computation procedures of the codes, and especially to the definition of the concrete's design fatigue strength. In the case of the MC10 and EC2, it results to be much smaller than the characteristic value given the variety of reducing parameters which influence its computation ($\gamma_{c,fat}$, β_{cc}, k_1, etc. Section 2.6.1 and Section 2.6.2), while only the partial load material for

concrete must be accounted on the DNV, leading to a much larger fatigue design strength of the material and therefore larger allowable stress levels.

The comments here made about the final results have been obtained for the set of cycles derived from the analysis of a specific structure subjected to a concrete set of loads. S-N curves account for each of the cycles present on the structure, presenting many result variations between the different possible combinations of maximal and minimal stress level. As it can be seen in Figure 28, curves intersect themselves for low values of maximum stress level, which would lead to different behaviours for the same cycle properties. Moreover, the curves on Figure 28 respond for the same value of minimum stress level. Varying it, would lead to many possible combinations of the output values. It is possible that a different relative behaviour of the three codes results could be observed for an input set of cycles of different characteristics.

It can be therefore concluded that the influence of the S-N curve and its associated computation procedure is crucial over the design fatigue life of the structure. A complete fatigue design and verification shall therefore need of the S-N curve calibration and the procedure parametrization which can best describe the treated problem, including considerations on the structure type, the intensity of the acting loads, and the characteristics of the environmental conditions. The selected procedure shall account for enough reliable safety levels, while allowing to design a non-oversized structure. Further knowledge on the obtaining background of the three codes procedures shall be obtained in order to make decisions in this regard.

The general results and the derived verification analysis allow to justify that a structure like the WindCrete, placed on the by this Master Thesis proposed location, will not have problems in regard to fatigue processes, being it possible to disregard fatigue as a critical limit state.

The results of the further performed analysis on the mean stress level influence, taken to term in terms of an increment to the prestressing stress mean value, have shown as well interesting results from which important conclusions have been obtained.

On first term, the relation on the safety level of each of the curves is maintained through the different increment cases, from which the coherence of the model can be stated.

On a second place, a high growth of the damage rates can be seen for the increments on the mean stress level, turning highly critical in some of the curves for relative small increments of it. This leads to considerate the possibility of fatigue problems on localizations of the structure correspondent to severer seas, in which the harsh environmental conditions would cause higher loads and the associated higher prestressing levels, implying a significative variation on the

resulting damage, given the growth on both mean stress and stress range of the cycles.

A good and optimal design would have therefore to account adequately for the mean levels acting on the structure, evaluating the influence of prestressing stretches along the structure, and accounting adequately for increments on it due to structural details with special geometries or variations on the structure geometry.

The possibility of thickness variations shall be accounted as well as a design solution. Given the actual results, fatigue resistance would allow to diminish general areas of the structure through a wall thickness reduction, which would lead to economic benefits on the project. Contrariwise, the implications of a placement with more difficult sea states could be avoided on a wall thickness addition, increasing both inertia and area, and leading to both smaller stress variations and mean stress levels.

4. Conclusions

An extensive research has been conducted on the fatigue phenomena behavior on concrete structures for floating offshore wind turbines. It has been possible to establish a wide and deep knowledge base on the matter, which, furthermore, has been employed for the elaboration of an applied fatigue design method; including the proposal of a fatigue damage analysis method and its implementation as a computational tool on the Matlab programming language.

In a first term, the main topics of the state of the art regarding floating offshore wind turbines technology have been presented, allowing to obtain a global view on the necessities they face and the solutions that up to date have been engineered. As a key tool that is inherently attached to its development, its simulation procedures have been studied as well, obtaining a good perspective on the theories used and the level of simplicity and reliability involved. Both researches have allowed to obtain a deeper knowledge on the functioning principles of the WindCrete structure, providing a general description of the parameters and implications which its design involves.

Next, a complete summary on the state of the art knowledge of fatigue has been introduced. As it has been seen, the complexity of the phenomena has required of a global, but rigorous treatment. It has been considered necessary to conduct it on a deeper delve basis, for which a topic progression, from the more general historical review to the specifics of its evaluation on offshore structures, has been selected. The different related necessary concepts have been understood, along with its different approaches and the engineered characterization methods. Further details on the fatigue phenomena have accounted for the aspects regarding its practical treatment on real engineering problems and designs. The most important existing codes which include prescriptions concerning fatigue verification have been studied and compared.

As for a last section of the previous literature research, the results of the study on the limited existing references on the fatigue design of floating offshore wind turbine concrete structures have been detailed. It has appeared to be an indispensable part of the developed master thesis works, leading to the fundaments of the upcoming definition and proposal of a fatigue design procedure applied on a real floating offshore structural concept.

In the context of the practical developments of this Master Thesis, the results of using the knowledge extracted from all the gathered information on the matter are presented: a fatigue

design method is proposed as an approach to its application on the conceptual structure WindCrete.

As it has been possible to see, fatigue design extends much further than the characterization of fatigue damage. It requires of a solid process in which solutions must be found in order to obtain a reliable stress time history, a calculation procedure for its stress response must be defined, and finally an appropriate way to evaluate the fatigue damage which results of it must be selected. All of these aspects have been duly taken into account, providing an approach proposal which has resulted to be a reliable method on all its treated aspects. Its implementation on a Matlab code has allowed to obtain an optimized computation tool, which stands out for its flexibility on the incorporation of new concepts or parameters, and for the easy verification on the correct behavior of its intermediate process.

As a culmination, it has been possible to apply the produced model through its programmed tool on the verification of the WindCrete structure against fatigue. Given the conceptual state of this structure, considerations have been made on what could be a likely application of the concept. In this regard, a spatial location proposal has been made, for which environment and load characterization have been taken to term following the procedures of the proposed model. The mechanical response to those, including the forces distribution, has been obtained through a competent simulation, which has taken into account its more important loads and the dynamical character of the problem.

As for the final fatigue characterization, the verification prescriptions of three different codes have been employed, selected for its interesting contributions to the design calibrations. A comparison on the by each of them defined procedures and the obtained results has been realized as a practical way of analyzing its validity, obtaining a global view on the fundamental parameters affecting the structure behavior and some insight on what would be its performance against fatigue in service conditions.

Such an extensive and complete global research has led to many observations on the different procedures which are worth commenting as a final completion of the work developed. In a first term, the complexity of the fatigue phenomena and the difficulties for the characterization of its effects on real problems are existent. The S-N curve method, as the only approach to the fatigue damage computation defined by the existing design codes, results to be a variable procedure with a high dependence of its results over the calibration used.

In general, it has been observed that the fatigue analysis process is based on different assumptions and many qualitative approaches that result into problem resolution proposals

which are based on, either assumptions that focus on guaranteeing high levels of safety, or on an approach usage that must be appropriate with the specific characteristics of the studied problem, for which particular previous experience and research is needed.

Moreover, the general fatigue design approach involves different parts which can result into engineering problems themselves, as it has been the case of the load determination approach on this thesis. The characterization of the time evolution and variation of the different parameters which condition the loads on the structure has resulted into a very demanding problem for which an effective solution has been found. It has required, on a first step, of the correct approach onto the selection of the parameters which more adequately represent the sea state climates that is trying to be described given its behavior and its simulations. On an even more challenging question, the combined variation of the different selected parameters has had to be carefully described, looking for an economic analysis process while guaranteeing reliability.

In similar terms, the necessity of a good mechanical simulation tool exists. A good representation of the forces that will appear on the structure while on service, along with an adequate characterization of its variations, turns out to be fundamental given its high conditioning on the fatigue damage resistance for some specific geometrical peculiarities.

The final proposed and implemented model, which accounts for the computation of all the values representing the results of all these mentioned previous step, and for the characterization of the final fatigue damage itself, has resulted to accomplish the proposed objectives of comprehensibility, practicality, flexibility, optimization and reliability.

A major innovation, which represents a high benefit for the necessary fatigue design verifications, is the possibility to compute the fatigue damage along every single point of the structure, providing an extensive description which can ensure to recall the correct section in terms of criticality, and optimize the structure by, for example, adding or removing material on the adequate zones as provided by the analysis. Such a complete procedure has proven to not require of an excess of computation resources, given its planned implementation in this sense. Fine enough results can be obtained on assumable times for adequate point discretization.

The results obtained have been proved to be reliable, through the duly verification of all the different intermediate processes and results. In the same sense, the final damage computation process has also been accounted, for which an explanation on the results disparity has been found on the differences on the parametrizations and procedures of the general calculations process which each of them prescribes. Final results on fatigue life of WindCrete

have shown different interesting aspects which is worth outlining. In a first term, it has been concluded that for the proposed design problem, given the spatial location accounted and the prestressing values derived, fatigue life would not be critical, having obtained large values of it.

The conceptual state of the WindCrete structure, with no specific or localization related application, has made it necessary to account for variations on its design parameters. Considerations on higher level of prestressing, which could be required on harsher environments have been taken to term. Results obtained in this regard, have showed a large influence on the mean stress level over the fatigue damage and consequently over the fatigue life of the structure. For relatively small increments on the mean stress level of the structure, critical fatigue levels are reached on some of the code's results.

It can be therefore concluded that the spatial location of the WindCrete will be a determinant parameter on its fatigue resisting behavior. Severe sea will imply at the same time, higher stress levels and greater variations due to stronger environmental actions; and higher loads of prestressing to avoid the larger tensile stresses originated by those loads, which will as well increment the mean stress level on the structure.

A milestone has been set on the development of fatigue design procedures for floating offshore wind turbines, and, more specifically, on the description of the resistant behavior and development of the WindCrete, framed in its previous design phase. The presented model, grounded on a wide theoretical basis which is too included, will serve as a very interesting design tool for the description of the fatigue strength of the WindCrete, being possible as well to adapt it for its use on other concrete floating offshore structures. The procedure taken to term in the realization of this Thesis, its documentation and the model implementation will allow to easily take advantage of the work done, being possible to use it as a solid base from which further developments shall depart.

4.1 Suggestions for Future Research

As for a future look on the related research at this progress point of this Master Thesis, different appreciations can be made regarding future developments on the matter which shall help reducing uncertainty and understanding better the fatigue process implications on the WindCrete.

On a previous stage to the necessary fatigue damage computation, a finer representation

of the joint wind and wave climate representation shall be taken to term. This would include, on a first step, the inclusion of different directions for wind and waves acting at the same time. It would result interesting to describe the influence of this new consideration and its causes. Further refinement could be performed on the resolution for which the parameters describing the sea states have been presented, guaranteeing that the final employed values distribution accounts sufficiently accurately for the structure's resistive behavior.

In a similar sense, the application of different simulation codes, or the inclusion of different modelling procedures for the different subsystems, shall be studied in order to optimize the fatigue design, for which high levels of result reliability are needed, given that the application of global safety factor as the ones that could be applied on an ultimate limit state design, will incur into an oversize. The same study process would allow as well to state the process reliability.

A deeper analysis shall be obtained from the detailed definition of parameters such as the prestressing and structural details, in which it is possible that stress concentrations might appear. This task, which would be as well useful on a long term basis for the verification of particular real applications designs, shall provide interesting information on the influence on the different design parameters over the WindCrete, allowing to dispose of a wider knowledge base from which design decisions, both conceptual and detailed, can be made.

As an extended analysis, fatigue resistance on concrete against shear, and general fatigue behavior of the reinforcement, both passive and active, shall be verified. Although not being treated in this document, given its global approach, its check would be as critical as the normal compression fatigue response.

As a final remark, it can be stated that, despite the broad extension of the related knowledge areas and its youth, research regarding floating offshore structures applications is proving to advance on a constant pace. As proven by this Master Thesis, advantages can be taken from the related matters, facilitating general design procedures, which shall be easily verified and developed on the basis of specific experimental research and testing.

5. Literature Index

[1] BTM Consult, “International Wind Energy Development. World Market Update 2010.” Ringkøbig, 2011.

[2] EWEA, “Wind in our Sails. The coming of Europe's Offshore Wind Energy Industry.” Brussels, 2011.

[3] GWEC, “Global Wind Report. Annual Market Update 2014.” Brussels, 2014.

[4] ERNST & YOUNG, “Offshore Wind in Europe. Walking the Tightrope to Success.” 2015.

[5] EWEA, “The European Offshore Wind Industry - Key Trends and Statistics 1st Half 2015.” 2015.

[6] EWEA, “Deep Water. The Next Step for Offshore Wind Energy.” Brussels, 2013.

[7] EESI, “Fact Sheet. Offshore Wind Energy.” Washington, 2010.

[8] S. Butterfield, W. Musial, J. Jonkman and P. Sclavounos, “Engineering Challenges for Floating Offshore Wind Turbines.” in *2005 Copenhagen Offshore Wind Conference*, Copenhagen, 2005.

[9] L. Sethuraman, V. Venugopal and M. Mueller, “Drive-Train Configurations for Floating Wind Turbines.” in *Eigth International Conference and Exhibition on Ecological Vehicles and Renewable Energies (EVER)*, 2013.

[10] Roland Berger, “Offshore Wind Toward 2020. On the Pathway to Cost Competitiveness.” 2013.

[11] J. Best, “Future Offshore Wind Turbine Foundations Needs.” in *Offshore Energy 12*, Amsterdam, 2012.

[12] C. Molins, A. Campos, F. Sandner and D. Matha, “Monolithic Concrete Offshore Floating Structure for Wind Turbines.” in *EWEA 2014 Annual Event*, Barcelona, 2014.

[13] D. Matha, “Model Development and Loads Analysis of an Offshore Wind Turbine on a Tension Leg Platform, with a Comparison to Other Floating Turbine Concepts.” Boulder, 2009.

[14] A. R. Henderson, D. Witcher and C. A. Morgan, “Floating Support Structures. Enabling New Markets for Offshore Wind Energy.” in *European Wind Energy Conference*, Marseille, 2009.

[15] S. K. Chakrabarti, Handbook of Offshore Engineering. London: ELSEVIER, 2005.

[16] H. Karadeniz, Stochastic Analysis of Offshore Steel Structures. An Analytical Appraisal. London: Springer-Verlag, 2003.

[17] M. Hofmann and I. B. Sperstad, “Will 10 MW Wind Turbines Bring Down the Operation and Maintenance Cost of Offshore Wind Farms?,” in *EERA DeepWind'2014, 11th Deep Sea Offshore Wind R&D Conference*, 2014.

[18] N. Perisic, P. H. Kirkegaard and U. T. Tygesen, “Load Identification of Offshore Platform for Fatigue Life Estimation.” in *Conference Proceedings of the Society for Experimental Mechanics Series*, 2014.

[19] European Commitee for Standardization, Eurocode 2: Design of Concrete Structures (EN 1992). 2004.

[20] X. Zheng, “On some Basic Problems of Fatigue Research in Engineering.” *International Journal of Fatigue,* vol. 23, no. 9, pp. 751-766, 2001.

[21] Scottish Enterprise, “A Guide to Offshore Wind and Oil&Gas Capability.” Glasgow, 2011.

[22] CARBON TRUST, “Floating Offshore Wind: Market and Technology Review.” London, 2015.

[23] A. Athanasia and A. B. Genachte, “Deeo Offshore and New Foundation Concepts.” in *DeepWind'2013*, Trondheim, 2013.

[24] J. M. Jonkman and D. Matha, “Dynamics of Offshore Floating Wind Turbines - Analysis of Three Concepts.” *Wind Energy,* no. 14, pp. 557-569, 2011.

[25] DNV, DNV-OS-J103. Design of Floating Wind Turbine Structures. Det Norske Veritas AS, 2013.

[26] FIP, Design and Construction of Concrete Ships. London: Thomas Telford, 1986.

[27] I. Holand, O. T. Gudmestad and J. Erik, Design of Offshore Concrete Structures. London: SPON PRESS, 2000.

[28] K. Sandvik, A. Godejord, K. O. Haereid and K. Hoyland, “Offshore Structure - A New Challenge.” in *XIV National Conference on Structural Engineering*, Acapulco, 2004.

[29] V. Arskog, M. Ferreira and O. E. Gjorv, “Durability and Performance of Norwegian Concrete Harbour Structures.” in *CONSEC '04*, Seoul, 2004.

[30] A01 Committee A934, Specification for Epoxy-Coated Prefabricated Steel Reinforcing Bars. West Conshoshocken: ASTM International, 2016.

[31] A01 Committee A775, Specification for Epoxy-Coated Steel Reinforcing Bars. West Conshohocken: ASTM International, 2016.

[32] O. E. Gjorv, Durability Design of Concrete Structures in Severe Environments. Boca Raton: CRC Press Taylor & Francis Group, 2014.

[33] J. B. Herbich and K. A. Ansari, Developments in Offshore Engineering. Houston: Gulf Publications Co. 1998.

[34] K. C. Tong, “Technical and Economic Aspects of a Floating Offshore Wind Farm.” *Journal of Wind Engineering ans Industrial Aerodynamics,* no. 74-76, pp. 399-410, 1998.

[35] T. Burton, N. Jenkins, D. Sharpe and E. Bossanyi, Wind Energy Handbook. Chichester: John Wiley & Sons, 2011.

[36] C. Östergaard and T. E. Schellin, “Comparison of Experimental and Theoretical Wave Actions on Floating and Compliant Offshore Structures.” *Applied Ocean Research,* vol. 9, no. 4, pp. 192-213, 1987.

[37] J. Jonkman and W. Musial, “Final Technical Report, IEA Wind Task 23, Subtask 2, Offshore Code Comparison Collaboration (OC3).” 2010.

[38] H. O. Berteaux, Buoy Engineering. New York: Wiley & Sons Inc. 1976.

[39] M. E. McCormick, Ocean Engineering Mechanics. New York: Cambridge Univeristy Press, 2010.

[40] T. Sarpkaya, Wave Force on Offshore Structures. Cambridge: Cambridge University Press, 2014.

[41] J. R. Morison, J. W. Johnson and S. A. Schaaf, “The Force Exerted by Surface Waves on Piles.” *Society of Petroleum Engineers,* vol. 2, no. 5, pp. 149-154, 1950.

[42] D. Matha, U. Fechter, M. Kühn and P. W. Cheng, “Non-Linear Multi-Body Mooring System Model for Floating Offshore Wind Turbines.” 2011.

[43] C. Zanuy Sánchez, Análisis Seccional de Elementos de Hormigón Armado sometidos a Fatiga, incluyendo Secciones entre Fisuras, Madrid: ANCI, 2009.

[44] J. Murcia Vela, A. R. Marí Bernat y A. Aguado de Cea, Hormigón Armado y Pretensado II. Barcelona: Univ. Politèc. de Catalunya, 2010.

[45] Comisión Permanente del Hormigón, EHE-08. Instrucción de Hormigón Estructural. Ministerio de Fomento, 2011.

[46] W. A. J. Albert, “Über Treibseile am Harz.” *Archiv für Mineralogie, Geognosie und Bergbau,* vol. 10, pp. 215-234, 1837.

[47] R. Louks, B. Gerin, J. Draper, H. Askes and L. Susmel, “On the Multiaxial Fatigue Assessment of Complex Three-Dimensional Stress Concentrators.” *International Journal of Fatigue,* vol. 63, pp. 12-24, 2014.

[48] W. J. M. Rankine, “On the Causes of the Unexpected Breakage of the Journals of Railway Axles, and on the Means of Preventing Such Accidents by Observing the Law of Continuity in their Construction.” *Institution of Civil Engineers, Minutes of Proceedings,* vol. 2, pp. 105-108, 1842.

[49] J. O. York, “An Account of a Series of Experiments on hte Comparative Strength of olid and Hollow Axles.” *Institution of Civil Engineers, Minutes of Proceedings,* vol. 2, pp. 105-108, 1842.

[50] A. Morin, Leçons de Mécanique Practique - Résistance des Matérieaux. Paris: Librairie de L. Hachette et Cie. 1853.

[51] F. Braithwaite, “On the Fatigue and Consequent Fracture of Metals.” *Institution of Civil Engineers, Minutes of Proceedings,* vol. XII, pp. 463-474, 1854.

[52] W. Schütz, “A History of Fatigue.” *Engineering Fracture Mechanics,* vol. 54, no. 2, pp. 263-300, 1996.

[53] A. Wöhler, “Versuche zur Ermittlung der auf die Eisenbahnwegenachsen einwikenden Krafte und fie Wiederstandsfähigkeit der Wagen-Achsen.” *Zeitschrift für Bauwesen,* pp. 583-616, 1860.

[54] L. Spangenberg, Über das Verhalten der Metalle bei wiederholten Anstrengungen. Berlon: Ernst and Korn, 1875.

[55] W. Z. Gerber, “Calculation of the Allowable Stresses in Iron Structures.” *Bayer Architecture & Engineering,* vol. 6, pp. 101-110, 1874.

[56] J. Goodman, Mechanics Applied to Engineering. London: Longmans, Green & Co. 1914.

[57] R. E. Peterson, “Discussion of a Century Ago Concerning the Nature of Fatigue, and Review of Some of the Subsequent Researches Concerning the Mechanism of Fatigue.” *ASTM Bulletin,* no. 164, pp. 50-60, 1950.

[58] S. Timoshenko, History of Strength of Materials. New York: McGraw-Hill Book Company, 1953.

[59] A. A. Griffith, “The Phenomena of Rupture and Flow in Solids.” *Philosphical Transactions of The Royal Society A Mathematical Physical and Engineering Sciences,* vol. 221, no. 582-593, pp. 163-198, 1921.

[60] H. J. Gough, “Crystalline Structure in Relation to Failure of Metals, especially by Fatigue.” *ASTM Proceedings,* vol. 33, pp. 3-114, 1933.

[61] E. Orowan, “Theory of the Fatigue of Metals.” *Royal Society Proceedings,* no. A171, pp. 79-106, 1939.

[62] A. N. Stroh, “The Formation of Cracks as a Result of Plastic Flow.” *Proceedings of the Royal Society A Mathematical Physical and Engineering Sciences,* vol. 223, no. 1154, pp. 404-414, 1954.

[63] P. J. E. Forsyth, “Fatigue Fracture.” *Aircraft Engineering and Aerospace Technology,* vol. 32, no. 4, pp. 96-99, 1960.

[64] D. A. Ryder, “Some Quantitative Information Obtained from the Examination of Fatigue Fracture Surfaces.” *Royal Aircraft Establishment,* no. 257, 1957.

[65] E. Paris and A. Taliercio, “Anisotropic Damage Model for the Multiaxial Static and Fatigue Behaviour of Plain Concrete.” *Engineering Fracture Mechanics,* vol. 55, no. 2, pp. 163-179, 1996.

[66] G. R. Irwin, “Analysis of Stresses and Strains Near the End of a Crack Traversing a Plate.” *Journal of Applied Mechanics,* vol. 24, no. 36, pp. 1-4, 1957.

[67] J. O. Holmen, Fatigue of Concrete by Constant and Variable Amplitude Loading. Trondheim: Norges Tekniske Hogskole, 1979.

[68] L. Kaechele, “Review and Analysis of Cumulative-Fatigue-Damage Theories.” The Rand Corporation, 1963.

[69] A. Palmgren, “Die Lebensdauer von Kugellagern.” *Z. VDI Bd.* no. 68, p. 339, 1924.

[70] B. F. Langer, “Fatigue Failure from Stress Cycles of Varying Amplitude.” *Journal of Applied Mechanics,* vol. 4, pp. A160-A200, 1937.

[71] M. A. Miner, “CUmulative Damage in Fatigue.” *Journal of Applied Mechanics,* vol. 12, pp. A64-A159, 1945.

[72] E. S. Machlin, “Dislocation Theory of the Fatigue of Metals.” NACA, 1949.

[73] L. F. Coffin, E. E. Baldwin and G. Sokol, “Cyclic Strain Fatigue Studies on AISI 347 Stainless Steel.” *ASTM Proceedings,* no. 57, pp. 567-586, 1957.

[74] H. J. Grover, “An Observation Concerning the Cycle Ratio in Cumulative Damage.” in *Symposyum on Fatigue Aircraft Structures*, 1960.

[75] S. S. Manson, “Interfaces between Fatigue, Creep and Fracture.” *International Journal of Fracture Mechanics,* vol. 2, no. 1, 1966.

[76] O. Bilir, “Experimental Investigation of Fatigue Damage Acumulation in 1100 Al Alloy.” *International Journal of Fatigue,* vol. 13, no. 1, pp. 3-6, 1991.

[77] S. S. Manson and G. R. Halford, “Complexities of High Temperature Metal Fatigue: Some Steps Toward Understanding.” in *Annual Conference on Aeronautics and Astronautics*, Haifa, 1983.

[78] S. S. Manson and G. R. Halford, “Practical Implementation of the Double Linear Damage Rule and Damage Curve Approach for Treating Cumulative Fatigue Damage.” *International Journal of Fracture,* vol. 17, no. 2, pp. 169-192, 1981.

[79] L. M. Kachanov, Introduction to Continuum Damage Mechanics. Dordrecht: Springer Netherlands, 1986.

[80] A. Fatemi and L. Yang, “Cumulative Fatigue Damage and Life Prediction Theories: A Survey of the State of the Art for Homgeneous Materials.” *nternational Journal of Fatigue,* vol. 20, no. 1, pp. 9-34, 1998.

[81] J. Schijve, “Fatigue of Structures and Materials in the 20th Century and the State of the Art.” *International Journal of Fatigue,* vol. 25, pp. 679-702, 2003.

[82] G. P. Sendeckyj, “Constant Life Diagrams - A Historical Review.” *International Journal of Fatigue,* vol. 23, pp. 347-353, 2001.

[83] R. Jones, L. Molent and K. Walker, “Fatigue Crack Growth in a Diverse Range of Materials.” *International Journal of Fatigue,* vol. 40, pp. 43-50, 2012.

[84] H. Agerskov, “Fatigue in Steel Structures Under Random Loading.” *Journal of Constructional Steel Research,* vol. 53, pp. 283-305, 2000.

[85] X. Zheng, “On Some Basic Problems of Fatigue Research Under Random Loading.” *International Journal of Fatigue,* vol. 23, pp. 751-766, 2001.

[86] C. Weicheng, X. P. Huang and T. Moan, “An Engineering Model of Fatigue Crack Growth under Variable Amplitude Loading.” *International Journal of Fatigue,* vol. 30, pp. 2-10, 2007.

[87] J. L. Van Ornum, “Fatigue of Concrete.” *ASTM Transactions,* vol. 58, pp. 294-320, 1907.

[88] G. M. Nordby, “Fatigue of Concrete - A Review of Research.” *Journal of the American Concrete Institute,* vol. 30, no. 2, pp. 191-215, 1958.

[89] G. M. Murdock, “A Critical Review of Research on Fatigue of Plain Concrete.” Univeristy of Illinois, 1965.

[90] J. C. Antrim and J. F. McLaughlin, “Fatigue Study of Air-Eintrained Concrete.” *Journal of the American Concrete Institute,* vol. 30, no. 2, pp. 191-215, 1958.

[91] W. H. Gray, J. F. McLaughlin and J. C. Antrim, “Fatigue Properties of Lightweight Aggregate Concrete.” *Journal of the American Concrete Institute,* vol. 58, no. 2, 1961.

[92] J. P. Lloyd, J. L. Lott and C. E. Kesler, “Fatigue of Concrete.” University of Illinois, 1967.

[93] K. Aas-Jakobsen, “Fatigue of Concrete Beams and Columns.” University of Trondheim, Division of Concrete Structures, 19970.

[94] R. Tepfers and T. Kutti, “Fatigue Strength of Plain, Ordinary and Lightweight Concrete.” *ACI Journal,* vol. 76, no. 5, pp. 635-52, 1979.

[95] B. Zhang, D. V. Phillips and K. Wu, “Effects of Loading Frequency and Stress Reversal on Fatigue Life of Plain Concrete.” *Magazine of Concrete Research,* vol. 48, no. 177, pp. 31-75, 1996.

[96] G. Petkovic, R. Lenschow, H. Stemland and S. Rosseland, “Fatigue of High Stength Concrete.” *International Concrete Abstract,* vol. 121, pp. 505-526, 1990.

[97] H. A. W. Cornelissen and H. W. Reinardt, “Uniaxial Tensile Fatigue Failure of Concrete under Constant Amplitude and Programme Loading.” *Magazine of Concrete Research,* vol. 23, no. 129, pp. 219-260, 1984.

[98] H. F. Clemmer, "Fatigue of Concrete." *ASTM Proceedings,* vol. 22, 1922.

[99] W. K. Hatt, “Fatigue of Concrete.” in *Proceedings, 4th Annual Meeting, Highway Research Board, National Research Council*, 1924.

[100] H. A. Williams, “Fatigue Tests of Lightweight Aggreggate Concrete Beams.” *Proceedings, American Concrete Institute,* vol. 39, pp. 441-447, 1943.

[101] J. T. McCall, “Probability of Fatigue Failure of Plain Concrete.” *Journal of the American Concrete Institute,* vol. 30, no. 2, pp. 233-245, 1958.

[102] F. S. Opie and C. L. Hulsbos, “Probable Fatigue Life of Plain Concrete with Stress Gradient.” *ACI Journal,* vol. 63, no. 1, pp. 59-82, 1966.

[103] R. R. Dillmann, “Die Spannungsverteilung in der Biegedruckzone von Stahlbetonquerschnitten bei Häufig Wiederholter Belastung.” Technischen Hochschule Darmstadt, 1981.

[104] K. Aas-Jakobsen and R. Lenschow, “Behaviour of Reinforced Concrete Beams.” *ACI Journal,* vol. 70, no. 20, pp. 199-206, 1973.

[105] T. S. Chang and C. E. Kesler, “Fatigue Behaviour of Reinforced Concrete Beams.” *ACI Journal,* vol. 30, no. 2, pp. 245-254, 1958.

[106] L. Eskola, “Fatigue Behaviour of Prestressed Concrete.” ETH Zürich, 1996.

[107] V. Ciampi, R. Eligehausen, V. V. Bertero and E. P. Popow, “Analytical Model for Concrete Anchorages of Reinforced Bars under Generalized Excitations.” University of California, Berkeley, 1982.

[108] R. Eligehausen, E. P. Popov and V. V. Bertero, “Local Bond Stress-Slip Relationships of Deformed Bars under Generalized Excitations.” University of California, Berkeley, 1983.

[109] H. Kreller, “Non-Linear Strain Behaviour of Reinforced Concrete Beam Structures under Uniaxial Forces.” Universität Stuttgart, 1990.

[110] K. Terai, Y. Tmita, K. Hashimoto and N. Osawa, “Fatigue Design Method of Ship Structural Members Based on Fatigue Crack Growth Analysis.” in *Proceedings of the International Offshore and Polar Engineering Conference*, 2001.

[111] E. Peeker and E. Niemi, “Fatigue Crack Propagation Model Based on a Local Strain Approach.” vol. Journal of Constructional Steel Research, pp. 139-155, 1999.

[112] L. B. R. Robles, M. A. Buelta, E. Gonçalves and G. F. M. Souza, “A Method for the Evaluation of the Fatigue Operational Life of Submarine Pressure Hulls.” *International Journal of Fatigue,* pp. 41-52, 2000.

[113] K. Waagard, “Fatigue of Offshore Concrete Structures. Design and Experimental Investigations.” in *The 0th Annual OTC in Houston*, 1977.

[114] B. C. Gerwick and W. J. Venuti, “High and Low Cycle Fatigue Behaviour of Prestressed Concrete in Offshore Structures.” *Transcripts of the SOciety of Petroleum Engineers,* vol. 269, pp. 34-310, 1980.

[115] P. Stemberk and F. Hejnic, “Fuzzy Model for Fatigue of Concrete Including Chloride Penetration.” in *National and 1st International COnference on Technological Trends, College of Engineering Trivandrum*, 2010.

[116] FIB, Model Code for Concrete Structures 2010. Lausanne: Ernst & Sohn, 2013.

[117] F. S. Ople and C. L. Hulsbos, “Probable Fatigue Life of Plain Concrete with Stress Gradient.” *ACI Journal,* vol. 63, no. 1, pp. 59-82, 1966.

[118] J. Mazars, “Mechanical Damage and Fracture of Concrete Structures.” in *Proceedings ICF 5*, Cannes, 1981.

[119] J. Mazars, “A Description of Micro- and Macroscale Damage of Concrete Structures.” *Engineering Fracture Mechanics,* vol. 25, no. 5/6, pp. 729-737, 1986.

[120] E. Papa, “A Damage Model for Concrete Subjected to Fatigue Loading.” *European Journal of Mechanics,* vol. 12, no. 3, pp. 429-440, 1993.

[121] E. Papa and A. Taliercio, “Anisotropic Damage Model for the Multiaxial Static and Fatigue Behaviour of Plain Concrete.” *Engineering Fracture Mechanics,* vol. 55, no. 2, pp. 163-179, 1996.

[122] D. Pfanner, “Degradation of Concrete Structures Subjected to Fatigue Loading.” Ruh-Universität Bochum, 2002.

[123] A. Alliche, “Damage Model for Fatigue Loading of Concrete.” *International Journal of Fatigue,* vol. 26, pp. 915-921, 2004.

[124] A. Dragon, D. Halm and T. Desoyer, “Anisotropic Damage in Quasi-Brittle Solids. Modelling, Computational Issues and Application.” *Computational Methods Applied Mechanics Engineering,* vol. 26, pp. 331-352, 2000.

[125] C. Zanuy, L. Albajar and P. De la Fuente, “The Fatigue Process of Concrete and its Structural Influence.” Universidad Politécnica de Madrid, 2010.

[126] S. H. Mai, F. Le-Corre, G. Foret and B. Nedjar, “A Continuum Damage Modelling of Quasi-Static Fatigue Strength of Plain Concrete.” University Paris-Est, 2011.

[127] J. J. Marigo, “Modelling of Brittle and Fatigue Damage for Elastic material by Growth of Microvoids.” *Engineering Fracture Mechanics,* vol. 21, no. 4, pp. 986-974, 1985.

[128] B. Zhang, D. V. Phillips and K. Wu, “Further Research on Fatigue Properties of Plain Concrete.” *Magazine of Concrete Research,* vol. 49, no. 180, pp. 241-252, 1997.

[129] DNV, DNV-OS-C502. Offshore Concrete Structures. Det Norske Veritas, 2012.

[130] DNV, DNV-OS-J101. Design of Offshore Wind Turbine Structures. Det Norske Veritas AS, 2014.

[131] DNV, DNV-OS-C205. Environmental Conditions and Environmental Loads. Det Norske Veritas AS, 2014.

[132] DNV, DNV-OS-F205. Global Performance Analysis of Deepwater Floating Structures. Det Norske Veritas AS, 2010.

[133] DNV-GL, DNVGL-OS-C106. Structural Design of Deep Draught Floating Units. Det Norske Veritas AS, 2015.

[134] ABS, Global Performance Analysis for Floating Offshore Wind Turbine Installations. Houston: American Bureau of Shipping, 2014.

[135] IEC, IEC 61400-3. Wind Turbines - Part 3: Design Requirements for Offshore Wind Turbines. International Electrotechnical Commission, 2008.

[136] A. Campos, C. Molins, X. Gironella and P. Trubat, “Spar Concrete Monolithic Design for Offshore Wind Turbines.” *Proceedings of the Institution of Civil Engineering - Maritim Engineering,* vol. 169, no. 2, pp. 49-63, 2016.

[137] D. Matha, F. Lemmer, C. Molins, A. Campos and P. W. Cheng, “Efficient Preliminary Floating Offshore Wind Turbine Design and testing Methodologies and Application to a Concrete Spar Design.” *Philosphical Transactions of The Royal Society A Mathematical Physical Engineering Sciences,* vol. 373, no. 2035, 2015.

[138] L. H. Holthuijsen, Waves in Oceanic and Coastal Waters. Cambridge: Cambridge Univrsity Press, 2010.

[139] J. Mathisen and E. Bitner-Gregersen, “Joint Distributions for Significant Wave Height and Wave Zero-Up-Crossing Perios.” *Applied Ocean Research,* vol. 12, no. 2, pp. 93-103, 1990.

[140] E. Bitner-Gregersen, “Joint Probability Description for Combined Seas.” in *Proceedings of the 24th International Conference on Offshore Mechanics and Arctic Engineering (OMAE)*, 2005.

[141] C. Whelan, The Principles od Dynamics. TJ Bentley, 2000.

[142] MaTS, “Fatigue of Concrete. Part 4: Compressive Stresses.” MaTS, 1993.

[143] C. Molins, P. Trubat, X. Gironella and A. Campos, “Design optimization for a Truncated Catenary Mooring System for Scale Model Test.” *Journal of Marine Science and Engineering,* vol. 3, no. 4, pp. 1362-1381, 2015.

Appendix A. Codirectional Analysis, Origin Direction Distribution.

Origin direction distribution according to the defined groups, given the employed metocean data for the Windcrete's selected location (Section 3.3.4.5).

Direction Group		Direction Range	Occurrences	Probability
1	N	349º - 11º	*73109*	0.1448
2	NNE	12º - 33º	*26479*	0.0524
3	NE	34º - 56º	*16684*	0.0330
4	ENE	57º - 78º	*14407*	0.0285
5	E	79º - 101º	*15920*	0.0315
6	ESE	102º - 123º	*16291*	0.0323
7	SE	124º - 146º	*19090*	0.0378
8	SSE	147º - 168º	*25359*	0.0502
9	S	169º - 191º	*44015*	0.0872
10	SSW	192º - 213º	*51036*	0.1011
11	SW	214º - 236º	*33573*	0.0665
12	WSW	237º - 258º	*17628*	0.0349
13	W	259º - 281º	*12948*	0.0256
14	WNW	282º - 303º	*12437*	0.0246
15	NW	304º - 326º	*25505*	0.0505
16	NNW	327º - 348º	*100563*	0.1991
		TOTAL	505 044	1

Appendix B. Environmental Parameters Distributions Fit Results

Defining parameters of the probabilistic distributions characterizing the necessary environmental variables.

10-Minute Mean Wind Velocity Fit (Section 3.3.4.6.1)

Variable	Section	Parameters	
		Scale (α)	*Shape (β)*
Wind U_{10} *2-Parameter Weibull*	***1***	11.69	2.27
	2	7.29	2.08
	3	5.95	1.91
	4	6.32	1.56
	5	6.73	1.48
	6	6.55	1.66
	7	6.05	1.98
	8	6.45	2.26
	9	7.65	2.37
	10	8.56	2.27
	11	7.59	1.85
	12	5.46	1.95
	13	4.53	2.17
	14	4.72	2.15
	15	7.78	1.64
	16	14.31	2.31

Root Mean Square Wave Height Fit (Section 3.3.4.6.2)

Variable	Section	Parameters		
		Scale (α)	*Shape (β)*	*Location (γ)*
Wave H_{RMS} *3-Parameter Weibull*	***1***	0.77	1.58	0.07
	2	0.39	0.92	0.21
	3	0.36	0.70	0.23
	4	0.69	0.84	0.11
	5	0.86	0.94	0.03
	6	0.69	0.91	0.08
	7	0.44	0.86	0.12
	8	0.33	0.89	0.13
	9	0.33	1.07	0.12
	10	0.33	1.00	0.18
	11	0.48	1.17	0.06
	12	0.35	1.00	0.08
	13	0.28	0.98	0.09
	14	0.31	1.07	0.08
	15	0.46	1.12	0.12
	16	0.76	1.29	0.27

Conditioned Fit of the 10-Minute Mean Wind Velocity on the Root Mean Square Wave Height (Section 3.3.4.6.3)

Variable	Section	Parameters					
		c_1	c_2	c_3	c_4	c_5	c_6
Wind and Wave U_{10} on H_{RMS} *3-Parameter Weibull on 2-Parameter Weibull*	***1***	3.51	0.21	3.17	1.54	11.92	0.59
	2	2.62	0.33	2.01	4.25	4.61	1.11
	3	2.29	0.72	1.46	3.11	4.20	1.11
	4	2.97	0.05	3.69	2.83	4.10	1.12
	5	3.77	0.00	5.31	2.07	5.42	0.90
	6	2.67	0.18	2.71	2.58	5.24	0.90
	7	2.62	0.30	1.52	2.95	5.19	0.77
	8	2.99	0.00	14.77	2.32	6.71	0.46
	9	3.09	-0.22	1.36	2.88	6.69	0.35
	10	2.60	0.58	0.00	2.09	8.97	0.34
	11	2.50	0.71	0.15	1.90	9.45	0.56
	12	2.12	0.60	1.48	2.20	6.58	0.67
	13	2.27	0.04	3.63	2.05	4.12	0.33
	14	2.22	0.00	21.03	2.50	3.67	0.39
	15	0.07	1.06	2.69	2.11	9.92	0.73
	16	4.23	0.96	1.94	0.53	14.12	0.51

Conditioned Fit of the Mean Wave Period on the Root Mean Square Wave Height (Section 3.3.4.6.4)

Variable	Section	Parameters					
		a_0	a_1	a_2	b_0	b_1	b_2
Wave T_m on H_{RMS} *Lognormal on 2-Parameter Weibull*	***1***	0.71	0.65	0.44	8.19	-8.04	0.00
	2	0.75	0.66	0.47	14.50	-14.33	0.00
	3	0.84	0.61	0.47	16.21	-16.05	0.00
	4	0.85	0.60	0.47	12.97	-12.83	0.00
	5	0.81	0.63	0.45	10.58	-10.43	0.00
	6	0.88	0.56	0.51	9.83	-9.67	0.00
	7	0.79	0.63	0.47	12.05	-11.87	0.00
	8	0.82	0.58	0.54	11.98	-11.79	0.00
	9	0.75	0.65	0.52	9.10	-8.90	0.01
	10	0.79	0.59	0.60	9.53	-9.34	0.01
	11	0.74	0.66	0.53	21.46	-21.28	0.00
	12	0.82	0.63	0.51	11.06	-10.85	0.01
	13	0.81	0.69	0.52	25.37	-25.16	0.00
	14	0.82	0.68	0.52	12.70	-12.52	0.00
	15	0.74	0.65	0.44	6.10	-5.92	0.01
	16	0.66	0.69	0.40	11.50	-11.39	0.00

Appendix C. Discrete Joint Wind and Wave Climate Characterization

Resulting sea states defining the joint wind and wave climate on the given parameters for the stated spatial location, given the selected analysis method and the proposed value resolution (Section 3.3.4.6.5). Includes the design load case consideration and assignation (Section 3.3.4.7).

Sea State	H_{RMS}	U_{10}	**Dir. Section**	T_m	**Probability**	**DLC**
#	*m*	*m/s*	#	*Sec.*	-	*POWP/PARK*
1	0.25	1	0	2.75	0.0006	PARK
2	0.75	1	0	3.75	0.0001	PARK
3	0.25	1	1	3.25	0.0020	PARK
4	0.75	1	1	3.75	0.0005	PARK
5	0.25	1	2	3.25	0.0020	PARK
6	0.75	1	2	3.75	0.0005	PARK
7	0.25	1	3	3.25	0.0022	PARK
8	0.75	1	3	3.75	0.0003	PARK
9	0.25	1	4	3.25	0.0019	PARK
10	0.75	1	4	3.75	0.0001	PARK
11	0.25	1	5	3.25	0.0020	PARK
12	0.75	1	5	3.75	0.0004	PARK
13	0.25	1	6	3.25	0.0027	PARK
14	0.75	1	6	3.75	0.0003	PARK
15	0.25	1	7	3.25	0.0012	PARK
16	0.75	1	7	3.75	0.0002	PARK
17	0.25	1	8	2.75	0.0015	PARK
18	0.75	1	8	3.75	0.0003	PARK
19	0.25	1	9	2.75	0.0007	PARK
20	0.75	1	9	3.75	0.0002	PARK
21	0.25	1	10	2.75	0.0018	PARK
22	0.75	1	10	3.75	0.0001	PARK
23	0.25	1	11	3.25	0.0034	PARK
24	0.75	1	11	3.75	0.0004	PARK
25	0.25	1	12	3.25	0.0028	PARK
26	0.75	1	12	4.25	0.0004	PARK

Sea State	H_{RMS}	U_{10}	Dir. Section	T_m	Probability	DLC
#	*m*	*m/s*	#	*Sec.*	-	*POWP/PARK*
27	0.25	1	13	3.25	0.0026	PARK
28	0.75	1	13	4.25	0.0005	PARK
29	0.25	1	14	3.25	0.0065	PARK
30	0.75	1	14	3.75	0.0053	PARK
31	1.25	1	14	4.25	0.0002	PARK
32	0.25	3	0	2.75	0.0056	POWP
33	0.25	5	0	2.75	0.0131	POWP
34	0.25	7	0	2.75	0.0147	POWP
35	0.25	9	0	2.75	0.0098	POWP
36	0.25	11	0	2.75	0.0042	POWP
37	0.25	13	0	2.75	0.0011	POWP
38	0.25	15	0	2.75	0.0001	POWP
39	0.75	3	0	3.75	0.0014	POWP
40	0.75	5	0	3.75	0.0049	POWP
41	0.75	7	0	3.75	0.0098	POWP
42	0.75	9	0	3.75	0.0138	POWP
43	0.75	11	0	3.75	0.0140	POWP
44	0.75	13	0	3.75	0.0104	POWP
45	0.75	15	0	3.75	0.0056	POWP
46	0.75	17	0	3.75	0.0022	POWP
47	0.75	19	0	3.75	0.0006	POWP
48	0.75	21	0	3.75	0.0001	POWP
49	1.25	3	0	4.25	0.0002	POWP
50	1.25	5	0	4.25	0.0007	POWP
51	1.25	7	0	4.25	0.0017	POWP
52	1.25	9	0	4.25	0.0032	POWP
53	1.25	11	0	4.25	0.0047	POWP
54	1.25	13	0	4.25	0.0056	POWP
55	1.25	15	0	4.25	0.0054	POWP
56	1.25	17	0	4.25	0.0041	POWP
57	1.25	19	0	4.25	0.0023	POWP
58	1.25	21	0	4.25	0.0010	POWP
59	1.25	23	0	4.25	0.0003	POWP
60	1.75	7	0	4.75	0.0002	POWP

Sea State	H_{RMS}	U_{10}	Dir. Section	T_m	Probability	DLC
#	*m*	*m/s*	#	*Sec.*	-	*POWP/PARK*
61	1.75	9	0	4.75	0.0004	POWP
62	1.75	11	0	4.75	0.0007	POWP
63	1.75	13	0	4.75	0.0011	POWP
64	1.75	15	0	4.75	0.0015	POWP
65	1.75	17	0	4.75	0.0017	POWP
66	1.75	19	0	4.75	0.0014	POWP
67	1.75	21	0	4.75	0.0010	POWP
68	1.75	23	0	4.75	0.0005	POWP
69	1.75	25	0	4.75	0.0001	POWP
70	2.25	15	0	5.25	0.0002	POWP
71	2.25	17	0	5.25	0.0003	POWP
72	2.25	19	0	5.25	0.0004	POWP
73	2.25	21	0	5.25	0.0004	POWP
74	2.25	23	0	5.25	0.0003	POWP
75	0.25	3	1	3.25	0.0088	POWP
76	0.25	5	1	3.25	0.0114	POWP
77	0.25	7	1	3.25	0.0069	POWP
78	0.25	9	1	3.25	0.0021	POWP
79	0.25	11	1	3.25	0.0003	POWP
80	0.75	3	1	3.75	0.0026	POWP
81	0.75	5	1	3.75	0.0047	POWP
82	0.75	7	1	3.75	0.0049	POWP
83	0.75	9	1	3.75	0.0032	POWP
84	0.75	11	1	3.75	0.0013	POWP
85	0.75	13	1	3.75	0.0004	POWP
86	1.25	3	1	4.25	0.0003	POWP
87	1.25	5	1	4.25	0.0007	POWP
88	1.25	7	1	4.25	0.0011	POWP
89	1.25	9	1	4.25	0.0013	POWP
90	1.25	11	1	4.25	0.0010	POWP
91	1.25	13	1	4.25	0.0006	POWP
92	1.25	15	1	4.25	0.0002	POWP
93	1.75	7	1	5.25	0.0002	POWP
94	1.75	9	1	5.25	0.0003	POWP

Sea State	H_{RMS}	U_{10}	Dir. Section	T_m	Probability	DLC
#	*m*	*m/s*	#	*Sec.*	-	*POWP/PARK*
95	1.75	11	1	5.25	0.0004	POWP
96	1.75	13	1	5.25	0.0003	POWP
97	1.75	15	1	5.25	0.0002	POWP
98	1.75	17	1	5.25	0.0001	POWP
99	2.25	15	1	5.75	0.0001	POWP
100	0.25	3	2	3.25	0.0061	POWP
101	0.25	5	2	3.25	0.0050	POWP
102	0.25	7	2	3.25	0.0016	POWP
103	0.25	9	2	3.25	0.0002	POWP
104	0.75	3	2	3.75	0.0022	POWP
105	0.75	5	2	3.75	0.0031	POWP
106	0.75	7	2	3.75	0.0022	POWP
107	0.75	9	2	3.75	0.0008	POWP
108	0.75	11	2	3.75	0.0002	POWP
109	1.25	3	2	4.75	0.0003	POWP
110	1.25	5	2	4.75	0.0007	POWP
111	1.25	7	2	4.75	0.0009	POWP
112	1.25	9	2	4.75	0.0008	POWP
113	1.25	11	2	4.75	0.0004	POWP
114	1.25	13	2	4.75	0.0001	POWP
115	1.75	7	2	5.25	0.0003	POWP
116	1.75	9	2	5.25	0.0004	POWP
117	1.75	11	2	5.25	0.0004	POWP
118	1.75	13	2	5.25	0.0002	POWP
119	2.25	11	2	5.75	0.0002	POWP
120	2.25	13	2	5.75	0.0002	POWP
121	2.25	15	2	5.75	0.0001	POWP
122	0.25	3	3	3.25	0.0079	POWP
123	0.25	5	3	3.25	0.0038	POWP
124	0.25	7	3	3.25	0.0004	POWP
125	0.75	3	3	3.75	0.0020	POWP
126	0.75	5	3	3.75	0.0029	POWP
127	0.75	7	3	3.75	0.0017	POWP
128	0.75	9	3	3.75	0.0005	POWP

Sea State	H_{RMS}	U_{10}	Dir. Section	T_m	Probability	DLC
#	*m*	*m/s*	#	*Sec.*	-	*POWP/PARK*
129	1.25	3	3	4.75	0.0004	POWP
130	1.25	5	3	4.75	0.0009	POWP
131	1.25	7	3	4.75	0.0011	POWP
132	1.25	9	3	4.75	0.0008	POWP
133	1.25	11	3	4.75	0.0004	POWP
134	1.75	5	3	5.25	0.0002	POWP
135	1.75	7	3	5.25	0.0004	POWP
136	1.75	9	3	5.25	0.0005	POWP
137	1.75	11	3	5.25	0.0004	POWP
138	1.75	13	3	5.25	0.0003	POWP
139	2.25	9	3	5.75	0.0002	POWP
140	2.25	11	3	5.75	0.0003	POWP
141	2.25	13	3	5.75	0.0002	POWP
142	2.25	15	3	5.75	0.0002	POWP
143	2.75	13	3	6.25	0.0001	POWP
144	2.75	15	3	6.25	0.0002	POWP
145	2.75	17	3	6.25	0.0001	POWP
146	0.25	3	4	3.25	0.0082	POWP
147	0.25	5	4	3.25	0.0031	POWP
148	0.25	7	4	3.25	0.0002	POWP
149	0.75	3	4	3.75	0.0015	POWP
150	0.75	5	4	3.75	0.0033	POWP
151	0.75	7	4	3.75	0.0024	POWP
152	0.75	9	4	3.75	0.0006	POWP
153	1.25	3	4	4.75	0.0002	POWP
154	1.25	5	4	4.75	0.0008	POWP
155	1.25	7	4	4.75	0.0014	POWP
156	1.25	9	4	4.75	0.0013	POWP
157	1.25	11	4	4.75	0.0006	POWP
158	1.25	13	4	4.75	0.0002	POWP
159	1.75	5	4	5.25	0.0002	POWP
160	1.75	7	4	5.25	0.0004	POWP
161	1.75	9	4	5.25	0.0006	POWP
162	1.75	11	4	5.25	0.0006	POWP

Sea State	H_{RMS}	U_{10}	Dir. Section	T_m	Probability	DLC
#	*m*	*m/s*	#	*Sec.*	-	*POWP/PARK*
163	1.75	13	4	5.25	0.0004	POWP
164	1.75	15	4	5.25	0.0002	POWP
165	2.25	7	4	5.75	0.0001	POWP
166	2.25	9	4	5.75	0.0002	POWP
167	2.25	11	4	5.75	0.0003	POWP
168	2.25	13	4	5.75	0.0003	POWP
169	2.25	15	4	5.75	0.0002	POWP
170	2.25	17	4	5.75	0.0001	POWP
171	2.75	11	4	6.25	0.0001	POWP
172	2.75	13	4	6.25	0.0002	POWP
173	2.75	15	4	6.25	0.0002	POWP
174	2.75	17	4	6.25	0.0001	POWP
175	0.25	3	5	3.25	0.0067	POWP
176	0.25	5	5	3.25	0.0046	POWP
177	0.25	7	5	3.25	0.0012	POWP
178	0.25	9	5	3.25	0.0001	POWP
179	0.75	3	5	3.75	0.0018	POWP
180	0.75	5	5	3.75	0.0028	POWP
181	0.75	7	5	3.75	0.0023	POWP
182	0.75	9	5	3.75	0.0011	POWP
183	0.75	11	5	3.75	0.0003	POWP
184	1.25	3	5	4.75	0.0003	POWP
185	1.25	5	5	4.75	0.0008	POWP
186	1.25	7	5	4.75	0.0011	POWP
187	1.25	9	5	4.75	0.0010	POWP
188	1.25	11	5	4.75	0.0007	POWP
189	1.25	13	5	4.75	0.0003	POWP
190	1.75	5	5	5.25	0.0002	POWP
191	1.75	7	5	5.25	0.0004	POWP
192	1.75	9	5	5.25	0.0005	POWP
193	1.75	11	5	5.25	0.0005	POWP
194	1.75	13	5	5.25	0.0004	POWP
195	1.75	15	5	5.25	0.0002	POWP
196	2.25	9	5	5.75	0.0002	POWP

Sea State	H_{RMS}	U_{10}	Dir. Section	T_m	Probability	DLC
#	*m*	*m/s*	#	*Sec.*	-	*POWP/PARK*
197	2.25	11	5	5.75	0.0003	POWP
198	2.25	13	5	5.75	0.0003	POWP
199	2.25	15	5	5.75	0.0002	POWP
200	2.75	13	5	6.25	0.0001	POWP
201	2.75	15	5	6.25	0.0002	POWP
202	2.75	17	5	6.25	0.0001	POWP
203	0.25	3	6	3.25	0.0100	POWP
204	0.25	5	6	3.25	0.0092	POWP
205	0.25	7	6	3.25	0.0034	POWP
206	0.25	9	6	3.25	0.0006	POWP
207	0.75	3	6	3.75	0.0017	POWP
208	0.75	5	6	3.75	0.0029	POWP
209	0.75	7	6	3.75	0.0028	POWP
210	0.75	9	6	3.75	0.0016	POWP
211	0.75	11	6	3.75	0.0005	POWP
212	1.25	3	6	4.25	0.0003	POWP
213	1.25	5	6	4.25	0.0007	POWP
214	1.25	7	6	4.25	0.0009	POWP
215	1.25	9	6	4.25	0.0009	POWP
216	1.25	11	6	4.25	0.0006	POWP
217	1.25	13	6	4.25	0.0003	POWP
218	1.75	5	6	5.25	0.0002	POWP
219	1.75	7	6	5.25	0.0003	POWP
220	1.75	9	6	5.25	0.0003	POWP
221	1.75	11	6	5.25	0.0003	POWP
222	1.75	13	6	5.25	0.0002	POWP
223	2.25	11	6	5.75	0.0001	POWP
224	2.25	13	6	5.75	0.0001	POWP
225	0.25	3	7	3.25	0.0069	POWP
226	0.25	5	7	3.25	0.0115	POWP
227	0.25	7	7	3.25	0.0083	POWP
228	0.25	9	7	3.25	0.0029	POWP
229	0.25	11	7	3.25	0.0005	POWP
230	0.75	3	7	3.75	0.0013	POWP

Sea State	H_{RMS}	U_{10}	Dir. Section	T_m	Probability	DLC
#	*m*	*m/s*	#	*Sec.*	-	*POWP/PARK*
231	0.75	5	7	3.75	0.0029	POWP
232	0.75	7	7	3.75	0.0036	POWP
233	0.75	9	7	3.75	0.0027	POWP
234	0.75	11	7	3.75	0.0013	POWP
235	0.75	13	7	3.75	0.0004	POWP
236	1.25	3	7	4.25	0.0002	POWP
237	1.25	5	7	4.25	0.0005	POWP
238	1.25	7	7	4.25	0.0007	POWP
239	1.25	9	7	4.25	0.0008	POWP
240	1.25	11	7	4.25	0.0006	POWP
241	1.25	13	7	4.25	0.0003	POWP
242	1.25	15	7	4.25	0.0001	POWP
243	1.75	7	7	4.75	0.0002	POWP
244	1.75	9	7	4.75	0.0002	POWP
245	1.75	11	7	4.75	0.0002	POWP
246	1.75	13	7	4.75	0.0001	POWP
247	0.25	3	8	2.75	0.0098	POWP
248	0.25	5	8	2.75	0.0199	POWP
249	0.25	7	8	2.75	0.0202	POWP
250	0.25	9	8	2.75	0.0112	POWP
251	0.25	11	8	2.75	0.0035	POWP
252	0.25	13	8	2.75	0.0006	POWP
253	0.75	3	8	3.75	0.0019	POWP
254	0.75	5	8	3.75	0.0044	POWP
255	0.75	7	8	3.75	0.0060	POWP
256	0.75	9	8	3.75	0.0055	POWP
257	0.75	11	8	3.75	0.0034	POWP
258	0.75	13	8	3.75	0.0014	POWP
259	0.75	15	8	3.75	0.0004	POWP
260	1.25	3	8	4.25	0.0003	POWP
261	1.25	5	8	4.25	0.0006	POWP
262	1.25	7	8	4.25	0.0009	POWP
263	1.25	9	8	4.25	0.0010	POWP
264	1.25	11	8	4.25	0.0008	POWP

Sea State	H_{RMS}	U_{10}	Dir. Section	T_m	Probability	DLC
#	*m*	*m/s*	#	*Sec.*	-	*POWP/PARK*
265	1.25	13	8	4.25	0.0005	POWP
266	1.25	15	8	4.25	0.0002	POWP
267	1.75	7	8	5.25	0.0001	POWP
268	1.75	9	8	5.25	0.0002	POWP
269	1.75	11	8	5.25	0.0001	POWP
270	0.25	3	9	2.75	0.0054	POWP
271	0.25	5	9	2.75	0.0131	POWP
272	0.25	7	9	2.75	0.0177	POWP
273	0.25	9	9	2.75	0.0143	POWP
274	0.25	11	9	2.75	0.0069	POWP
275	0.25	13	9	2.75	0.0020	POWP
276	0.25	15	9	2.75	0.0003	POWP
277	0.75	3	9	3.75	0.0015	POWP
278	0.75	5	9	3.75	0.0041	POWP
279	0.75	7	9	3.75	0.0067	POWP
280	0.75	9	9	3.75	0.0077	POWP
281	0.75	11	9	3.75	0.0062	POWP
282	0.75	13	9	3.75	0.0035	POWP
283	0.75	15	9	3.75	0.0013	POWP
284	0.75	17	9	3.75	0.0003	POWP
285	1.25	3	9	4.25	0.0002	POWP
286	1.25	5	9	4.25	0.0006	POWP
287	1.25	7	9	4.25	0.0010	POWP
288	1.25	9	9	4.25	0.0014	POWP
289	1.25	11	9	4.25	0.0014	POWP
290	1.25	13	9	4.25	0.0011	POWP
291	1.25	15	9	4.25	0.0007	POWP
292	1.25	17	9	4.25	0.0003	POWP
293	1.75	7	9	5.25	0.0002	POWP
294	1.75	9	9	5.25	0.0002	POWP
295	1.75	11	9	5.25	0.0003	POWP
296	1.75	13	9	5.25	0.0003	POWP
297	1.75	15	9	5.25	0.0002	POWP
298	0.25	3	10	2.75	0.0099	POWP

Sea State	H_{RMS}	U_{10}	Dir. Section	T_m	Probability	DLC
#	*m*	*m/s*	#	*Sec.*	-	*POWP/PARK*
299	0.25	5	10	2.75	0.0144	POWP
300	0.25	7	10	2.75	0.0103	POWP
301	0.25	9	10	2.75	0.0046	POWP
302	0.25	11	10	2.75	0.0014	POWP
303	0.25	13	10	2.75	0.0002	POWP
304	0.75	3	10	3.75	0.0011	POWP
305	0.75	5	10	3.75	0.0030	POWP
306	0.75	7	10	3.75	0.0047	POWP
307	0.75	9	10	3.75	0.0050	POWP
308	0.75	11	10	3.75	0.0037	POWP
309	0.75	13	10	3.75	0.0019	POWP
310	0.75	15	10	3.75	0.0007	POWP
311	0.75	17	10	3.75	0.0002	POWP
312	1.25	3	10	4.25	0.0001	POWP
313	1.25	5	10	4.25	0.0004	POWP
314	1.25	7	10	4.25	0.0007	POWP
315	1.25	9	10	4.25	0.0011	POWP
316	1.25	11	10	4.25	0.0012	POWP
317	1.25	13	10	4.25	0.0010	POWP
318	1.25	15	10	4.25	0.0007	POWP
319	1.25	17	10	4.25	0.0004	POWP
320	1.25	19	10	4.25	0.0002	POWP
321	1.75	9	10	5.25	0.0002	POWP
322	1.75	11	10	5.25	0.0002	POWP
323	1.75	13	10	5.25	0.0003	POWP
324	1.75	15	10	5.25	0.0002	POWP
325	1.75	17	10	5.25	0.0002	POWP
326	0.25	3	11	3.25	0.0083	POWP
327	0.25	5	11	3.25	0.0070	POWP
328	0.25	7	11	3.25	0.0034	POWP
329	0.25	9	11	3.25	0.0011	POWP
330	0.25	11	11	3.25	0.0003	POWP
331	0.75	3	11	3.75	0.0014	POWP
332	0.75	5	11	3.75	0.0021	POWP

Sea State	H_{RMS}	U_{10}	Dir. Section	T_m	Probability	DLC
#	*m*	*m/s*	#	*Sec.*	-	*POWP/PARK*
333	0.75	7	11	3.75	0.0021	POWP
334	0.75	9	11	3.75	0.0014	POWP
335	0.75	11	11	3.75	0.0007	POWP
336	0.75	13	11	3.75	0.0002	POWP
337	1.25	3	11	4.75	0.0001	POWP
338	1.25	5	11	4.75	0.0003	POWP
339	1.25	7	11	4.75	0.0004	POWP
340	1.25	9	11	4.75	0.0005	POWP
341	1.25	11	11	4.75	0.0004	POWP
342	1.25	13	11	4.75	0.0002	POWP
343	0.25	3	12	3.25	0.0074	POWP
344	0.25	5	12	3.25	0.0062	POWP
345	0.25	7	12	3.25	0.0026	POWP
346	0.25	9	12	3.25	0.0006	POWP
347	0.75	3	12	4.25	0.0014	POWP
348	0.75	5	12	4.25	0.0016	POWP
349	0.75	7	12	4.25	0.0010	POWP
350	0.75	9	12	4.25	0.0004	POWP
351	1.25	3	12	4.75	0.0002	POWP
352	1.25	5	12	4.75	0.0003	POWP
353	1.25	7	12	4.75	0.0002	POWP
354	0.25	3	13	3.25	0.0067	POWP
355	0.25	5	13	3.25	0.0056	POWP
356	0.25	7	13	3.25	0.0024	POWP
357	0.25	9	13	3.25	0.0006	POWP
358	0.75	3	13	4.25	0.0015	POWP
359	0.75	5	13	4.25	0.0017	POWP
360	0.75	7	13	4.25	0.0011	POWP
361	0.75	9	13	4.25	0.0005	POWP
362	0.75	11	13	4.25	0.0001	POWP
363	1.25	3	13	4.75	0.0002	POWP
364	1.25	5	13	4.75	0.0003	POWP
365	1.25	7	13	4.75	0.0002	POWP
366	0.25	3	14	3.25	0.0009	POWP

Sea State	H_{RMS}	U_{10}	Dir. Section	T_m	Probability	DLC
#	*m*	*m/s*	#	*Sec.*	-	*POWP/PARK*
367	0.25	5	14	3.25	0.0005	POWP
368	0.25	7	14	3.25	0.0004	POWP
369	0.25	9	14	3.25	0.0003	POWP
370	0.25	11	14	3.25	0.0002	POWP
371	0.25	13	14	3.25	0.0002	POWP
372	0.25	15	14	3.25	0.0002	POWP
373	0.25	17	14	3.25	0.0002	POWP
374	0.25	19	14	3.25	0.0001	POWP
375	0.25	21	14	3.25	0.0001	POWP
376	0.75	3	14	3.75	0.0017	POWP
377	0.75	5	14	3.75	0.0012	POWP
378	0.75	7	14	3.75	0.0009	POWP
379	0.75	9	14	3.75	0.0007	POWP
380	0.75	11	14	3.75	0.0006	POWP
381	0.75	13	14	3.75	0.0005	POWP
382	0.75	15	14	3.75	0.0004	POWP
383	0.75	17	14	3.75	0.0004	POWP
384	0.75	19	14	3.75	0.0003	POWP
385	0.75	21	14	3.75	0.0003	POWP
386	0.75	23	14	3.75	0.0002	POWP
387	0.75	25	14	3.75	0.0002	POWP
388	1.25	3	14	4.25	0.0004	POWP
389	1.25	5	14	4.25	0.0005	POWP
390	1.25	7	14	4.25	0.0005	POWP
391	1.25	9	14	4.25	0.0006	POWP
392	1.25	11	14	4.25	0.0006	POWP
393	1.25	13	14	4.25	0.0005	POWP
394	1.25	15	14	4.25	0.0004	POWP
395	1.25	17	14	4.25	0.0004	POWP
396	1.25	19	14	4.25	0.0003	POWP
397	1.25	21	14	4.25	0.0002	POWP
398	1.25	23	14	4.25	0.0001	POWP
399	1.75	11	14	4.75	0.0001	POWP
400	1.75	13	14	4.75	0.0002	POWP

Sea State	H_{RMS}	U_{10}	Dir. Section	T_m	Probability	DLC
#	*m*	*m/s*	#	*Sec.*	-	*POWP/PARK*
401	1.75	15	14	4.75	0.0002	POWP
402	1.75	17	14	4.75	0.0003	POWP
403	1.75	19	14	4.75	0.0002	POWP
404	0.25	3	15	2.75	0.0011	POWP
405	0.25	5	15	2.75	0.0051	POWP
406	0.25	7	15	2.75	0.0116	POWP
407	0.25	9	15	2.75	0.0137	POWP
408	0.25	11	15	2.75	0.0081	POWP
409	0.25	13	15	2.75	0.0022	POWP
410	0.25	15	15	2.75	0.0002	POWP
411	0.75	3	15	3.75	0.0005	POWP
412	0.75	5	15	3.75	0.0026	POWP
413	0.75	7	15	3.75	0.0080	POWP
414	0.75	9	15	3.75	0.0162	POWP
415	0.75	11	15	3.75	0.0225	POWP
416	0.75	13	15	3.75	0.0207	POWP
417	0.75	15	15	3.75	0.0123	POWP
418	0.75	17	15	3.75	0.0045	POWP
419	0.75	19	15	3.75	0.0009	POWP
420	1.25	5	15	4.25	0.0002	POWP
421	1.25	7	15	4.25	0.0008	POWP
422	1.25	9	15	4.25	0.0024	POWP
423	1.25	11	15	4.25	0.0053	POWP
424	1.25	13	15	4.25	0.0092	POWP
425	1.25	15	15	4.25	0.0118	POWP
426	1.25	17	15	4.25	0.0106	POWP
427	1.25	19	15	4.25	0.0060	POWP
428	1.25	21	15	4.25	0.0018	POWP
429	1.25	23	15	4.25	0.0003	POWP
430	1.75	9	15	4.75	0.0002	POWP
431	1.75	11	15	4.75	0.0006	POWP
432	1.75	13	15	4.75	0.0015	POWP
433	1.75	15	15	4.75	0.0030	POWP
434	1.75	17	15	4.75	0.0047	POWP

Sea State	H_{RMS}	U_{10}	Dir. Section	T_m	Probability	DLC
#	*m*	*m/s*	#	*Sec.*	-	*POWP/PARK*
435	1.75	19	15	4.75	0.0053	POWP
436	1.75	21	15	4.75	0.0038	POWP
437	1.75	23	15	4.75	0.0014	POWP
438	1.75	25	15	4.75	0.0002	POWP
439	2.25	13	15	5.25	0.0001	POWP
440	2.25	15	15	5.25	0.0004	POWP
441	2.25	17	15	5.25	0.0009	POWP
442	2.25	19	15	5.25	0.0016	POWP
443	2.25	21	15	5.25	0.0022	POWP
444	2.25	23	15	5.25	0.0018	POWP
445	2.25	25	15	5.25	0.0007	POWP
446	2.75	19	15	5.75	0.0002	POWP
447	2.75	21	15	5.75	0.0005	POWP
448	2.75	23	15	5.75	0.0008	POWP
449	2.75	25	15	5.75	0.0007	POWP
450	3.25	23	15	5.75	0.0001	POWP
451	3.25	25	15	5.75	0.0003	POWP
452	0.75	27	14	3.75	0.0002	PARK
453	0.75	29	14	3.75	0.0002	PARK
454	0.75	31	14	3.75	0.0002	PARK
455	0.75	33	14	3.75	0.0001	PARK
456	2.75	27	15	5.75	0.0002	PARK
457	3.25	27	15	5.75	0.0002	PARK